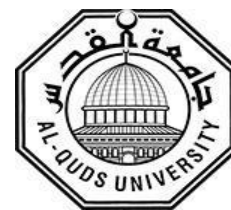


**Deanship of Graduate Studies  
Al-Quds University**



**Synthesis, Characterization and *In Vitro* Kinetic Study  
of Gabapentin Prodrugs**

**Fatma Isam Abdul Qadir Haddad**

**M.Sc. Thesis**

**Jerusalem-Palestine**

**1439/2018**

**Synthesis, Characterization and *In Vitro* Kinetics  
Study of Gabapentin Prodrugs**

**Prepared By:**

**Fatma Isam Abdul Qadir Haddad**

**B.Sc., Pharmacy, An-Najah National University,  
Palestine.**

**Supervisor: Prof. Dr. Rafik Karaman**

**A thesis submitted in partial fulfillment of  
requirements for the degree of Master of  
Pharmaceutical Science, Al-Quds University.**

**1439/2018**

Al-Quds University  
Deanship of Graduate Studies  
Pharmaceutical Science Program



## Thesis Approval

### Synthesis, Characterization and *In Vitro* Kinetics Study of Gabapentin Prodrugs

Prepared by: Fatma Isam Abdul Qadir Haddad

Registration No.: 21511147

Supervisor: Prof. Rafik Karaman

Master thesis Submitted and Accepted, Date:6/5/2018

The names and signatures of the examining committee members are as follows:

1-Head of Committee: Prof. Rafik Karaman

Signature:.....

2- Internal Examiner: Prof. Saleh Abu-Lafi

Signature:.....

3- External Examiner: Dr. Hatem Hejaz

Signature: .....

Jerusalem–Palestine

1439/2018

## **Dedication**

This thesis is dedicated to my parents who encouraged and inspired me throughout my educational journey. I am very grateful for their love, support, and prayers.

Special and loving thanks go out to all my sisters, my brothers, and my friends and to all whom I love who supported me spiritually throughout my research.

Fatma Haddad

## **Declaration**

I certify that the thesis submitted for the degree of the master is the result of my own research, except where otherwise acknowledged, and that this thesis (or any part of the same) has not be submitted for a higher degree to any other university or institution.

Signed: .....

Fatma Isam Abdul Qadir Haddad

Date: 6/5/2018

## **Acknowledgment**

First and foremost, I am deeply thankful to Almighty Allah from Whom I always receive help and protection.

I would like to express my special appreciation and thanks to my supervisor Professor Dr. Rafik Karaman, I would like to thank you for encouraging my research and for allowing me to grow as a researcher.

I would like to thank again my mother for giving me the strength to reach for the star and chase my dreams.

I am thankful for and fortunate enough to get constant encouragement, support and guidance from Yahya Khawaja, Anas Najjar, Ibrahim Ayyad, Dr. Hussein Hallak, and Ameen Thewabteh.

I also owe sincere gratitude to Dr. Saleh Abu-Lafi for his support, help and for carrying out liquid chromatography-mass spectrometry for the synthesized gabapentin prodrugs.

It gives me great pleasure in acknowledging the support and help of Mr. Munir Atrash at Jerusalem Pharmaceutical company in Ramallah, Palestine. I also thank Dr. Mohammed Abo Zneid for his wonderful skill in high-performance liquid chromatography techniques and his support.

I am very grateful to Ms. Rema Mofrh at Beit Jala Pharmaceutical Company for the support and her excellent high-performance liquid chromatography techniques.

## Abstract

Gabapentin has non-linear pharmacokinetics which limit its clinical effectiveness. The absorption of gabapentin occurs by L-amino acid transport system through a low-capacity nutrient transporter expressed in a narrow part of the upper small intestine. This is a carrier-mediated and saturable transport system leading to dose-dependent pharmacokinetics of gabapentin- as the dose increases, the bioavailability decreases.

Based on Kirby's enzyme model, three gabapentin prodrugs were proposed. They are expected to have higher and predictable bioavailability, in contrast to gabapentin, as a result of improving passive absorption. Moreover, the proposed prodrugs can be used in different dosage forms due to their potential solubility in organic and aqueous media. The prodrugs were synthesized and characterized by melting point, fourier transform infrared spectroscopy, proton nuclear magnetic resonance spectroscopy and liquid chromatography-mass spectrometry analytical techniques to guarantee pure gabapentin prodrugs. Hydrolysis of gabapentin prodrugs was investigated using high-performance liquid chromatography at constant temperature (37°C) using different buffer pHs, namely, 0.1N HCl, pH 3, pH 6.8 and pH 7.4 to resemble the physiological environments in the human body. Furthermore, *in silico* prediction of physiochemical parameters, absorption, distribution, metabolism, excretion, toxicity, and blood-brain barrier permeability for the three synthesized gabapentin prodrugs were studied.

Gabapentin prodrug 1 experimental half-life values in 0.1N HCl, buffer pH's 3, 6.8 and 7.4 were 16.57, 17.76, 101.91, and 119.48 hours, respectively.

Gabapentin prodrug 2 was hydrolyzed into its parent drug in 0.1N HCl, buffer pH's 3, 6.8, and 7.4 with experimental half-life values of 20.3, 22.70, 130.75 and 277.2 hours, respectively. However, gabapentin prodrug 3 was extremely insoluble in acidic environment and completely stable at pH 6.8 and pH 7.4. The *in silico* results revealed that all the synthesized gabapentin prodrugs comply with Lipinski's rule of five, have good and favorable pharmacokinetic properties, have positive central nervous system permeability, and none of the prodrugs had high risk of toxicity.

Three gabapentin prodrugs were synthesized and characterized and their *in vitro* intraconversion to their parent drugs showed that half-life was primarily affected by the pH of the medium, the distance between the two reactive centers, and the pka of the linker. *In vivo* pharmacokinetic studies will be done for both gabapentin prodrug 1-2 in order to determine the bioavailability and the duration of action of the tested prodrugs.

## Table of Contents

No.	Theme	Page
	<b>Declaration</b>	<b>i</b>
	<b>Acknowledgment</b>	<b>ii</b>
	<b>Abstract</b>	<b>iii</b>
	<b>Table of Contents</b>	<b>v</b>
	<b>List of Tables</b>	<b>ix</b>
	<b>List of Schemes</b>	<b>x</b>
	<b>List of Figures</b>	<b>xi</b>
	<b>List of Abbreviations</b>	<b>xiv</b>
	<b>Chapter One</b>	<b>2</b>
<b>1.</b>	<b>Introduction</b>	<b>2</b>
1.1	Neuropathic pain	2
1.1.1.	Types of neuropathic pain:	2
1.1.2.	Pharmacologic treatment of neuropathic pain:	4
1.2	Epilepsy	7
1.3	Restless leg syndrome (RLS)	8
1.4	Gabapentin	9
1.5	Prodrug	9
1.5.1.	Application of prodrug approach:	10
1.5.2.	Enzymatically versus chemically bioactivation:	12

1.6	Problem statement	14
1.7	Thesis objectives	15
1.7.1.	General objectives:	15
1.7.2.	Specific objectives:	16
1.8	Research questions	16
	<b>Chapter Two:</b>	<b>18</b>
<b>2.</b>	<b>Literature Review</b>	<b>18</b>
2.1	Novel gabapentin prodrugs classified according to their transport target	19
2.1.1.	Gabapentin prodrug that targets high capacity nutrient transporters:	19
2.1.2.	Gabapentin prodrugs that target the human apical sodium-dependent bile acid transporter (hASBT):	21
2.2	Enzyme models	23
	<b>Chapter Three</b>	<b>28</b>
<b>3.</b>	<b>Experimental part</b>	<b>28</b>
3.1	Part one	28
3.1.1.	Chemicals and instrumentation:	28
3.2	Part two	28
3.2.1.	Synthesis of gabapentin prodrugs:	32
3.3	Part three	37
3.3.1.	Kinetic methods:	37

3.4	Part four	40
3.4.1.	<i>In silico</i> prediction of physicochemical parameters, drug-likeness, ADMET for the synthesized gabapentin <b>ProD 1-3</b> :	40
3.4.2.	<i>In silico</i> prediction of BBB permeability of the synthesized gabapentin <b>ProD 1-3</b> :	41
	<b>Chapter Four</b>	43
<b>4.</b>	<b>Results and Discussion</b>	43
4.1	Gabapentin standard and prodrugs characterization using different analytical techniques	44
4.1.1.	Melting point, FT-IR, <sup>1</sup> H-NMR and LC-MS analysis of gabapentin standard:	44
4.1.2.	Melting point, FT-IR, <sup>1</sup> H-NMR and LC-MS analysis of gabapentin <b>ProD 1</b> :	46
4.1.3.	Melting point, FT-IR, <sup>1</sup> H-NMR and LC-MS analysis of gabapentin <b>ProD 2</b> :	48
4.1.4.	Melting point, FT-IR, <sup>1</sup> H-NMR and LC-MS analysis of gabapentin <b>ProD 3</b> :	51
4.2	Hydrolysis studies	53
4.2.1.	<i>In vitro</i> intraconversion of gabapentin <b>ProD 1-3</b> to their parent drug:	55
4.3	<i>In silico</i> prediction of physicochemical parameters, drug-likeness and CNS like properties for gabapentin <b>ProD 1-3</b>	73
4.3.1.	Drug-likeness:	73

4.3.2. Molecular lipophilicity:	74
4.3.3. Distribution coefficient ( $\log D$ ):	74
4.3.4. Aqueous solubility ( $\log S$ ):	75
4.3.5. <i>In silico</i> prediction of BBB permeability and $\log BB$ :	75
4.4 <i>In silico</i> ADMET prediction	78
<b>Chapter Five</b>	<b>80</b>
<b>5. Conclusion and Future directions</b>	<b>80</b>
5.1 Conclusion	80
5.2 Future directions	81
<b>References</b>	<b>82</b>
المخلص بالعربية	93

## List of Tables

<b>Table No.</b>	<b>Theme</b>	<b>Page</b>
<b>Table 4-1</b>	The $k_{\text{obs}}$ value and $t^{1/2}$ for the intraconversion of <b>ProD 1</b> in 0.1N HCl, pH 3, pH 6.8, and pH 7.4.	<b>72</b>
<b>Table 4-2</b>	The $k_{\text{obs}}$ value and $t^{1/2}$ for the intraconversion of <b>ProD 2</b> in 0.1N HCl, pH 3, pH 6.8, and pH 7.4.	<b>72</b>
<b>Table 4-3</b>	The $k_{\text{obs}}$ value and $t^{1/2}$ for the intraconversion of <b>ProD 3</b> in 0.1N HCl, pH 3, pH 6.8, and pH 7.4.	<b>72</b>
<b>Table 4-4</b>	Physiochemical properties and drug-likeness of the gabapentin and its synthesized prodrugs.	<b>76</b>
<b>Table 4-5</b>	CNS like properties for gabapentin and its synthesized prodrugs.	<b>77</b>
<b>Table 4-6</b>	ADMET prediction for <b>ProD 1</b> (a), <b>ProD 2</b> (b), and <b>ProD 3</b> (c).	<b>78</b>

## List of Schemes

<b>Scheme No.</b>	<b>Theme</b>	<b>Page</b>
<b>Scheme 3-1</b>	Gabapentin <b>ProD 1</b> ; synthesis scheme for the formation of two diastereomers of gabapentin <b>ProD 1</b> .	<b>34</b>
<b>Scheme 3-2</b>	Gabapentin <b>ProD 2</b> ; synthesis scheme for the formation of gabapentin <b>ProD 2</b> .	<b>35</b>
<b>Scheme 3-3</b>	Gabapentin <b>ProD 3</b> ; synthesis scheme for the formation of two diastereomers of gabapentin <b>ProD 3</b> .	<b>36</b>

## List of Figures

<b>Figure No.</b>	<b>Theme</b>	<b>Page</b>
<b>Figure 1-1</b>	Chemical structure of gabapentin (a), pregabalin (b), and GABA (c).	7
<b>Figure 2-1</b>	Chemical structure of gabapentin enacarbil.	20
<b>Figure 2-2</b>	Chemical structure of five gabapentin prodrugs that target the hASBT.	22
<b>Figure 2-3</b>	Chemical structures of Kemp's acid amides <b>1-11</b> .	24
<b>Figure 2-4</b>	Acid-catalyzed hydrolysis of N-alkylmaleamic acids <b>1-9</b> .	24
<b>Figure 2-5</b>	Acid-catalyzed hydrolysis of gabapentin <b>ProD 1</b> .	25
<b>Figure 2-6</b>	Acid-catalyzed hydrolysis of gabapentin <b>ProD 2</b> .	26
<b>Figure 2-7</b>	Acid-catalyzed hydrolysis of gabapentin <b>ProD 3</b> .	26
<b>Figure 4-1</b>	FT-IR spectrum of gabapentin.	44
<b>Figure 4-2</b>	<sup>1</sup> H-NMR spectrum of gabapentin, in CD <sub>3</sub> OD.	45
<b>Figure 4-3</b>	+ESI-LC-MS spectrum of gabapentin.	45
<b>Figure 4-4</b>	FT-IR spectrum of <b>ProD 1</b> .	47
<b>Figure 4-5</b>	<sup>1</sup> H-NMR spectrum of <b>ProD 1</b> , in CD <sub>3</sub> OD .	47
<b>Figure 4-6</b>	+ESI-LC-MS spectrum of <b>ProD 1</b> .	47
<b>Figure 4-7</b>	FT-IR spectrum of <b>ProD 2</b> .	49
<b>Figure 4-8</b>	<sup>1</sup> H-NMR spectrum of <b>ProD 2</b> , in CD <sub>3</sub> OD.	49
<b>Figure 4-9</b>	-ESI-LC-MS spectrum of <b>ProD 2</b> (Full scan mode).	50

<b>Figure 4-10</b>	-ESI-LC-MSMS spectrum of <b>ProD 2</b> (Product ion scan mode).	<b>50</b>
<b>Figure 4-11</b>	FT-IR spectrum of <b>ProD 3</b> .	<b>52</b>
<b>Figure 4-12</b>	<sup>1</sup> H-NMR spectrum of <b>ProD 3</b> , in CD <sub>3</sub> SOCD <sub>3</sub> .	<b>52</b>
<b>Figure 4-13</b>	+ESI-LC-MS spectrum of <b>ProD 3</b> .	<b>53</b>
<b>Figure 4-14</b>	Calibration curves for <b>ProD 1</b> (a), <b>ProD 2</b> (b), and <b>ProD 3</b> (c)	<b>54</b>
<b>Figure 4-15</b>	Chromatograms showing gabapentin standard (a) and both linker 1 diastereomers (b) at gabapentin <b>ProD 1</b> HPLC conditions.	<b>58</b>
<b>Figure 4-16</b>	Chromatograms showing the intraconversion of <b>ProD 1</b> at 0.1 NHCl after 15 min (a) and after 72 hrs (b).	<b>59</b>
<b>Figure 4-17</b>	Chromatograms showing the intraconversion of <b>ProD 1</b> at pH 3 after 9 hrs (a) and at end of the reaction (b).	<b>60</b>
<b>Figure 4-18</b>	Chromatograms showing the intraconversion of <b>ProD 1</b> at pH 6.8 after 24 hrs (a) and after 240 hrs (b).	<b>61</b>
<b>Figure 4-19</b>	Chromatograms showing the intraconversion of <b>ProD 1</b> at pH 7.4 after 30 hrs (a) and after 240 hrs (b).	<b>62</b>
<b>Figure 4-20</b>	Chromatograms showing gabapentin standard at gabapentin <b>ProD 2</b> HPLC conditions.	<b>63</b>
<b>Figure 4-21</b>	Chromatograms showing linker 2 standard at pH 0.1N HCl and pH 3 (a) and pH 6.8 and 7.4 (b) at gabapentin <b>ProD 2</b> HPLC conditions.	<b>63</b>

<b>Figure 4-22</b>	Chromatograms showing the intraconversion of <b>ProD 2</b> at pH 0.1 N HCl after 1 hr (a) and after 73 hrs (b).	<b>64</b>
<b>Figure 4-23</b>	Chromatograms showing the intraconversion of <b>ProD 2</b> at pH 3 after 2 hrs (a) and after 79 hrs (b).	<b>65</b>
<b>Figure 4-24</b>	Chromatograms showing the intraconversion of <b>ProD 2</b> at pH 6.8 after 1 hr (a) and after 380 hrs (b).	<b>66</b>
<b>Figure 4-25</b>	Chromatograms showing the intraconversion of <b>ProD 2</b> at pH 7.4 after 5 hrs (a) and after 355 hrs (b).	<b>67</b>
<b>Figure 4-26</b>	Chromatograms showing gabapentin standard (a) and linker 3 diastereomers (b) at gabapentin <b>ProD 3</b> HPLC conditions.	<b>68</b>
<b>Figure 4-27</b>	Chromatograms showing the stability of <b>ProD 3</b> at pH 7.4 after 1 hr (a) and after 168 hrs (b).	<b>69</b>
<b>Figure 4-28</b>	First order hydrolysis plot for both diastereomers of <b>ProD 1</b> in 0.1N HCL (a), buffer pH 3 (b), buffer pH 6.8 (c), and buffer pH 7.4 (d).	<b>70</b>
<b>Figure 4-29</b>	First order hydrolysis plot for <b>ProD 2</b> in 0.1N HCl (a), buffer pH 3 (b), buffer pH 6.8 (c), and buffer pH 7.4 (d).	<b>71</b>
<b>Figure 4-30</b>	BBB permeability prediction for <b>ProD 1</b> (a), <b>ProD 2</b> (b), and <b>ProD 3</b> (c)	<b>77</b>

## List of Abbreviations

ADMET	Absorption, distribution, metabolism, excretion and toxicity.
BBB	Blood-brain barrier
Caco 2	Colorectal adenocarcinoma cell lines
CDCA	Chenodeoxycholic acid
CD <sub>3</sub> OD	Deuterated methanol
CNS	Central nervous system
CYP	Cytochrome P450
Da	Dalton
d	Doublet
ddd	Doublet of doublet of doublets
DMSO-d <sub>6</sub>	Deuterated dimethyl sulfoxide
dq	Doublet of quartets
dtd	Doublet of triplet of doublets
ESI	Electrospray ionization
FT-IR	Fourier transform infrared spectrophotometer
hASBT	Human apical sodium-dependent bile acid transporter
HCl	Hydrochloric acid
HIA	Human intestinal absorption
HLB	Hydrophilic lipophilic balance
hrs	Hours
HPLC	High-performance liquid chromatography
GABA	Gamma-aminobutyric acid
K <sub>obs</sub>	The observed rate constant of hydrolysis
LC-MS	Liquid chromatography–mass spectrometry
Log <i>D</i>	Distribution coefficient
Log <i>P</i>	partition coefficient
Log <i>S</i>	Aqueous solubility
m	Multiplet
ml	Milliliter
mmol	Millimole
NaOH	Sodium hydroxide
PDA	Photodiode array
Pgp	P-glycoprotein
pH	potential of hydrogen
ppm	Part per million
ProD 1	Prodrug 1
ProD 2	Prodrug 2
ProD 3	Prodrug 3
PSA	Polar surface area
q	Quartet
RLS	Restless leg syndrome
s	Singlet
t	Triplet
TCA	Tricyclic antidepressants
THF	Tetrahydrofuran
TPSA	Topological Polar Surface Area
Å	Angstrom
R <sup>2</sup>	Coefficient of determination
<i>t</i> <sub>1/2</sub>	Half-life
<sup>1</sup> H-NMR	Proton nuclear magnetic resonance spectroscopy
0.1N HCl	Normalized hydrochloric acid

# **Chapter one**

## **Introduction**

## **Chapter one**

### **1. Introduction**

#### **1.1 Neuropathic pain**

Neuropathic pain is triggered by damage of the somatosensory nervous system affecting both its function and structure and leading to sudden onset of pain as well as pathological amplification of responses to innocuous and noxious stimuli [1]. It is commonly described as pricking, tingling, burning, coldness, itching, or stabbing [2-4]. Many animal studies of a neuropathic pain model showed alteration of voltage-gated sodium and/or potassium channels, and increases in transient receptor potential vanilloid 1 [5-7]. Also, the loss of gamma-aminobutyric acid (GABA) in the dorsal root ganglia after nerve damage contributes to the exaggerated response of nociceptive nerves of the spinal dorsal root ganglia [6].

It is estimated to distress millions of people worldwide [8-10], and also has a significant effect on health-related quality of life and is associated with high economic burden for the individual and society [11,12].

##### **1.1.1. Types of neuropathic pain:**

Neuropathic pain may result from dysfunctions of the central nervous system (CNS) or the peripheral nervous system. Therefore, neuropathic pain can be classified into central, peripheral, or mixed (central and peripheral ) neuropathic pain [13].

Central neuropathic pain frequently generates from spinal cord injury, stroke, or multiple sclerosis [13,14]. Peripheral neuropathic pain results from a multitude of conditions, including diabetes and other metabolic diseases, mechanical trauma, human immunodeficiency virus-related neuropathies, herpes zoster infection, neurotoxic chemicals, nutritional deficiencies, immune-mediated dysfunctions or tumor invasion [13,15,16].

While there are many types of neuropathic pain according to the cause of nerve injury, such as the aforementioned, common types include:

#### **1.1.1.1. Diabetic neuropathy:**

Diabetic neuropathy is a serious and most frequent chronic complication of diabetes mellitus [17]. Chronic hyperglycemia results in activation of several metabolic pathways in the peripheral nervous system, including increased activity of polyol pathway in neurons and Schwann cells [18], and increased protein kinase C activity. These metabolic disturbances induced oxidative stress, which is a mediator of hyperglycemia causing sensory neuron injury and consequently diabetic neuropathy [19].

#### **1.1.1.2. Post-herpetic neuralgia:**

Post-herpetic neuralgia is chronic pain caused by virus-induced nerve injury. It is the most common complication of herpes zoster and frequently results in significant reduction in the patient's health-related quality of life [20]. Approximately 20–35% of the population will develop herpes zoster in their life [21,22].

About 10-30% of individuals with herpes zoster will experience post-herpetic neuralgia [23,24]. It is well known that herpes zoster affects the central and peripheral nervous systems [2].

#### **1.1.1.3. Trigeminal neuralgia:**

Trigeminal neuralgia is a chronic, painful disorder involving the trigeminal nerve. There are two divided trigeminal nerves, which carry sensation from face to brain, one on each side of the face. There are two types: typical and atypical trigeminal neuralgia [26]. The typical form is characterized by episodes of sudden, severe pain on one side of the face which last for seconds and up to a few minutes. The atypical form is characterized by less severe constant burning pain. The same person may experience both forms [27]. Most frequently the trigeminal neuralgia is induced by demyelination of trigeminal sensory fibers. The demyelination of trigeminal nerve root is usually caused by compression by an overlying artery or vein, multiple sclerosis, and compressive masses in the posterior fossa [28].

#### **1.1.2. Pharmacologic treatment of neuropathic pain:**

Neuropathic pain is commonly nonresponsive to typical analgesics [29]. Moreover, there is no evidence that refutes or supports the efficacy of paracetamol and non-steroidal anti-inflammatory drugs for the management of neuropathic pain [30]. On the other hand, moderate to very low evidence demonstrates the efficacy of high concentration topical capsaicin (8%) to treat post-herpetic neuralgia, human immunodeficiency virus neuropathy, and painful diabetic neuropathy [31].

Moreover, according to a Cochrane review in 2018, there was no convincing evidence that supports the efficacy of opioids for the management of neuropathic pain [32-34]. In addition, there is uncertain evidence for the benefit from low concentration topical capsaicin or a topical lidocaine patch for neuropathic pain [35,36]. However, there is strong evidence for the efficacy and recommendations for the use of these three drug classes as first-line therapy in neuropathic pain [37]: the serotonin-nor-epinephrine reuptake inhibitors such as duloxetine [38-40], tricyclic antidepressants (TCAs), particularly amitriptyline [41], and the calcium channel alpha-2-delta ligands gabapentin and pregabalin were also recommended [42-44].

#### **1.1.2.1. Tricyclic antidepressants:**

TCAs have demonstrated analgesic efficacy in both depressed and non-depressed patients with neuropathic pain [45]. The major advantages of TCAs are their once-daily dosing, low cost, and favorable effects on depression, which is a common complication of neuropathic pain [46]. However, the main drawback of TCAs is the risk of anticholinergic side effects and orthostatic hypotension [47]. In addition, cardiac toxicity is another disadvantage of TCAs, therefore, it is recommended to use TCAs with caution in patients with cardiac disease [48,49].

#### **1.1.2.2. Selective serotonin and nor-epinephrine reuptake inhibitors:**

In many randomized clinical studies, two selective serotonin and nor-epinephrine reuptake inhibitors duloxetine, and venlafaxine have demonstrated efficacy in patients with peripheral neuropathic pain [50]. Duloxetine efficacy has been demonstrated to be continued over one year in painful diabetic peripheral neuropathy [51].

The biggest advantages of duloxetine are its once-daily dosing and that it effectively treats depression [52]. The most common reported side effects of duloxetine were nausea, dry mouth, fatigue, dizziness, and constipation [53].

Venlafaxine also has demonstrated efficacy in diabetic peripheral neuropathy and polyneuropathies of variant causes, but not in post-herpetic neuralgia [54]. It should be used with caution in patients with cardiovascular disease since it has been shown to be cardiotoxic in a small number of patients [55]. Many studies demonstrated a relationship between antidepressant treatment and thoughts of suicide. Therefore, concerns regarding the risks of TCAs and selective serotonin and nor-epinephrine reuptake inhibitors must be balanced versus the benefits in patients with neuropathic pain [56,57].

#### **1.1.2.3. Calcium channel alpha 2-delta ligands:**

In spite of gabapentin and pregabalin being structural analogs to GABA, (see Figure 1-1), they have no effect on the GABAergic system. They bind to voltage-gated calcium channels alpha 2-delta-1 subunit and antagonize it, inhibiting the release of excitatory neurotransmitters.

Both medications have been shown to be efficacious in many neuropathic pain conditions [58,59]. However, post-marketing surveillance has noted an increasing number of reports of heart failure in patients using pregabalin, but not gabapentin [60-62].

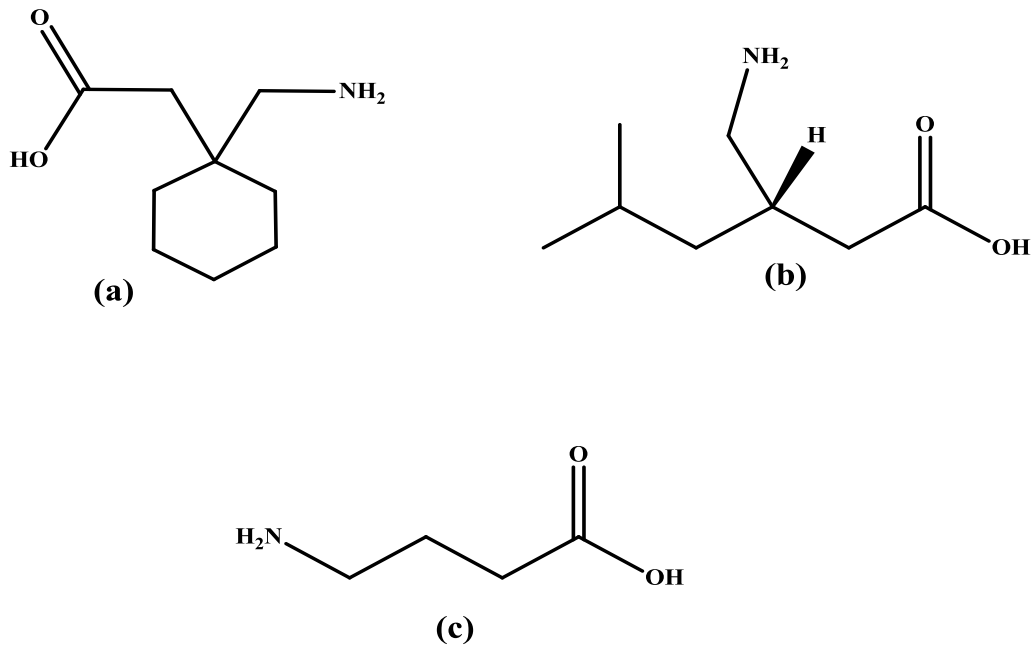


**Figure 1-1:** Chemical structure of gabapentin (a), pregabalin (b), and GABA (c).

## 1.2 Epilepsy

Epilepsy is a common, non-contagious, chronic, neurological, and heterogeneous collection of disorders affecting about 65 million people globally [63]. It is characterized by repeated incident of involuntary movements and unusual sensations accompanied by loss of awareness or not. The resulting recurrent seizure can be classified into either focal (partial) including only part of the body, or generalized, involving entire body which constitutes many types such as absence, atonic, myoclonic, and tonic-clonic seizures [64].

There is evidence from a review including 91 articles on gabapentin that gabapentin has efficacy as mono-therapy in adults and adolescents with newly recognized partial or mixed seizure diseases [65, 66]. Moreover, the discontinuation rate as a result of side effects was lower among patients on higher doses of gabapentin (13.5%) than those on carbamazepine (24%) [65].

### **1.3 Restless leg syndrome (RLS)**

RLS is a common neurological disease which is characterized by an urgent need to move the legs to alleviate unpleasant, not usually painful, and uncomfortable sensations [67]. The symptoms appear during the night or on rest particularly when lying or sitting [68]. It is divided into idiopathic and symptomatic (secondary) forms of RLS with the symptomatic form being associated with e.g. Parkinson's disease, iron deficiency, uremia, pregnancy, or chronic renal failure [68]. In 2016, evidence-based recommendations for the treatment of RLS were established. The alpha 2-delta ligands such as pregabalin and gabapentin were recommended for initial RLS management; these medications are effective and have a low risk of RLS augmentation [2]. Although dopaminergic drugs like levodopa and dopamine agonists are effective over the short-term, their efficacy declines in many patients over time, and/or augmentation develops [69].

## 1.4 Gabapentin

Gabapentin is 1-(aminomethyl)cyclohexaneacetic acid structurally resembling GABA, an inhibitory neurotransmitter that was shown to have a role in managing seizure states [70]. It antagonizes voltage-gated calcium channels by binding to them [71]. It is a zwitterion with two pKa values:  $pK_{a1} = 3.68$  (carboxylic acid) and  $pK_{a2} = 10.70$  (primary amine) [72], not metabolized by human and thus, excreted renally unchanged, has a short half-life ( $t_{1/2}$ ), and has non-linear pharmacokinetic which limits its clinical effectiveness [73]. Therefore, its bioavailability differs inversely with dose. For example, the bioavailability of a 300-mg dose is roughly 60%, while that of a 600-mg dose is roughly 40%. When the dose is tripled from 300 to 900 mg, its maximum concentration increases less than three times as a consequence of dose-dependent saturable absorption [71]. Additionally, the absorption of gabapentin varies from patient to patient [71]. Gabapentin first received approval for use as an anti-epileptic medication in 1993 [74]. Then in 2002, it received approval as a treatment for post-herpetic neuralgia [74]. Now, it has approval for the treatment of several types of neuropathic pain, epilepsy and RLS [69]. It is well tolerated but can cause dose-related dizziness and sedation [75].

## 1.5 Prodrug

The term ‘prodrug’ was first introduced by Albert in 1958 as a pharmacologically inactive moiety that undergoes conversion to its active form by metabolic and/or chemical processes prior to their therapeutic activity [76,77].

This term has been successfully used to alter the physicochemical, pharmacokinetic, and biopharmaceutical properties of the compound [78]. Thus, instead of designing and development of new chemical entities, which requires a lot of time and money [79], prodrug strategy can be used in order to modify the limitation and unfavorable physicochemical, biological, pharmacokinetic, and organoleptic properties of many existing medications [80].

About ten percent of all globally marketed drugs are considered as prodrugs. Between 2000 and 2008, twenty percent of drugs that were approved were shown to be prodrugs and when considering 2008 alone, 33% of all approved drugs were prodrugs. Consequently, in the present time, the prodrug strategy became progressively more popular and successful in pharmaceutical industries [81,82].

### **1.5.1. Applications of prodrug approach:**

#### **1.5.1.1. Enhancing permeability and absorption:**

Absorption and permeability have an important effect on drug efficacy: improving the lipophilicity of the parent drug, by masking polarly ionized or nonionized functional groups, will increase either topical or oral absorption, this can be achieved by the prodrug approach [83]. Hydrophilic functional groups on the parent drug like amino groups can be changed to more lipophilic groups, and these prodrugs are easily hydrolyzed to parent drugs [84,85]. Furthermore, increasing oral absorption can be achieved by designing prodrugs that have the same structural properties of substrates that are taken up by carrier-mediated transport [86].

#### **1.5.1.2. Improving solubility and dissolution rate of drugs:**

When dissolution is the rate-limiting step in the absorption of poorly aqueous soluble agents or when the parental or ophthalmic formulation of such agents is desired, hydrophilicity or water solubility is required [87]. Higher than thirty percent of newly discovered drugs have low aqueous solubility and have low bioavailability [88,89]. In order to solve this limitation, several formulation strategies including salt formation and solubilizing excipients have been applied. However, prodrugs provide another strategy to enhance the solubility of the compound in the aqueous media by binding ionizable or polar neutral groups [86,90-91].

#### **1.5.1.3. Taste masking:**

Bitterness and sourness of drugs are major reasons for a patient non-compliance and un-acceptance, particularly pediatrics. In order to overcome the bad taste of the drug, two approaches can be utilized: i) reducing drug solubility in saliva and ii) masking functional groups that are possibly responsible for the drug's attaching to taste receptors located on the tongue [92].

#### **1.5.1.4. Changing the distribution profile:**

In order to attain site-selective drug delivery, many efforts have been made to bind various macromolecular strategies and nanotechnologies, but these methods lack clinical success.

Today, the prodrug strategy is a promising site-selective drug liberation approach which utilizes endogenous enzymes and transporters of the target cell and tissue [86].

#### **1.5.1.5. Protecting from rapid metabolism:**

The beneficial effects of drugs can be impaired by extensive excretion and/or metabolic pathways. Oral bioavailability of many drug molecules is significantly reduced by first pass metabolism [93]. Therefore, many formulation such as sublingual and controlled release have been designed to overcome this drawback [94]. However, oral bioavailability can be increased by masking metabolically sensitive functional groups using prodrug strategy [95].

#### **1.5.2. Enzymatically versus chemically bioactivation:**

Prodrugs that are designed to be activated by natural enzymes such as esterases and amidases are susceptible to individual variation in the response to pharmacologic therapies due to genetic polymorphisms of these enzymes [96].

Recently, many studies have shown that the presence of functional genetic variants of carboxylesterases: carboxylesterase 1 and carboxylesterase 2 alters the pharmacokinetic and pharmacodynamic properties of several prodrugs [96]. Several studies suggested that the genetic variants of carboxylesterase 1 may be linked with increased plasma concentrations of clopidogrel and may elevate the risk of toxic or adverse side effects [96,97].

In addition, other studies demonstrated that genetic variants of carboxylesterase 1 and carboxylesterase 2 may decrease the activation of oseltamivir and irinotecan prodrugs, and obstruct prodrug activation, which may result in a decrease of the prodrugs' therapeutic effect [96,98-100]. Furthermore, seventy-five percent of enzymatically metabolized prodrugs are activated by cytochrome P450 enzymes [101], which are known to have genetic polymorphisms that lead to differing in prodrug effectivity and safety [102]. Moreover, the bioavailability and efficacy of prodrugs that are developed to liberate the active drugs by these natural enzymes may be reduced by premature hydrolysis during the absorption phase [103]. Consequently, the prediction of enzymatic hydrolysis of the prodrug becomes difficult and therefore clinical efficacy of the prodrugs will be unpredictable. Furthermore, bioconversion can be altered by a variety of factors like age, ethnicity, health, and gender [104-106].

Novel prodrugs for drugs having hydroxyl, phenol, or amine functional groups have been designed by employing recent computational process using molecular orbital and molecular mechanics methods. Most recently, Karaman's group have been computed many mechanisms of intramolecular methods for several enzyme models and utilized them for designing many prodrug linkers [107-110].

The conventional prodrug strategy was concentrated on affecting several physiochemical properties, whereas recent computational strategies work by designing prodrugs with a higher bioavailability than parent drugs by binding it with a suitable linker. The active drug will be released in a sustained manner when introduced to the physiological environment with the ability to control the release rate of the parent drug by binding the drug with different linkers [111].

## 1.6 Problem statement

Gabapentin has pharmacokinetic drawbacks which limit its clinical effectiveness. The absorption of gabapentin occurs by the L-amino acid transport system, due to its zwitterionic nature, through a low-capacity nutrient transporter expressed in a narrow part of the upper small intestine [73,112]. This is a carrier-mediated, and saturable transport system leading to the dose-dependent pharmacokinetics of gabapentin: as the dose increases, the bioavailability decreases [73]. For example, the bioavailability of gabapentin is approximately 60%, 47%, 34%, 33%, and 27% following 900, 1200, 2400, 3600, and 4800 mg per day taken in 3 divided doses, respectively [113,114]. All of these doses are within the recommended therapeutic dose range. For example, the recommended dose of gabapentin to treat epilepsy is 900 to 4800 mg divided three times per day [115]. Moreover, the saturable transport system led to variability of absorption of gabapentin from patient to patient [113].

As a consequence of these pharmacokinetic deficiencies of gabapentin, the prediction of its dose necessary to achieve an optimal therapeutic effect in a given patient is often difficult, and the desired treatment response may not be achieved. In addition, the short  $t_{1/2}$  of gabapentin (about 5–7 h) represents another limitation of its pharmacokinetics that necessitates frequent dosing which is a cause of noncompliance in epileptic patients and missed doses which can reduce clinical effectiveness [73,114].

On the other hand, the prodrug chemical strategy requiring enzyme catalysis has many disadvantages related to many intrinsic and extrinsic factors that can alter the catalysis process. Such as unpredictable clinical effects and safety of the most prodrug-activating enzymes owing to genetic polymorphisms, age-related physiological changes, or drug interactions [116].

Therefore, there is need to design new prodrugs of gabapentin that have potential for higher and predictable bioavailability than the current medication when given in different dosage forms, have the ability to be hydrolyzed to their parent drugs through intramolecular reaction and without any need for enzyme catalysis, and have the ability to liberate gabapentin in a controlled manner to solve the frequent dosing problem of gabapentin.

## **1.7 Thesis objectives**

### **1.7.1. General objectives:**

The main aim of this research was to synthesize prodrugs of gabapentin that have the potential of higher bioavailability and linear pharmacokinetics and have the ability to be hydrolyzed chemically to gabapentin without the need for enzymes.

In order to obtain this objective, the gabapentin prodrugs' physicochemical properties must have the following: (i) to have a moderate hydrophilic-lipophilic balance (HLB) value; (ii) to be soluble in the physicochemical environment; (iii) to give upon chemical hydrolysis non-toxic by-products.

By having these properties, the following features are expected to be obtained: (i) high bioavailability and linear pharmacokinetic properties; (ii) predictable plasma levels; (iii) a chemically driven programmable release system that releases gabapentin in a sustained manner; and (iv) the capability to use these prodrugs in different dosage forms.

### 1.7.2. Specific objectives:

Specific objectives to our study were:

1. To synthesize gabapentin prodrugs having the potential for dose-independent and higher bioavailability than gabapentin through binding it to different linkers.
2. To characterize these prodrugs using different analytical techniques.
3. To carry out *in vitro* kinetic studies for the synthesized gabapentin prodrugs at different pHs resembling physiological media.
4. To study the physiochemical parameters, pharmacokinetics, drug-likeness, and toxicity properties of the synthesized gabapentin prodrugs by *in silico* computational software.
5. To predict the ability of the synthesized prodrugs to cross the blood-brain barrier (BBB) by *in silico* software.

### 1.8 Research questions

1. Would it be possible to bind gabapentin to the linkers through chemical synthesis?
2. Do the proposed gabapentin prodrugs have physiochemical features which could result in a high and dose-independent bioavailability?
3. Would the synthesized prodrugs have the ability to liberate, *in vitro*, gabapentin in a programmable release manner?
4. Do the synthesized gabapentin prodrugs have the potential to be designed in several dosage forms?
5. Do the synthesized prodrugs penetrate BBB and have a favorable physiochemical and drug-like properties?

## **Chapter Two**

### **Literature review**

## **Chapter two**

### **2. Literature review**

In 1973, Satzinger group began the GABA project to search for an epilepsy treatment. Their study was based on compensation of GABA to the brain by passive diffusion by preparing lipophilic GABA analogs because GABA itself can't penetrate the BBB when given systemically [117]. In 1975, Satzinger and co-workers prepared gabapentin and demonstrated its effectivity in many animal models of epilepsy. Despite that gabapentin has much higher lipophilicity when compared to GABA, it was shown later that it did not enter the CNS by passive diffusion as Satzinger and Hartenstien had initially envisioned [117]. In 1995, it was discovered that it penetrates the BBB by L-type amino acid transporter [118].

Surprisingly, gabapentin demonstrates little or no interaction with GABA receptors and does not appear to alter GABA uptake, synthesis, or metabolism as had been initially imagined [119]. Most recently, it demonstrated that it exerts its effects by binding to the alpha-2-delta-1 subunit of voltage-gated calcium channels and causes reduced calcium influx, decreasing the release of many excitatory neurotransmitters including glutamate [120]. This explained its effect as an anti-epileptic and analgesic of neuropathic and other conditions [120,121].

Later, pregabalin demonstrated its effectiveness for the treatment of epilepsy and neuropathic pain through the same mechanism of action as gabapentin, by coupling to the alpha-2-delta-1 subunit of voltage-gated calcium channels [58,122], but with higher and more predictable bioavailability [123].

However, gabapentin is less addictive than pregabalin. Unlike gabapentin, pregabalin is scheduled as a schedule V controlled substance [124]. Pregabalin use is associated with increased risk of heart failure a side effect that has not been appeared with the less potent calcium channel antagonist gabapentin [60,62]. In addition, in 2017, Agarwal *et al.* showed that gabapentin is significantly more efficacious than pregabalin in reducing pain in chronic pelvic pain syndrome patients [125]. Moreover, pregabalin, like gabapentin, has a short  $t_{1/2}$  so it is required to be taken in 2 or 3 divided doses daily [126,127].

Many attempts have been made to synthesize prodrugs of gabapentin in order to overcome its pharmacokinetic limitations (previously mentioned) which include dose-dependent pharmacokinetics for example, the bioavailability of a 300-mg dose is about 60% while that of a 600-mg dose is about 40% [128,129], high interpatient variability [113], and potentially ineffective drug exposure as a result of saturable gabapentin absorption that occurs only in a limited region of the small intestine by L-amino acid transport system through a low-capacity nutrient transporter [73,112]. Moreover, its short  $t_{1/2}$  requires frequent dosing leading to non-compliance in patients [114].

## **2.1 Novel gabapentin prodrugs classified according to their transporter target**

### **2.1.1. Gabapentin prodrug that targets high-capacity nutrient transporters:**

XP13512 [1-({[1-(2-methylpropanoyl)oxy]ethyl}oxy)carbonyl]amino}methyl)cyclohexyl] acetic acid)) is gabapentin enacarbil (Figure 2-1). It was synthesized as a gabapentin prodrug [130].



### **2.1.2. Gabapentin prodrugs that target the human apical sodium-dependent bile acid transporter (hASBT):**

An alternative approach employed by Polli and coworkers was coupling gabapentin to a natural substrate of a transporter to yield several novel prodrugs to enhance gabapentin absorption through targeting high-capacity membrane transport systems in the gut [129]. Since the main limitation in gabapentin absorption results from its zwitterionic nature and its facilitated uptake by low-capacity transporters [73], these prodrugs were designed to target hASBT with the same high affinity and high capacity as native bile acids [129]. hASBT belongs to the solute carrier genetic superfamily, it is considered as an essential carrier protein expressed in the intestine. It mediates the intestinal absorption of bile salts through enterohepatic circulation [134], and many studies suggested it as potential prodrug target [135].

Five prodrugs were synthesized to which gabapentin was linked to chenodeoxycholic acid (CDCA) (Figure 2-2). These prodrugs differed in ionic properties and the existence or lack of glutamic acid linker between gabapentin and the bile acid. Among these prodrugs, only two were found to be likely prodrugs that may elevate gabapentin absorption *via* hASBT uptake: CDCA-gabapentin and CDCA-glutamic acid-gabapentin methyl ester which they represented in Figure 2-2 as A and D compounds, respectively. These two prodrugs were tested for their inhibition and uptake properties. The inhibition study with taurocholate showed that the gabapentin conjugates are potent inhibitors, with strong interaction with the transporter. Based on this study, the researcher concluded that these both derivatives are novel prodrugs of gabapentin.

However, these two prodrugs were chemically stable but they degraded by a catalyst to gabapentin [129]. We need the prodrugs to be hydrolyzed chemically and not enzymatically because the activity of many prodrug activating enzymes may be varied due to: genetic polymorphisms, age-related physiological change and drug interactions. Therefore, the clinical response may be varied [116].

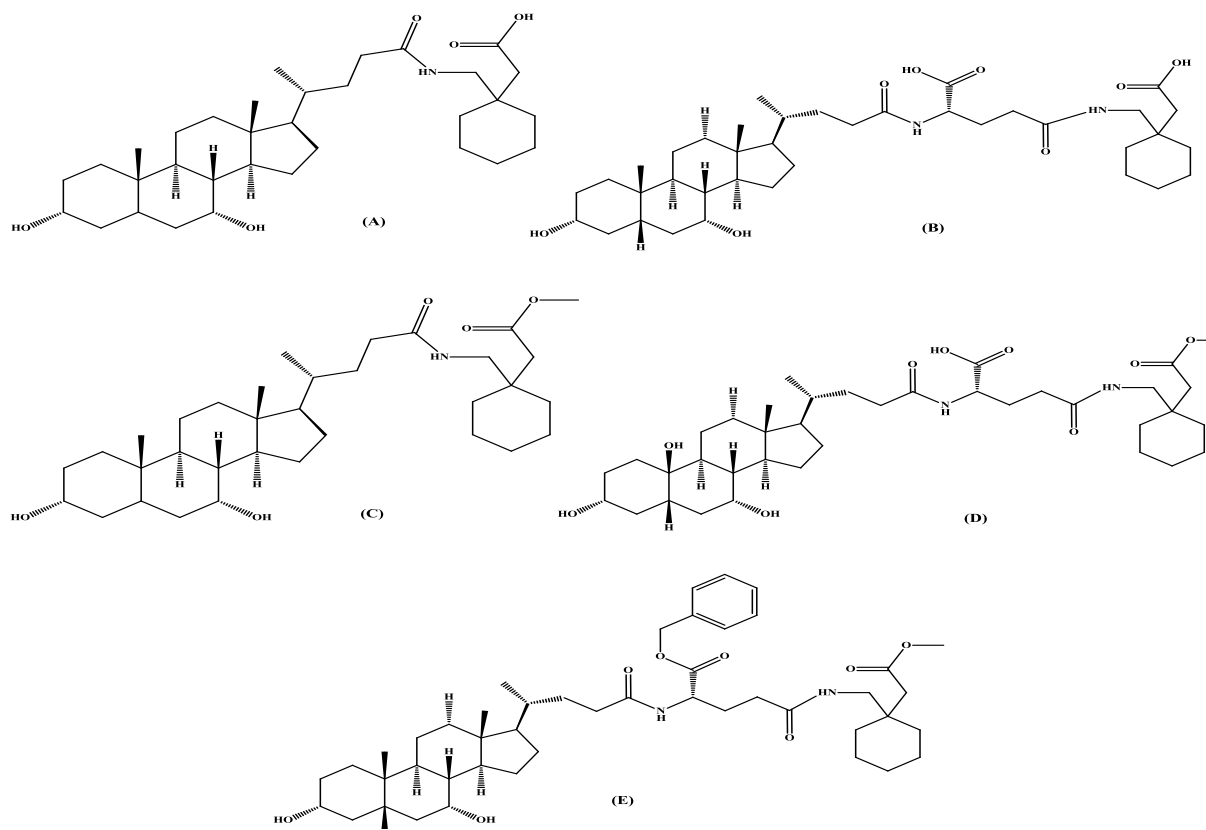


**Figure 2-2:** Chemical structure of five gabapentin prodrugs that target the hASBT.

## 2.2 Enzyme models

Prodrugs of gabapentin were utilized to provide gabapentin in adequate predictable concentrations and a controlled release manner. Although, some achievement has been obtained using diverse approaches in which, all synthesized gabapentin prodrugs are enzymatically converted to gabapentin, this prodrug chemical strategy requiring enzyme catalysis has several drawbacks as a result of several intrinsic and extrinsic factors. Drawbacks which can alter the transformation of the prodrug to its parent drug for instance; the activity of many prodrug-activating enzymes may differ as a result of age-associated physiological changes, genetic polymorphisms, or drug interactions, causing differences in therapeutic response [116,136-138]. However, no attempt was made to develop prodrugs of gabapentin using the chemical approach to release the parent drug in a predictable and programmable manner [139].

Therefore, there is need to synthesize new prodrugs of gabapentin with higher and dose-independent bioavailability which have the potential to release gabapentin in a sustained manner *via* intramolecular chemical conversion without the need for enzyme catalysis.

Karaman's group have explored a number of intramolecular processes to gain insight into enzyme catalysis, toward the development of prodrug linkers with improved bioavailability over existing medications using *ab initio* and density functional theory molecular orbital methods [140-156]. They studied the proton transfer reaction in some of Kemp's acid amide derivatives **1-11** (Figure **2-3**) by using enzyme models as potential linkers to be linked to amine-drugs [157].

Moreover, Kirby's group have studied the acid-catalyzed hydrolysis of N-alkylmaleamic acids **1-9** (Figure 2-4); they found that the intramolecular nucleophilic group is responsible for the amide bond cleavage [158].

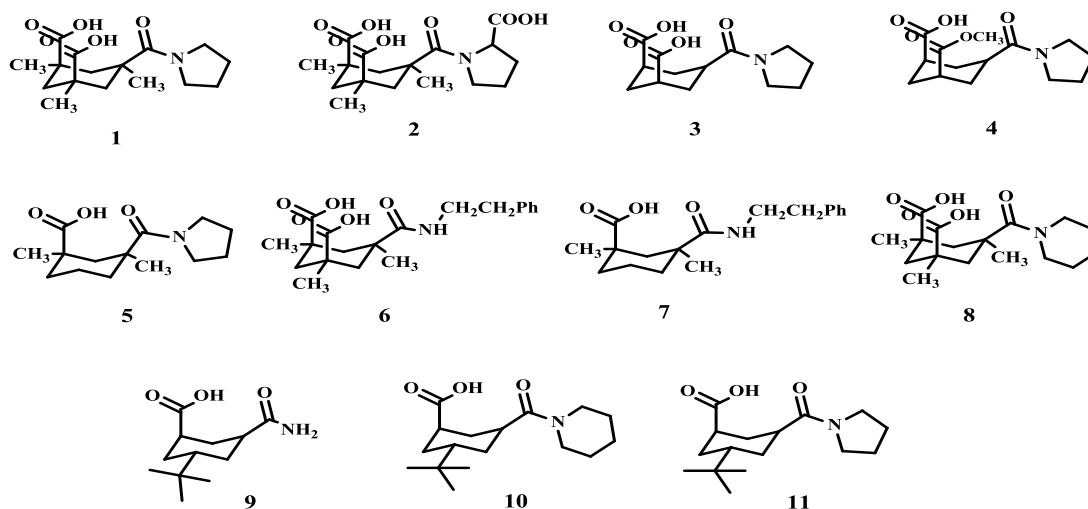


**Figure 2-3:** Chemical structures of Kemp's acid amides **1-11**.

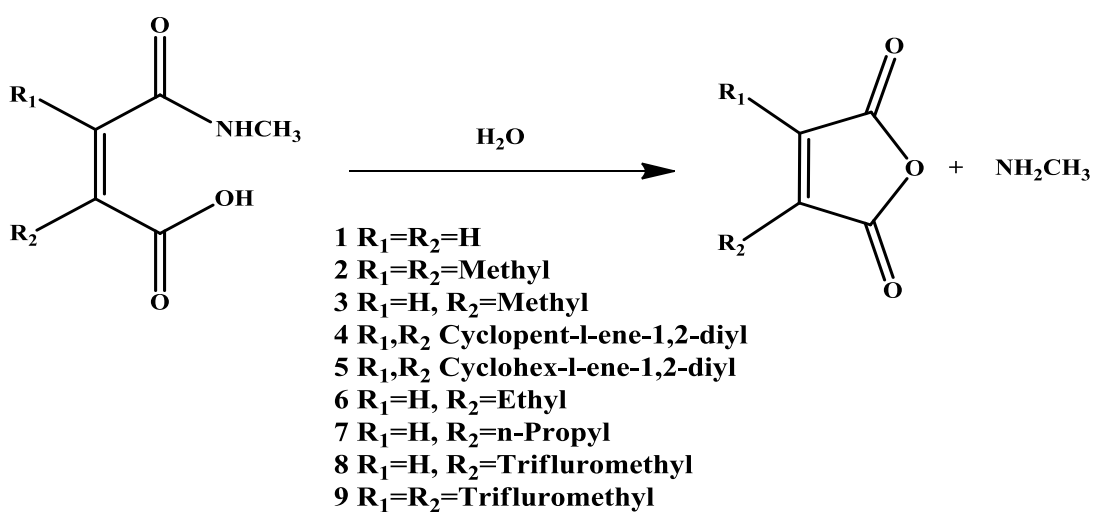


**Figure 2-4: Acid-catalyzed hydrolysis of N-alkylmaleamic acids 1-9.**

Based on density functional theory calculations of proton transfer mechanism of these acid amides, three gabapentin prodrugs were proposed (Figures 2-5 to 2-7). These proposed gabapentin prodrugs **1-3 (ProD 1-3)** have a modified HLB, due to the presence of both hydrophilic and lipophilic moieties. In addition, at physiological pH in the intestine and blood circulation, the calculated predominant form of gabapentin is the ionized form whereas **ProD 1-3** are predicted to exist in the free acid and ionic forms. Thus, gabapentin **ProD 1-3** were expected to have higher and more predictable bioavailability than gabapentin as a result of increased its passive absorption.

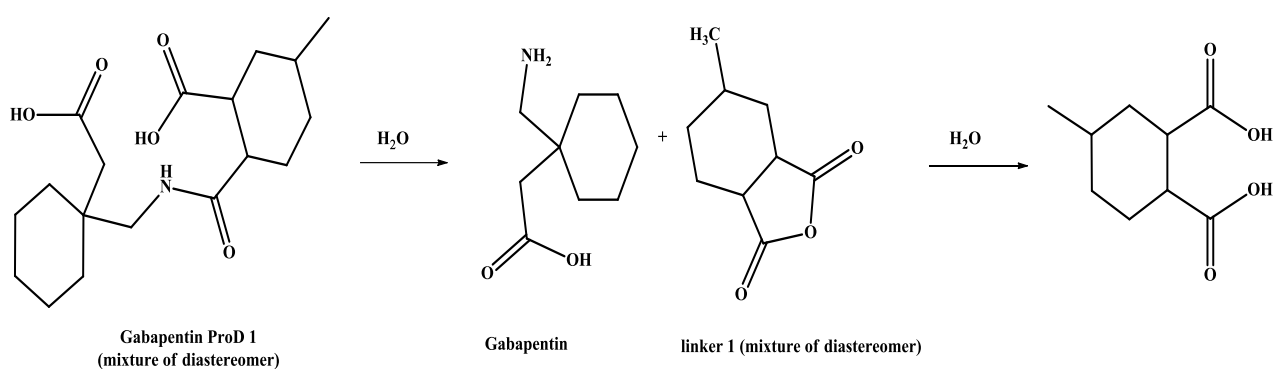


**Figure 2-5: Acid-catalyzed hydrolysis of gabapentin ProD 1.**

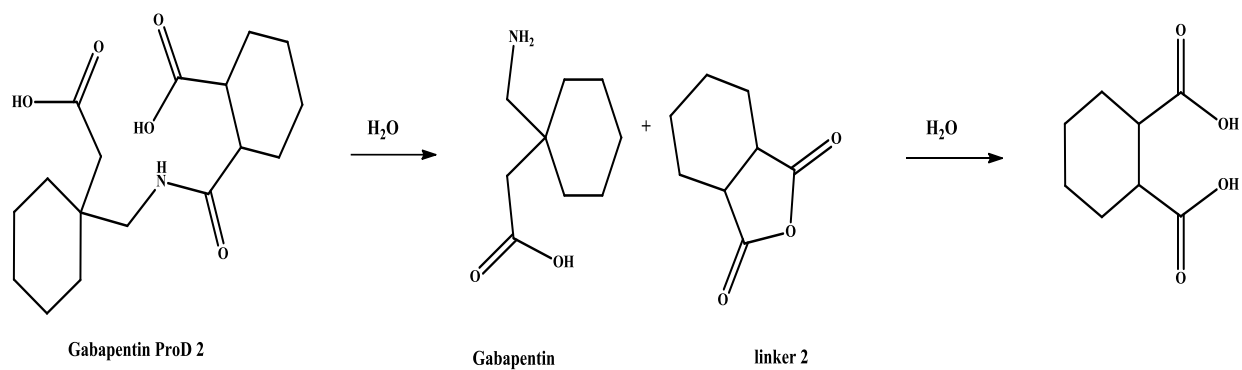


**Figure 2-6:** Acid-catalyzed hydrolysis of gabapentin **ProD 2**.

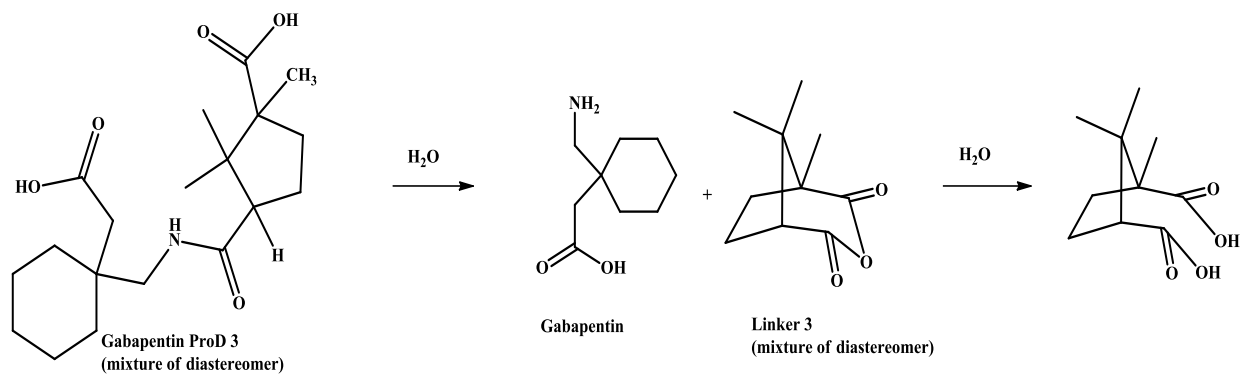


**Figure 2-7:** Acid-catalyzed hydrolysis of gabapentin **ProD 3**.

# **Chapter Three**

## **Experimental**

## Chapter Three

### 3. Experimental Part

This chapter consists of four main parts: Part one describes all material, chemicals, and instruments used in this study. The second is the synthetic part which concerns with the synthetic methods and identification of the synthesized prodrugs. Third one is the kinetic studies part that illustrates the specific preparations and analysis used to study gabapentin prodrugs intraconversion in different four potential of hydrogen (pH) solutions by the high-performance liquid chromatography (HPLC). The fourth part is an *in silico* prediction of the physiochemical parameters, drug-likeness, ADMET (absorption, distribution, metabolism, excretion, and toxicity) properties, and CNS penetrability of the synthesized prodrugs.

#### 3.1 Part one

##### 3.1.1. Chemicals and Instrumentation:

###### 3.1.1.1. Reagents:

A pure standard of gabapentin was obtained from Beit Jala Pharmaceutical Company. The diastereomeric mixture of hexahydro-4-methylphthalic anhydride, *cis*-1,2-cyclohexanedicarboxylic anhydride, mixture of diastereomers of camphoric acid anhydride, sodium hydroxide (NaOH) and thin layer chromatography were all purchased from Sigma Aldrich.

### **3.1.1.2. Solvents:**

Tetrahydrofuran (THF), hexane, chloroform, and diethyl ether were all obtained from Sigma Aldrich. Distilled water was obtained from a distillatory device available at Karaman's lab. HPLC grade solvents of methanol, acetonitrile, and water were purchased from J.T. Baker.

### **3.1.1.3. Instrumentation and substance identification:**

Chemical hazards fuming hood, hotplates, pH meter and rotary evaporator are available at Karaman's Lab in the Faculty of Pharmacy, Al-Quds University. The melting point and FT-IR were done at Beit Jala Pharmaceutical Company in Bethlehem. HPLC was done at Beit Jala Pharmaceutical Company in Bethlehem and at Jerusalem Pharmaceutical Company in Ramallah. Proton nuclear magnetic resonance spectroscopy ( $^1\text{H-NMR}$ ) was done at the Hebrew University. Liquid chromatography-mass spectroscopy (LC-MS) was done at Al-Quds University.

#### **3.1.1.3.1. pH meter:**

pH meter model HM-30G: TOA electronics<sup>TM</sup> was used to measure the pH values for all buffers and reaction media involved in this research.

### 3.1.1.3.2. FT-IR:

All infrared spectra (FTIR) were obtained from potassium bromide matrix(4000–400  $\text{cm}^{-1}$ ) using a Perkin-Elmer Precisely, Spectrum 100, FT-IR spectrometer.

### 3.1.1.3.3. HPLC:

HPLC measurements for gabapentin **ProD 1** were performed using Shimadzu prominence HPLC-Photodiode array (PDA) system, (Shimadzu Corp. Japan). The HPLC system consisted of a model LC-2030C 3D equipped with a PDA. Data acquisition and control of the gabapentin **ProD 1** were carried out using Lab solutions software. However, the HPLC measurements for the gabapentin **ProD 2** and **ProD 3** were performed using a Dionex HPLC system (USA). The data acquisition and control were performed using Chromeleon software.

Analytes were separated on a 4 mm x 250 mm, 5  $\mu\text{m}$  Purospher® RP-18 endcapped column in **ProD 1** kinetic study. However, for **ProD 2-3** kinetic studies, analytes were separated on a 4 mm x 250 mm, 5  $\mu\text{m}$  particle size C18 Phenomenex Luna® column.

#### 3.1.1.3.4. <sup>1</sup>H-NMR:

All <sup>1</sup>H-NMR spectra were conducted using the 500 MHz Varian NMR spectrometer. **ProD 1-2** samples were run in deuterated methanol (CD<sub>3</sub>OD), but **ProD 3** sample was run in deuterated dimethyl sulfoxide (DMSO-d<sub>6</sub>). For <sup>1</sup>H-NMR, chemical shifts are reported in parts per million (ppm, δ) downfield from tetramethylsilane. Spin multiplicities are described as doublet (d), doublet of doublets (ddd), doublet of quartets (dq), doublet of triplet of doublet (dtd), singlet (s), triplet (t), quartet (q), and multiplet (m). Data were processed on-line at [www.nmrdb.org](http://www.nmrdb.org).

#### 3.1.1.3.5. LCMS:

The synthesized prodrugs were subject to LCMS analysis in the electrospray ionization mode (ESI) using LC-MSMS instrument of Thermo Fisher scientific at Al-Quds University. LC-MS analysis for both **ProD 1** and **ProD 3** was performed in positive electrospray ionization mode(+ESI). **ProD 1** and **ProD 3** MS conditions were as follows: direct injection was utilized, flow rate equals 0.05 ml/min of 20% methanol and 80% water and 0.1% formic acid. Full scan of 100-1200 Dalton (Da), positive ion voltage of 3500 volts, ion transfer tube temperature of 325°C, vaporizer temperature of 275°C. **ProD 2** analysis was carried out in negative electrospray ionization mode(-ESI). The mobile phase was composed of 80% water, 20% methanol, and 0.1% formic acid. Both full scan and product ion scan modes were performed for **ProD 2**.

The MS conditions for full scanning mode for **ProD 2** were as follows: negative ion voltage was 2500 volts, ion transfer tube temperature was 320°C, full scan range was between 100-400 Da, quadrupole resolution was 0.7 full width at half maximum, and scan rate was 1000 Da per second. Product ion scan mode conditions for **ProD 2** were as follows: m/z scan range was between 150-400 Da, m/z precursor was 324 Da, quadrupole resolution was 0.7 full width at half maximum, scan rate was 1000 Da per second, collision energy was 15 volts, negative ion voltage was 2500 volts, ion transfer tube temperature was 320°C, and vaporizer temperature 275°C.

## 3.2 Part two

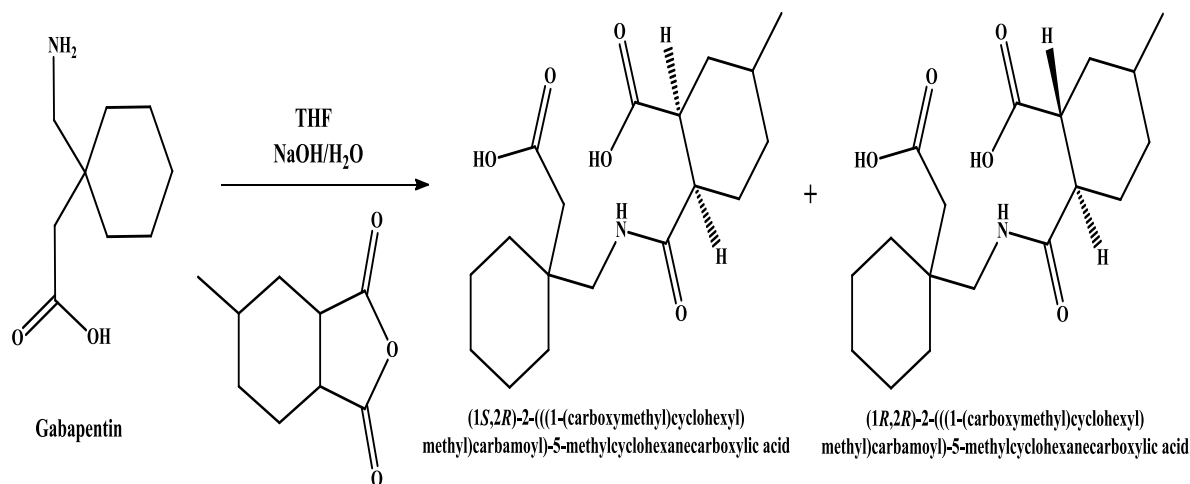
### 3.2.1. Synthesis of gabapentin Prodrugs:

Gabapentin **ProD 1** preparation: In a 250 milliliter (ml) round-bottom flask, 0.85g of gabapentin (5 millimole (mmol)) was dissolved in 50 ml THF, 0.20 g NaOH was dissolved in 50 ml THF. The resulting solution was stirred for 30 minutes, then (0.715 ml) 5 mmol of mixture of diastereomers of hexahydro-4-methylphthalic anhydride was slowly added to the reaction mixture and stirred at room temperature for 4 days. The reaction was monitored by thin layer chromatography which was performed on regular basis to check the reactions completion using chloroform and methanol (7:1) system as an eluent. The solvent was evaporated by the rotary evaporator and the resulting precipitate was washed with ethyl acetate and hexane, respectively. The white precipitate was dried at 37°C. The resulting yield was 93% (Scheme 3-1). Melting point is 110°C. The product consisted of two diastereomers of **ProD 1** with 89% and 11% for (1S, 2R) diastereomer and (1R, 2R) diastereomer of **ProD 1**, respectively, as revealed by HPLC.

(1S,2R) diastereomer of the **ProD 1**,  $^1\text{H-NMR}$  (500 MHz) (ppm,  $\delta$ )  $\text{CD}_3\text{OD}$  - 0.8797-0.8977 (d, 3H,  $\text{CH}_2\text{-CH-CH}_3$ ), 0.95-1.2 (m, 2H,  $\text{CH}_2\text{-CH}_2\text{-CH}$ ), 1.4006-1.4644 (m, 5H,  $\text{C-CH}_2\text{-CH}_2\text{-CH}_2\text{-CH}_2$ ,  $\text{CH}_2\text{-CH}_2\text{-CH}(\text{CH}_3)\text{-CH}_2$ ), 1.4940-1.5395 (m, 6H,  $\text{C-CH}_2\text{-CH}_2\text{-CH}_2\text{-CH}_2\text{-CH}_2$ ), 1.7649-1.810 (ddd, 2H,  $\text{CH}_2\text{-CH}_2\text{-CH-CH}_2\text{CH}$ ), 2.09-2.179 (q, 1H,  $\text{NH-C=O-CH-CH}(\text{CH}_2)\text{-COOH}$ ), 2.1733 (s, 2H,  $\text{C-CH}_2\text{-COOH}$ ), 2.2305-2.443 (dq, 2H,  $\text{NH-C=O-CH-CH}_2\text{CH}_2$ ), 3.02-3.08 (q, 1H,  $\text{NH-C=O-CH}(\text{CH})\text{-CH}_2$ ), 3.2662 (s, 2H,  $\text{C-CH}_2\text{NHC=O}$ ).

(1R,2R) diastereomer of the **ProD 1**,  $^1\text{H-NMR}$  (500 MHz) (ppm,  $\delta$ )  $\text{CD}_3\text{OD}$ - 0.9474-0.9660 (d, 3H,  $\text{CH}_2\text{-CH-CH}_3$ ), 1.07-1.2 (m, 2H,  $\text{CH}_2\text{-CH}_2\text{-CH}$ ), 1.4006-1.4644 (m, 5H,  $\text{C-CH}_2\text{-CH}_2\text{-CH}_2\text{-CH}_2$ ,  $\text{CH}_2\text{-CH}_2\text{-CH}(\text{CH}_3)\text{-CH}_2$ ), 1.4940-1.5395 (m, 6H,  $\text{C-CH}_2\text{-CH}_2\text{-CH}_2\text{-CH}_2\text{-CH}_2$ ), 1.808-1.862 (ddd, 2H,  $\text{CH}_2\text{-CH}_2\text{-CH-CH}_2\text{CH}$ ), 2.16-2.217 (q, 1H,  $\text{NH-C=O-CH-CH}(\text{CH}_2)\text{-COOH}$ ), 2.173 (s, 2H,  $\text{C-CH}_2\text{-COOH}$ ), 2.2305-2.443 (dq, 2H,  $\text{NH-C=O-CH-CH}_2\text{CH}_2$ ), 3.08-3.14 (q, 1H,  $\text{NH-C=O-CH}(\text{CH}_2)\text{-CH}$ ), 3.303 (s, 2H,  $\text{C-CH}_2\text{NHC=O}$ ).

IR ( $\text{KBr}/\nu_{\text{max}}\text{cm}^{-1}$ ) 1706.74 (C=O), 1646.82 (C=O), 1566.42 (C=O), 2926.55(OH), 2863.63(OH) and 3390.08 (NH).  $m/z$  340.19 Da  $[\text{M}+1]^+$ .

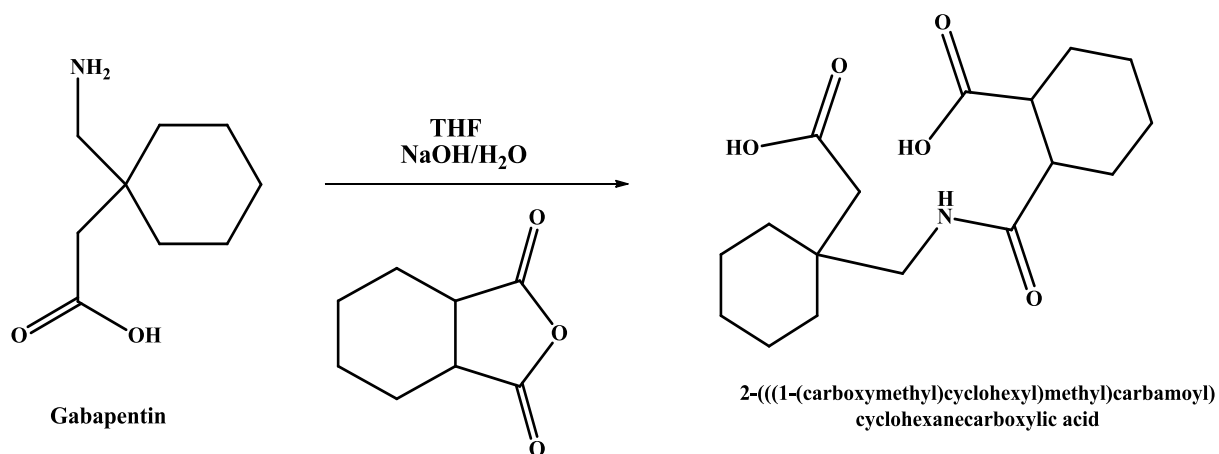


**Scheme 3-1:** Gabapentin **ProD 1**; synthesis scheme for the formation of two diastereomers of gabapentin **ProD 1**.

Gabapentin **ProD 2**: We followed the same procedure for gabapentin **ProD 1** but instead of using mixture of diastereomers of hexahydro-4-methylphthalic anhydride linker, *cis*-1,2-cyclohexanedicarboxylic anhydride was used (0.765g) 5 mmol (Scheme 3-2). The yield was 92%. Melting point is 180°C.

Gabapentin **ProD 2**,  $^1\text{H-NMR}$  (500 MHz) (ppm,  $\delta$ )  $\text{CD}_3\text{OD}$ - 1.3799-1.4253 (m, 8H, C- $\text{CH}_2\text{-CH}_2\text{-CH}_2\text{-CH}_2\text{-CH}_2$ , CH- $\text{CH}_2\text{-CH}_2\text{-CH}_2\text{-CH}_2\text{-CH}$ ), 1.4885-1.5291 (m, 4H, C- $\text{CH}_2\text{-CH}_2\text{-CH}_2\text{-CH}_2$ ), 1.59-1.67 (m, 2H, CH- $\text{CH}_2\text{-CH}_2\text{-CH}_2\text{-CH}_2\text{-CH}$ ), 1.7039-1.738 (m, 2H, CH- $\text{CH}_2\text{-CH}_2\text{-CH}_2\text{-CH}_2\text{-CH}$ ), 2.08 (q, 1H, CH- $\text{CH}(\text{CH}_2)\text{-COOH}$ ), 2.1026 (m, 2H, CH- $\text{CH}_2\text{-CH}_2\text{-CH}_2\text{-CH}_2\text{-CH}$ ), 2.26 (q, 1H, NH-C=O- $\text{CH}(\text{CH}_2)\text{-CH-COOH}$ ), 2.738 (s, 2H, C- $\text{CH}_2\text{-COOH}$ ), 3.23 (s, 2H, C- $\text{CH}_2\text{-NH}$ ).

IR (KBr/ $\nu_{\text{max}}$   $\text{cm}^{-1}$ ) 1707.44 (C=O), 1654.94 (C=O), 1565.16 (C=O), 2926.47(OH), 2856.88(OH) and, 3389.80(NH).  $m/z$  324.3 Da [ $\text{M}-1$ ].

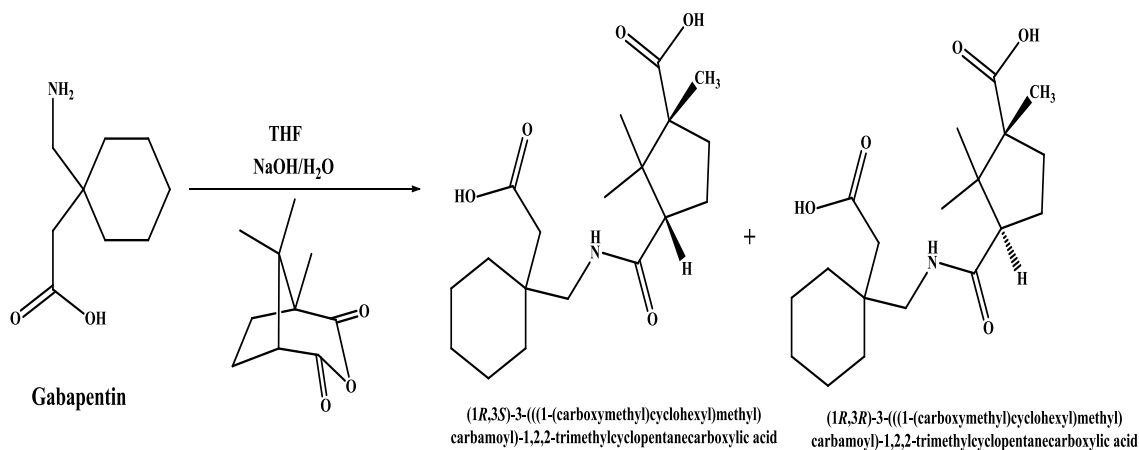


**Scheme 3-2:** Gabapentin **ProD 2**; synthesis scheme for the formation of gabapentin **ProD 2**.

Gabapentin **ProD 3**: We followed the same procedure as for gabapentin **ProD 1** but instead of using mixture of diastereomers of hexahydro-4-methylphthalic anhydride linker, a mixture of diastereomers of the camphoric acid anhydride was used (0.912g) 5 mmol (Scheme 3-3). The product yield was 93%. Melting point is 99°C. The product of **ProD 3** consists of two diastereomers. With 21% and 79% for (1S,2R) diastereomer and (1R,2R) diastereomer of **ProD 3**, respectively, as revealed by HPLC.

(1S,3R) diastereomer of the **ProD 3**,  $^1\text{H-NMR}$  (500 MHz) (ppm,  $\delta$ ) DMSO- $d_6$  0.72 (s, 3H, C-C- $\underline{\text{CH}}_3$ ), 1.2 (s, 3H, C-C- $\underline{\text{CH}}_3$ ), 1.29 (s, 3H, COOH-C- $\underline{\text{CH}}_3$ ), 1.25-1.35 (m, 2H, C- $\underline{\text{CH}}_2$ - $\underline{\text{CH}}_2$ - $\underline{\text{CH}}_2$ - $\underline{\text{CH}}_2$ ), 1.39-1.49 (m, 4H, C- $\underline{\text{CH}}_2$ - $\underline{\text{CH}}_2$ - $\underline{\text{CH}}_2$ - $\underline{\text{CH}}_2$ ), 1.49-1.65 (m, 4H, C- $\underline{\text{CH}}_2$ - $\underline{\text{CH}}_2$ - $\underline{\text{CH}}_2$ - $\underline{\text{CH}}_2$ ), 1.7-1.9 (ddd, 2H, NH-C=O-CH- $\underline{\text{CH}}_2$ - $\underline{\text{CH}}_2$ -C), 1.9-2.09 (dtd, 2H, NH-C=O-CH- $\underline{\text{CH}}_2$ - $\underline{\text{CH}}_2$ -C), 2.1 (s, 2H, C- $\underline{\text{CH}}_2$ -COOH), 2.5 (t, 1H, NH-C=O- $\underline{\text{CH}}_2$ -C), 3.25 (s, 2H, C- $\underline{\text{CH}}_2$ -NH-C=O).

(1*R*,3*R*) diastereomer of the **ProD 3**, <sup>1</sup>H-NMR (500 MHz) (ppm, δ) DMSO-d<sub>6</sub> 0.75 (s, 3H, C-C-CH<sub>3</sub>), 0.95 (s, 3H, C-C-CH<sub>3</sub>), 1.12 (s, 3H, COOH-C-CH<sub>3</sub>), 1.25-1.39 (m, 2H, C-CH<sub>2</sub>-CH<sub>2</sub>-CH<sub>2</sub>-CH<sub>2</sub>), 1.39-1.49(m, 4H, C-CH<sub>2</sub>-CH<sub>2</sub>-CH<sub>2</sub>-CH<sub>2</sub>), 1.49-1.65 (m, 4H, C-CH<sub>2</sub>-CH<sub>2</sub>-CH<sub>2</sub>-CH<sub>2</sub>), 1.7-1.9 (ddd, 2H, NH-C=O-CH-CH<sub>2</sub>-CH<sub>2</sub>-C), 1.9-2.09 (dtd, 2H, NH-C=O-CH-CH<sub>2</sub>-CH<sub>2</sub>-C), 2.25 (s, 2H, C-CH<sub>2</sub>-COOH), 2.56 (t, 1H, NH-C=O-CH-CH<sub>2</sub>-CH<sub>2</sub>-C), 3.27 (s, 2H, C-CH<sub>2</sub>-NH-C=O). IR (KBr/*v*<sub>max</sub> cm<sup>-1</sup>) 1760.93 (C=O), 1697.61 (C=O), 1612.25 (C=O), 2800-3000 (OH) and 3405.95(NH). *m/z* 354.21 Da [M+1]<sup>+</sup>.



**Scheme 3-3:** Gabapentin **ProD 3**; synthesis scheme for the formation of two diastereomers of gabapentin **ProD 3**.

### **3.3 Part three**

#### **3.3.1. Kinetic Methods:**

##### **3.3.1.1. Buffer Preparation:**

0.1 normalized hydrochloric acid (0.1 N HCl) was prepared by diluting 8.5 ml of hydrochloric acid with water to 1000 ml. Moreover, pH 3 was prepared by dissolving 6.8 g of potassium dihydrogen phosphate in 900 ml water for HPLC then it was adjusted by diluted orthophosphoric acid and water was added to a final volume of 1000 ml. The same procedure was done for the preparation of buffers pH 6.8 and 7.4, however, the required pH was adjusted using 1N NaOH.

Intraconversion of 500 ppm gabapentin **ProD 1**, **ProD 2**, and **ProD 3** solutions, in 0.1N HCl and buffers with pHs of 3, 6.8 and 7.4, to gabapentin was followed by HPLC at a wavelength of 210 nanometers. This wavelength was selected since the prodrugs lack absorption at higher lambda. Hydrolysis reactions were run mostly at 37°C.

##### **3.3.1.2. Calibration curves:**

###### **3.3.1.2.1. Calibration curve for ProD 1:**

A 50 mg of gabapentin **ProD 1** was dissolved in 100 ml methanol in order to prepare a stock solution with a concentration of 500 ppm. Subsequently, diluted solutions with the following concentrations (31.25, 62.5, 125, 250 and 500 ppm) were prepared from the stock.

20  $\mu\text{l}$  of each solution was injected into the HPLC and all the peaks were recorded using the following HPLC conditions: 4 mm x 250 mm, 5  $\mu\text{m}$  Purospher® RP-18 endcapped column, a mobile phase of 75% (5.28g  $(\text{NH}_4)_2\text{HPO}_4$  to 1000 ml with purified water and then pH was adjusted to 6.5 with orthophosphoric acid), 10% methanol and 15% Acetonitrile, a flow rate of 1 ml  $\text{minute}^{-1}$  and ultraviolet detection at a wavelength of 210 nanometers.

Peak area vs. concentration curves for gabapentin **ProD 1** was then plotted, and a coefficient of determination ( $R^2$ ) of the plot was calculated.

#### **3.3.1.2.2. Calibration curve for ProD 2:**

A 50 mg of gabapentin **ProD 2** was dissolved in 100 ml methanol in order to prepare a stock solution with a concentration of 500 ppm. Subsequently, diluted solutions with the following concentrations (31.25, 62.5, 125, 250 and 500 ppm) were prepared from the stock. 20  $\mu\text{l}$  of each solution was injected into the HPLC and the peak for the pharmaceuticals was recorded using the following HPLC conditions: 4 mm x 250 mm, 5  $\mu\text{m}$  phenomenex Luna® RP-18 end-capped column using mobile phase contains: 80% (5.28g  $(\text{NH}_4)_2\text{HPO}_4$  to 1000 ml with purified water and then pH was adjusted to 6.5 with orthophosphoric acid), 10% methanol and 10% acetonitrile, a flow rate of 1 ml  $\text{minute}^{-1}$  and ultraviolet detection at a wavelength of 210 nanometers.

Peak area vs. concentration curve for gabapentin **ProD 2** was then plotted, and  $R^2$  of the plot was calculated.

### **3.3.1.2.3. Calibration curve for ProD 3:**

A 50 mg of gabapentin **ProD 3** was dissolved in 100 ml methanol in order to prepare a stock solution with a concentration of 500 ppm. Subsequently, diluted solutions with the following concentrations (31.25, 62.5, 125, 250 and 500 ppm) were prepared from the stock. 20  $\mu$ l of each solution was injected into the HPLC and the peak for the pharmaceuticals was recorded using the following HPLC conditions: 4 mm x 250 mm, 5  $\mu$ m phenomenex Luna<sup>®</sup> RP-18 end-capped column using mobile phase contains: 77% (5.28g (NH<sub>4</sub>)<sub>2</sub>HPO<sub>4</sub> to 1000 ml with purified water and then pH was adjusted to 6.5 with orthophosphoric acid), 10% methanol and 13% acetonitrile, a flow rate of 1 ml minute<sup>-1</sup> and ultraviolet detection at a wavelength of 210 nanometers.

Peak area vs. concentration curve was then plotted, and R<sup>2</sup> of the plot was calculated.

### **3.3.1.3. Preparation of gabapentin standard and sample solution:**

A 500 ppm of gabapentin standard was prepared by dissolving 50 mg of gabapentin in 100 ml of 0.1N hydrochloric acid (HCl), buffer pH 3, buffer pH 6.8 and buffer pH 7.4, then each sample was injected into HPLC to detect the retention time of gabapentin.

A 500 ppm of the linkers standard (mixture of diastereomers of hexahydro-4-methylphthalic anhydride, *cis*-1,2-cyclohexanedicarboxylic anhydride, and mixture of diastereomers of camphoric acid anhydride) was prepared by dissolving 50 mg of each linker in 100 ml of 0.1N HCl, buffer pH 3, buffer pH 6.8 and buffer pH 7.4, then each sample was injected into HPLC to detect the retention time of the linkers.

A 500 ppm of each gabapentin **ProD 1-3** was prepared by dissolving 50 mg of the gabapentin **ProD 1-3** in 100 ml of 0.1N HCl, buffer pH 3, buffer pH 6.8 or buffer pH 7.4 then each sample was injected into HPLC to detect the retention time. The progression of the reactions was followed by monitoring the disappearance of the prodrugs and appearance of gabapentin and the linkers attached versus time.

Gabapentin **ProD 1-3** were incubated at 37°C to be monitored on the HPLC for several days to detect the intraconversion of the three prodrugs to their corresponding parent drug, to calculate the  $t_{1/2}$  of each prodrug.

### **3.4 Part Four**

#### **3.4.1. *In silico* prediction of physicochemical parameters, drug-likeness, ADMET for the synthesized gabapentin ProD 1-3:**

*In silico* prediction approaches increase our ability to predict physicochemical, pharmacokinetic, metabolic, and toxicity properties of drugs at the preclinical stage, thereby accelerating the drug discovery process and reducing the associated time, costs, and animal experiments [159].

Three software were used in this study to predict the physicochemical properties and number of ADMET values for the synthesized gabapentin prodrugs. ADMET are considered as the main reason for the failure of drug candidates at the later phases of drug development [159]. The first one is ACD/Lab software, version: v12.1, that can predict physicochemical, ADME, and toxicity features from the structure of the compound [160].

The second one is an online web server, Chemicalize, which was developed and is owned by ChemAxon and provides many cheminformatics tools to predict many physicochemical properties for the chemical compound [161]. The third software is preADME version 2.0; an online platform for predicting drug-likeness properties, ADME data, and toxicity of the chemical structure [162, 163]. Then by using Lipinski's rule of five, we assessed the drug-likeness and determined if these compounds will be orally active substances in human [164].

#### **3.4.2. *In silico* prediction of BBB permeability of the synthesized gabapentin ProD 1-3:**

Predicting BBB permeability is very significant to the development of drugs that target CNS; since a molecule must pass this barrier in order to display a pharmacological activity in the brain [165]. *In silico* BBB permeability was predicted for gabapentin **ProD 1-3** by utilizing an online program at <http://www.cbligand.org/BBB/> [166]. This uses AdaBoost and supports vector machine (SVM) combining 4 diverse fingerprints to expect if a compound can enter through the BBB (BBB+) or cannot enter through the BBB (BBB-) [166].

## **Chapter Four**

### **Results and Discussion**

## Chapter Four

### 4. Results and Discussion:

Three gabapentin prodrugs were proposed to synthesize utilizing three different linkers. As indicated above in Schemes **3-1** to **3-3**, these gabapentin prodrugs are composed of a promoiety containing a carboxylic acid group (hydrophilic moiety) and the rest of the prodrug molecule (a lipophilic moiety). The combination of both, the hydrophilic and lipophilic groups, provides a prodrug entity with potential to have high permeability (a modified HLB). Therefore; these prodrugs will be expected to be absorbed by passive diffusion to provide higher and dose-independent bioavailability. We have successfully synthesized these proposed gabapentin prodrugs with three various linkers. They were characterized by melting points, FT-IR, <sup>1</sup>H-NMR, and LC-MS analytical techniques, to guarantee pure gabapentin prodrugs.

**ProD 1** and **ProD 3** linkers consist of a mixture of diastereomers and produced prodrugs with two diastereomers. **ProD 1** diastereomers were 89% (1S, 1R) and 11% (1R,2R), while, **ProD 3** had diastereomers with 21% and 79% for (1S, 3R) and (1R, 3R), respectively. In contrast, the linker of **ProD 2** was *cis* isomer and therefore produced *cis* isomer of the prodrug.

## 4.1 Gabapentin standard and prodrugs characterization using different analytical techniques

### 4.1.1. Melting point, FT-IR, <sup>1</sup>H-NMR and LC-MS analysis of gabapentin standard:

1) The melting point of gabapentin is 167-169°C.

2) FT-IR (KBr/ $\nu_{\max}$   $\text{cm}^{-1}$ ) 1614.82  $\text{cm}^{-1}$  (C=O stretch of carboxylic acid), 2930.55  $\text{cm}^{-1}$  and 2856  $\text{cm}^{-1}$  (CH stretching) (Figure 4-1).

3) <sup>1</sup>H-NMR (500 MHz) (ppm,  $\delta$ ) CD<sub>3</sub>OD- 1.39-1.59 (m, 10 H, C-CH<sub>2</sub>-CH<sub>2</sub>-CH<sub>2</sub>-CH<sub>2</sub>-CH<sub>2</sub>), 2.45 (s, 2H, C-CH<sub>2</sub>-COOH), 2.9 (s, 2H, C-CH<sub>2</sub>-NH<sub>2</sub>) (Figure 4-2).

4) Gabapentin molecular formula is C<sub>9</sub>H<sub>17</sub>NO<sub>2</sub>. LC-MS (+ESI)  $m/z$  172.15 Da [M+1]<sup>+</sup> (Figure 4-3).

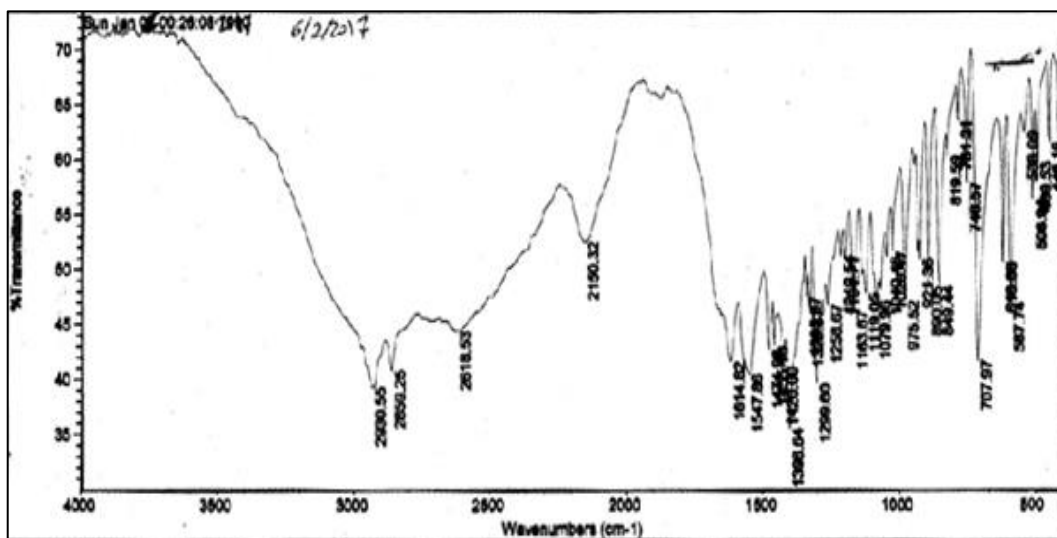
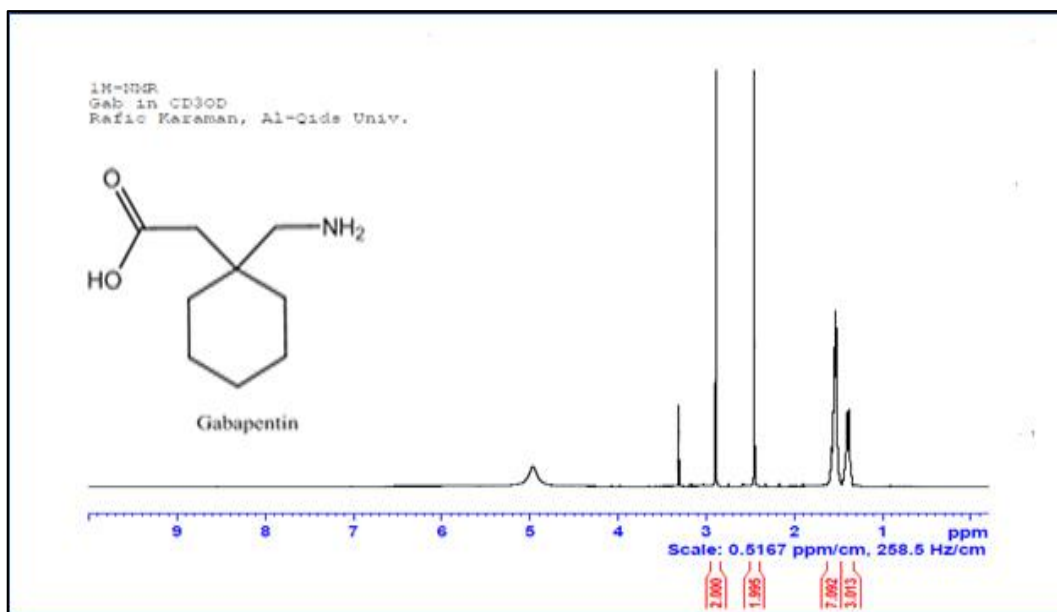
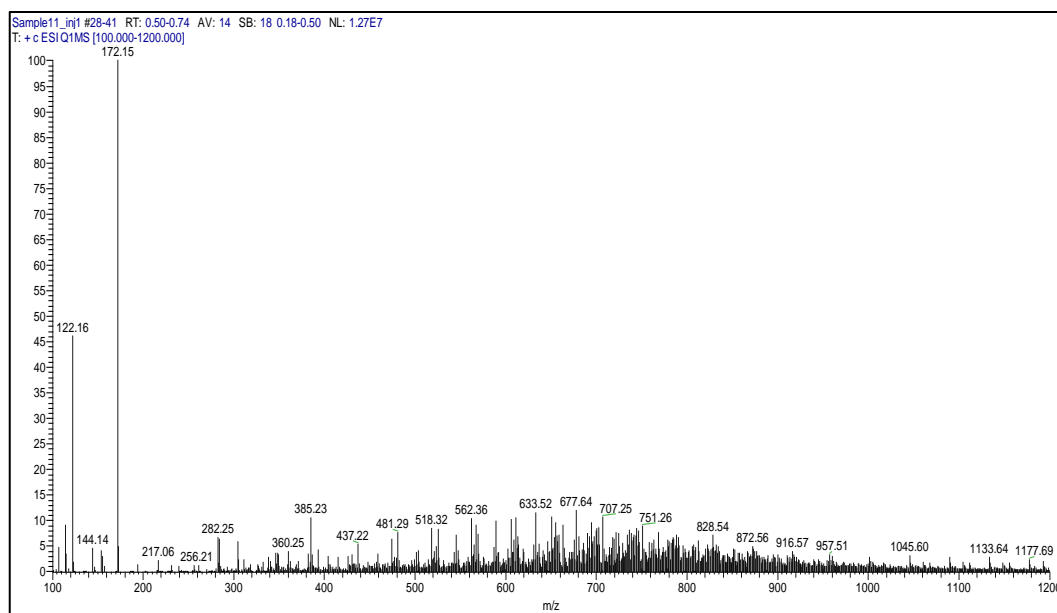


Figure 4-1: FT-IR spectrum of gabapentin.



**Figure 4-2:**  $^1\text{H}$ -NMR spectrum of gabapentin.



**Figure 4-3:** +ESI-LC-MS spectrum of gabapentin.

#### 4.1.2. Melting point, FT-IR, <sup>1</sup>H-NMR and LC-MS analysis of gabapentin ProD 1:

1) The melting point of **ProD 1** is 110 °C.

2) FT-IR (KBr/ $\nu_{\max}$ cm<sup>-1</sup>) 1706.74 (C=O of the carboxylic acid), 1646.82 (C=O of the amide), 1566.42 (N-H bending of the amide), 2926.55 (C-H stretching), 2863.63 (C-H stretching) and 3399.08 (NH) (Figure 4-4).

3) <sup>1</sup>H-NMR (500 MHz) (ppm,  $\delta$ ) of the (1S,2R) diastereomer of **ProD 1** CD<sub>3</sub>OD- 0.8797-0.8977 (d, 3H, CH<sub>2</sub>-CH-CH<sub>3</sub>), 0.95-1.07 (m, 2H, CH<sub>2</sub>-CH<sub>2</sub>-CH), 1.4006-1.4644 (m, 5H, C-CH<sub>2</sub>-CH<sub>2</sub>-CH<sub>2</sub>-CH<sub>2</sub>, CH<sub>2</sub>-CH<sub>2</sub>-CH(CH<sub>3</sub>)-CH<sub>2</sub>), 1.4940-1.5395 (m, 6H, C-CH<sub>2</sub>-CH<sub>2</sub>-CH<sub>2</sub>-CH<sub>2</sub>-CH<sub>2</sub>), 1.7649-1.810 (ddd, 2H, CH<sub>2</sub>-CH<sub>2</sub>-CH(CH<sub>3</sub>)-CH<sub>2</sub>CH), 2.09-2.179 (q, 1H, NH-C=O-CH-CH(CH<sub>2</sub>)-COOH), 2.1733 (s, 2H, C-CH<sub>2</sub>-COOH), 2.2305-2.443 (dq, 2H, NH-C=O-CH-CH<sub>2</sub>CH<sub>2</sub>), 3.02-3.08 (q, 1H, NH-C=O-CH(CH<sub>2</sub>)-CH<sub>2</sub>), 3.2662 (s, 2H, C-CH<sub>2</sub>NHC=O) (Figure 4-5).

<sup>1</sup>H-NMR (500 MHz) (ppm,  $\delta$ ) of the (1R,2R) diastereomer of **ProD 1** CD<sub>3</sub>OD- 0.9474-0.9660 (d, 3H, CH<sub>2</sub>-CH-CH<sub>3</sub>), 1.07-1.2 (m, 2H, CH<sub>2</sub>-CH<sub>2</sub>-CH), 1.4006-1.4644 (m, 5H, C-CH<sub>2</sub>-CH<sub>2</sub>-CH<sub>2</sub>-CH<sub>2</sub>, CH<sub>2</sub>-CH<sub>2</sub>-CH(CH<sub>3</sub>)-CH<sub>2</sub>), 1.4940-1.5395 (m, 6H, C-CH<sub>2</sub>-CH<sub>2</sub>-CH<sub>2</sub>-CH<sub>2</sub>-CH<sub>2</sub>), 1.808-1.862 (ddd, 2H, CH<sub>2</sub>-CH<sub>2</sub>-CH(CH<sub>3</sub>)-CH<sub>2</sub>CH), 2.16-2.217 (q, 1H, NH-C=O-CH-CH(CH<sub>2</sub>)-COOH), 2.173 (s, 2H, C-CH<sub>2</sub>-COOH), 2.2305-2.443 (dq, 2H, NH-C=O-CH-CH<sub>2</sub>CH<sub>2</sub>), 3.08-3.14 (q, 1H, NH-C=O-CH(CH<sub>2</sub>)-CH), 3.303 (s, 2H, C-CH<sub>2</sub>NHC=O) (Figure 4-5). The purity of the compound calculated from NMR is 93.8%.

4) The product molecular formula is C<sub>18</sub>H<sub>29</sub>NO<sub>5</sub> (yield 93%).

5) LC-MS (+ESI mode)  $m/z$  340.19 Da [M+H]<sup>+</sup>: the molecular mass of **ProD 1** is 339.4 Da. The positive electrospray ionization gave the protonated [M+H]<sup>+</sup> at  $m/z$  of 340.19 Da. Sodiated adduct peak appeared at  $m/z$  of 362.18 Da advocating the [M+ Na]<sup>+</sup> ion existence (Figure 4-6).

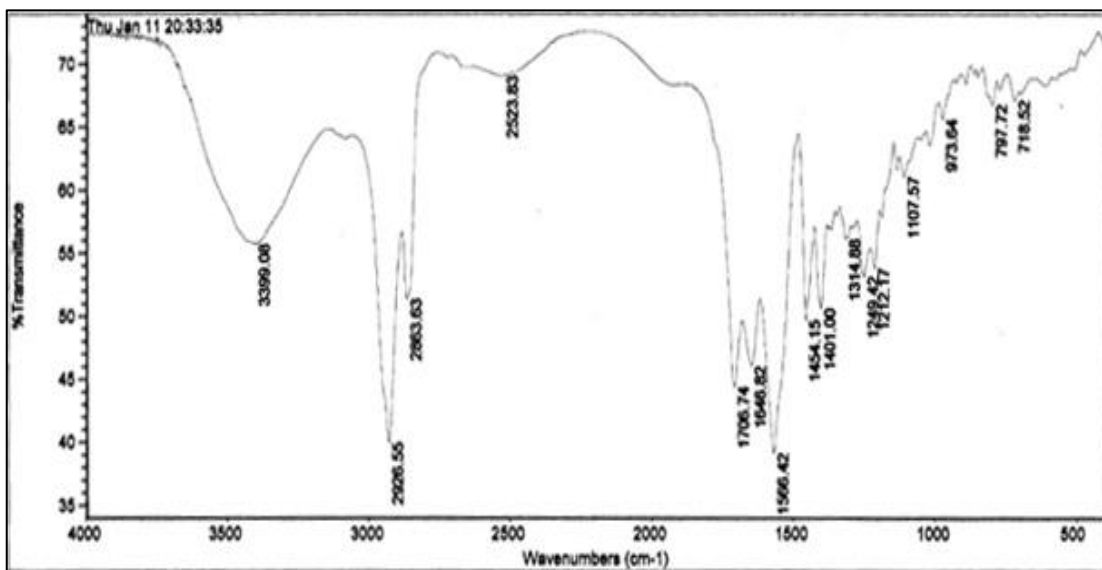


Figure 4-4: FT-IR spectrum of **ProD 1**.

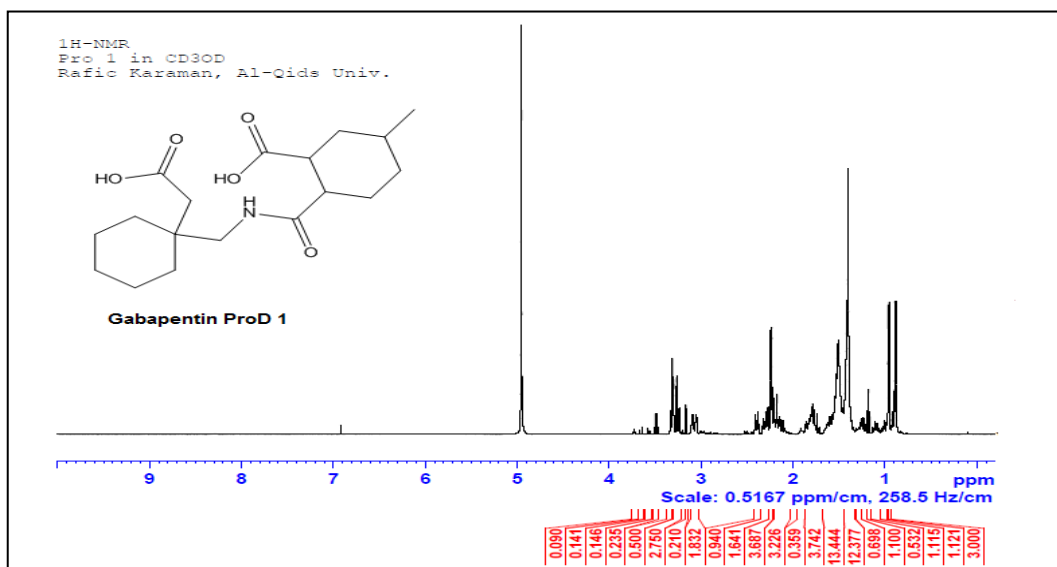
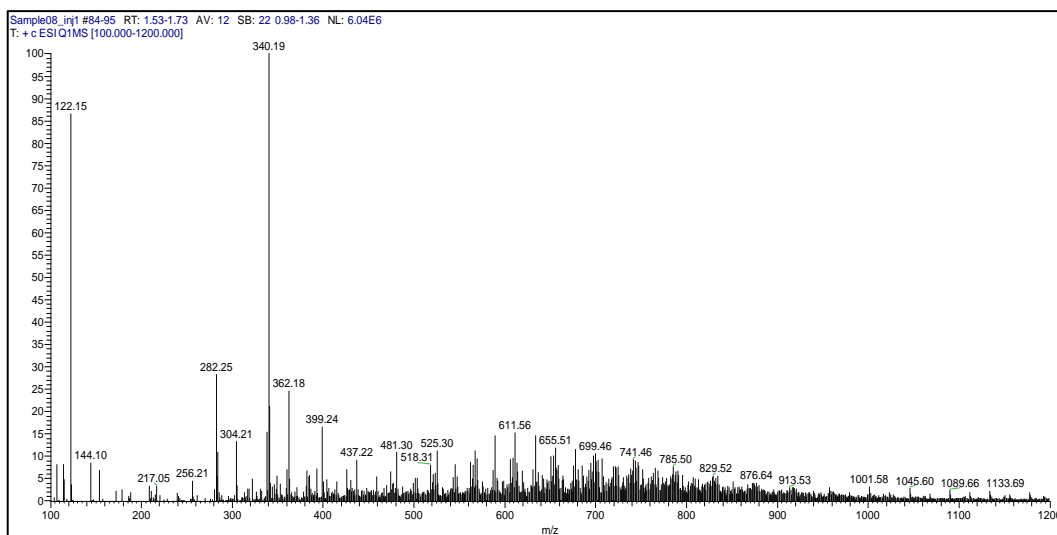


Figure 4-5:  $^1\text{H-NMR}$  spectrum of **ProD 1** in  $\text{CD}_3\text{OD}$ .



**Figure 4-6:** +ESI- LC-MS spectrum of **ProD 1**.

#### 4.1.3. Melting point, FT-IR, $^1\text{H-NMR}$ and LC-MS analysis of gabapentin **ProD 2**:

1) The melting point of **ProD 2** was 180 °C.

2) FT-IR (KBr/ $\nu_{\text{max}}$   $\text{cm}^{-1}$ ) 1707.44 (C=O of the carboxylic acid), 1654.94 (C=O of the amide), 1565.16 (N-H bending of the amide), 2926.47 (C-H stretching), 2856.88 (C-H stretching) and 3389.80 (NH) (Figure 4-7).

3)  $^1\text{H-NMR}$  (500 MHz) (ppm,  $\delta$ )  $\text{CD}_3\text{OD}$ - 1.3799-1.4253 (m, 8H, C- $\text{CH}_2$ - $\text{CH}_2$ - $\text{CH}_2$ - $\text{CH}_2$ - $\text{CH}_2$ , CH- $\text{CH}_2$ - $\text{CH}_2$ - $\text{CH}_2$ - $\text{CH}_2$ -CH), 1.4885-1.5291 (m, 4H, C- $\text{CH}_2$ - $\text{CH}_2$ - $\text{CH}_2$ - $\text{CH}_2$ - $\text{CH}_2$ ), 1.59-1.67 (m, 2H, CH- $\text{CH}_2$ - $\text{CH}_2$ - $\text{CH}_2$ - $\text{CH}_2$ -CH), 1.7039-1.738 (m, 2H, CH- $\text{CH}_2$ - $\text{CH}_2$ - $\text{CH}_2$ - $\text{CH}_2$ -CH), 2.08 (q, 1H, CH- $\text{CH}(\text{CH}_2)$ -COOH), 2.1026 (m, 2H, CH- $\text{CH}_2$ - $\text{CH}_2$ - $\text{CH}_2$ - $\text{CH}_2$ -CH), 2.26 (q, 1H, NH-C=O- $\text{CH}(\text{CH}_2)$ -CH-COOH), 2.738 (s, 2H, C- $\text{CH}_2$ -COOH), 3.23 (s, 2H, C- $\text{CH}_2$ -NH) (Figure 4-8). The purity of the compound calculated from NMR is 92.7 %.

4) The product molecular formula is  $\text{C}_{17}\text{H}_{27}\text{NO}_5$  (yield 92%).



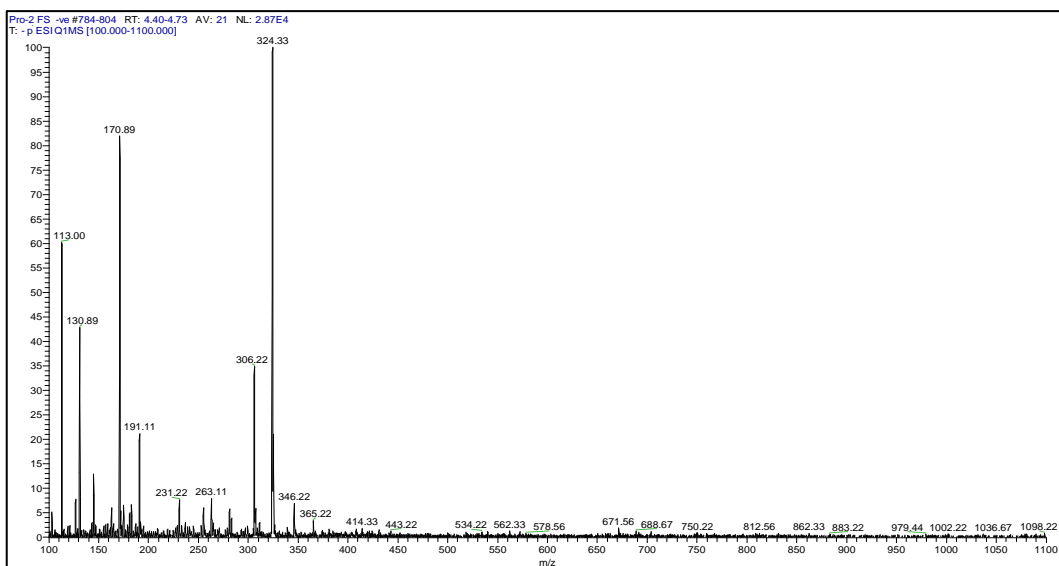


**Figure 4-9:** -ESI-LC-MS spectrum of **ProD 2** (Full scan mode).

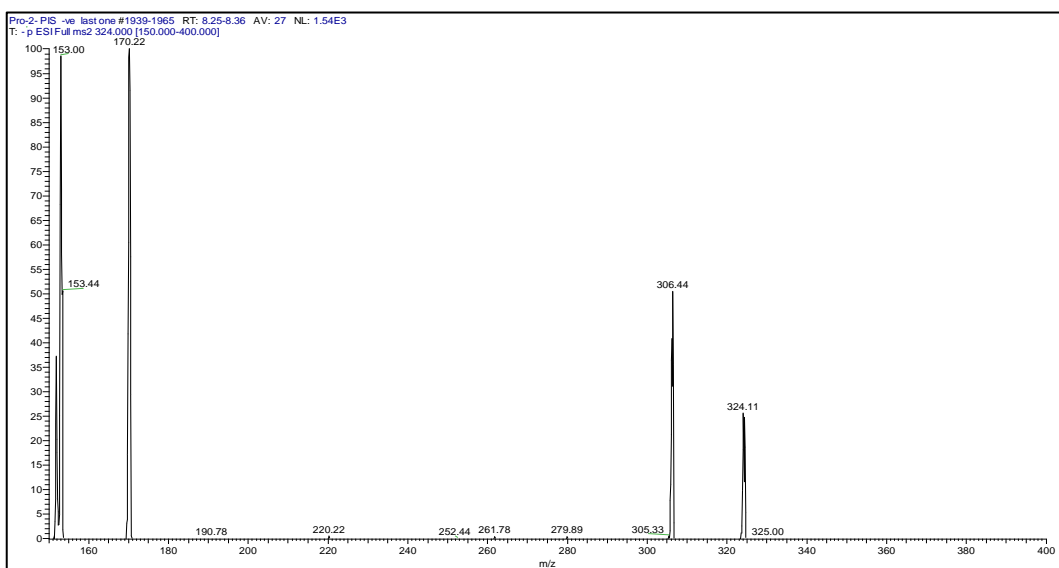


**Figure 4-10:** -ESI-LC-MSMS spectrum of **ProD 2** (Product ion scan mode).

#### 4.1.4. Melting point, FT-IR, <sup>1</sup>H-NMR and LC-MS analysis of gabapentin ProD 3:

1) The melting point of **ProD 3** was 99 °C.

2) IR (KBr/ $\nu_{\max}$  cm<sup>-1</sup>) 1760.93 (C=O of the carboxylic acid), 1697.61 (C=O of the amide), 1612.25 (N-H bending of the amide), 2800-3000 (C-H stretching) and 3405.95 (NH) (Figure 4-11).

3) <sup>1</sup>H-NMR (500 MHz) (ppm,  $\delta$ ) for the (1S,3R) diastereomer of the **ProD 3** (DMSO-d<sub>6</sub>) 0.72 (s, 3H, C-C-CH<sub>3</sub>), 0.95 (s, 3H, C-C-CH<sub>3</sub>), 1.12 (s, 3H, COOH-C-CH<sub>3</sub>), 1.25-1.35 (m, 2H, C-CH<sub>2</sub>-CH<sub>2</sub>-CH<sub>2</sub>-CH<sub>2</sub>), 1.39-1.49 (m, 4H, C-CH<sub>2</sub>-CH<sub>2</sub>-CH<sub>2</sub>-CH<sub>2</sub>), 1.49-1.65 (m, 4H, C-CH<sub>2</sub>-CH<sub>2</sub>-CH<sub>2</sub>-CH<sub>2</sub>), 1.7-1.9 (ddd, 2H, NH-C=O-CH-CH<sub>2</sub>-CH<sub>2</sub>-C), 1.9-2.09 (dtd, 2H, NH-C=O-CH(C)-CH<sub>2</sub>-CH<sub>2</sub>-C), 2.1 (s, 2H, C-CH<sub>2</sub>-COOH), 2.5 (t, 1H, NH-C=O-CH(C)-CH<sub>2</sub>), 3.25 (s, 2H, C-CH<sub>2</sub>-NH-C=O) (Figure 4-12).

<sup>1</sup>H-NMR (500 MHz) (ppm,  $\delta$ ) for the (1R,3R) diastereomer of the **ProD 3** (DMSO-d<sub>6</sub>) -0.75 (s, 3H, C-C-CH<sub>3</sub>), 1.2 (s, 3H, C-C-CH<sub>3</sub>), 1.29 (s, 3H, COOH-C-CH<sub>3</sub>), 1.25-1.39 (m, 2H, C-CH<sub>2</sub>-CH<sub>2</sub>-CH<sub>2</sub>-CH<sub>2</sub>), 1.39-1.49 (m, 4H, C-CH<sub>2</sub>-CH<sub>2</sub>-CH<sub>2</sub>-CH<sub>2</sub>), 1.49-1.65 (m, 4H, C-CH<sub>2</sub>-CH<sub>2</sub>-CH<sub>2</sub>-CH<sub>2</sub>), 1.7-1.9 (ddd, 2H, NH-C=O-CH-CH<sub>2</sub>-CH<sub>2</sub>-C), 1.9-2.09 (dtd, 2H, NH-C=O-CH-CH<sub>2</sub>-CH<sub>2</sub>-C), 2.25 (s, 2H, C-CH<sub>2</sub>-COOH), 2.56 (t, 1H, NH-C=O-CH-CH<sub>2</sub>), 3.27 (s, 2H, C-CH<sub>2</sub>-NH-C=O) (Figure 4-12). Peak appeared at 3.45 is due to the amount of water present in DMSO, as DMSO is highly miscible with water, during handling DMSO absorbs moisture and the broad peak at 3.45 is most likely due to the moisture present.

4) The product molecular formula is C<sub>19</sub>H<sub>31</sub>NO<sub>5</sub> (yield 93%).

5) LC-MS (positive mode)  $m/z$  354.21 Da  $[M+1]^+$ : the molecular mass of the **ProD 3** is 353.25 Da. The positive electrospray ionization gave the protonated  $[M+H]^+$  at  $m/z$  of 354.21 Da. Sodiated adduct peak appeared at  $m/z$  of 376.20 Da advocating the  $[M+Na]^+$  ion existence (Figure 4-13).

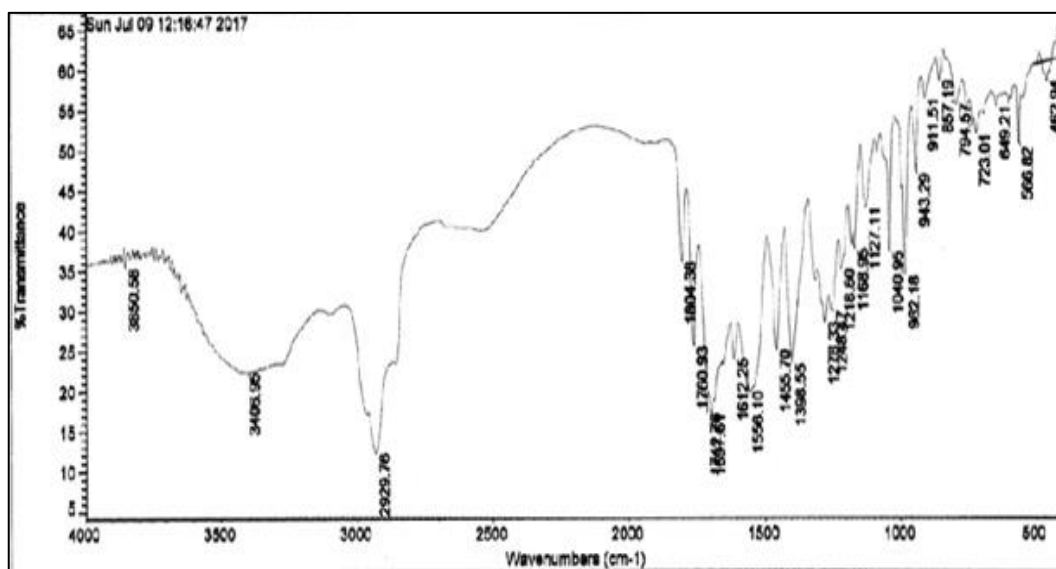


Figure 4-11: FT-IR spectrum of **ProD 3**.

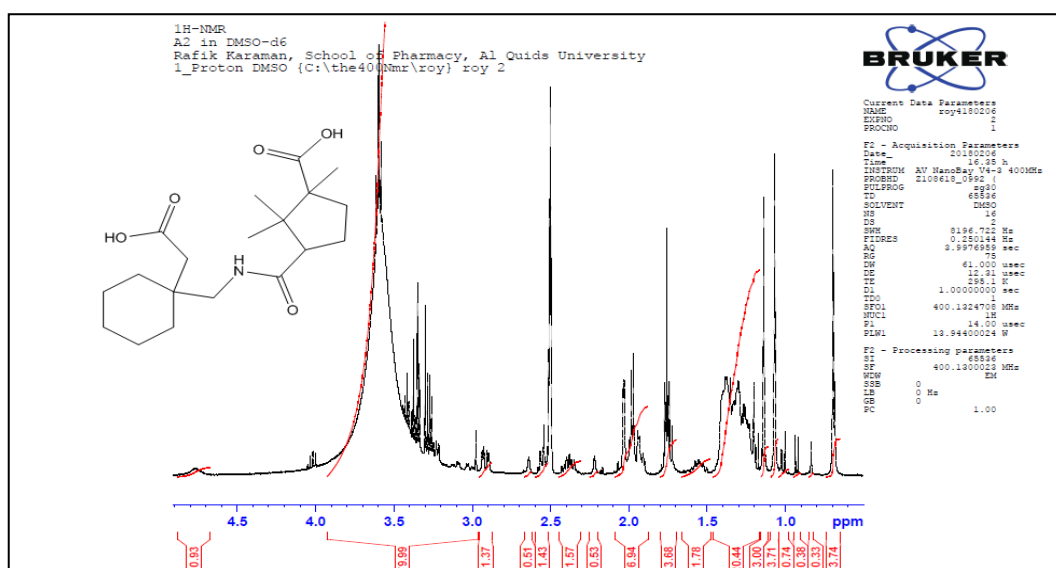
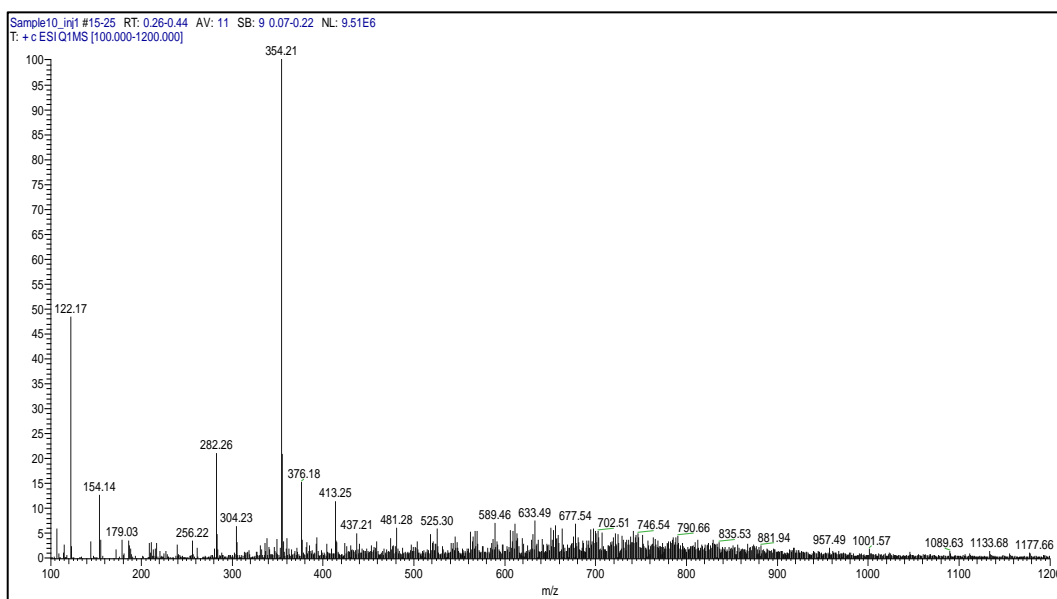


Figure 4-12:  $^1\text{H-NMR}$  spectrum of **ProD 3** in  $\text{CD}_3\text{SOCD}_3$ .



**Figure 4-13:** LC-MS spectrum of **ProD 3**.

## 4.2 Hydrolysis studies

Hydrolysis of gabapentin prodrugs was investigated using HPLC. Peaks of standards and degradation products were monitored to determine the rate of cleavage of the three synthesized gabapentin prodrugs. Kinetic studies were performed at constant temperature (37°C) and at different pH in buffers such as 0.1N HCl, pH 3, pH 6.8, and pH 7.4 which resemble the physiological environments in the human body. The 0.1N HCl and pH 3 were chosen to study the intraconversion of the gabapentin prodrugs in pH as of the stomach because the mean stomach pH of the adult is approximately 1-3, whereas, buffer pH 6.8 represents the small intestine pathway. pH 7.4 was selected to study the intraconversion of the tested prodrugs in pH as of the blood circulation system.

Calibration curves were obtained by plotting peak area of the prodrugs versus concentration. As shown in Figure 4-14, excellent linearity with  $R^2$  of 0.997 for gabapentin **ProD 1** and 0.999 for both gabapentin **ProD 2** and **ProD 3** were obtained.

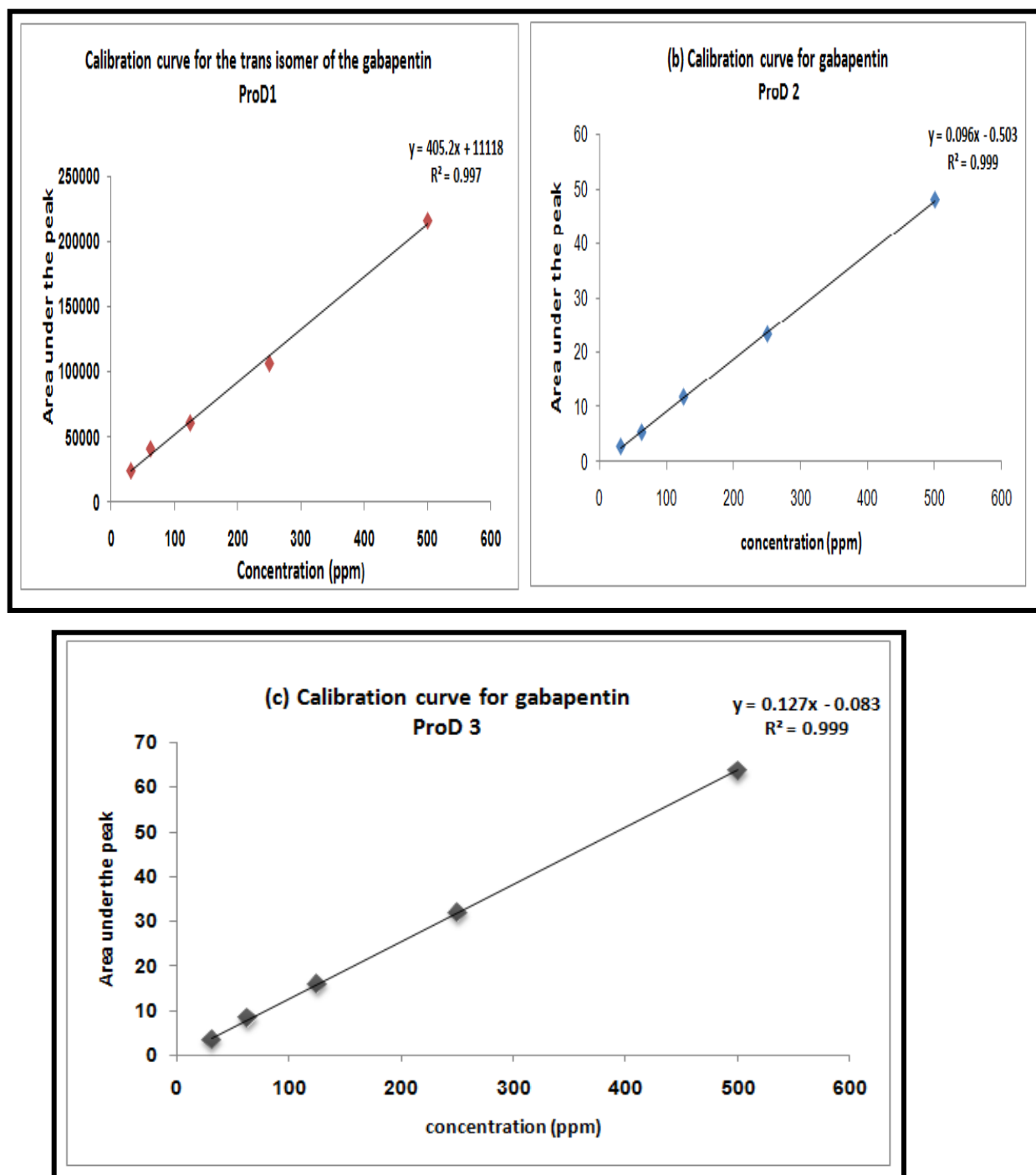


**Figure 4-14:** Calibration curves of **ProD 1** (a), **ProD 2** (b), and **ProD 3** (c).

#### 4.2.1. *In vitro* intraconversion of gabapentin ProD 1-3 to their parent drug:

The hydrolysis kinetic studies of gabapentin **ProD 1-3** were done in aqueous buffers in the same method to that carried out by Kirby *et al.* on maleamic acids **1-9** (Figure 2-4) [167]. This is to explore if the gabapentin prodrugs undergo hydrolysis in an aqueous medium and measure the rate of the hydrolysis should it occur, indicating the fate of the prodrugs in the system. The kinetics of the acid-catalyzed hydrolysis of the synthesized gabapentin **ProD 1-3** were conducted in four different aqueous media: 0.1 N HCl, buffer pH 3, buffer pH 6.8 and buffer pH 7.4. The results and chromatograms of the kinetic study are summarized in Figures 4-15 to 4-27.

Under experimental conditions, **ProD 1-2** were hydrolyzed to liberate the parent drug, gabapentin, as demonstrated by HPLC analysis (Figures 4-15 to 4-25). At constant temperature and pH, the reactions display strict first-order kinetics as an observed rate constants of hydrolysis ( $k_{\text{obs}}$ ) were markedly constant and straight lines were acquired by plotting  $\ln$  concentration of residual prodrugs versus time (Figures 4-28 to 4-29), whereas the gabapentin **ProD 3** was shown to be extremely stable at constant pH and temperature as evident by HPLC analysis indicated in Figure 4-26 to 4-27.

**ProD 1** HPLC conditions gave good resolution between the two **ProD 1** diastereomeric peaks (resolution ( $R_s$ ) > 2.5) as depicted in Figure 4-16 to 4-19. However, improper separation ( $R_s$  < 1.2) between the two diastereomer peaks of **ProD 3** was observed by using **ProD 3** HPLC conditions (Figure 4-27). Both **ProD 3** diastereomers were shown to be very stable. Thus, improving the resolution between **ProD 3** diastereomers will only consume time and money.

The  $k_{\text{obs}}$  and the corresponding  $t_{1/2}$  for gabapentin prodrugs in different media were estimated from the linear regression equation correlating the ln concentration of the residual prodrug versus time (Tables 4-1 to 4-3).

Acid-catalyzed hydrolysis of the gabapentin **ProD 1-2** was found to be much higher at 0.1N HCl and pH 3 (acidic media) than pH 6.8 and pH 7.4 (Figures 4-15 to 4-25). Gabapentin **ProD 1** experimental half-life values in 0.1N HCl, buffer pH's 3, 6.8 and 7.4 were 16.57, 17.76, 101.91, and 119.48 hrs, respectively. **ProD 2** was hydrolyzed into its parent drug in 0.1N HCl, buffer pH's 3, 6.8, and 7.4 with experimental half-life values of 20.3, 22.70, 130.75 and 277.2 hrs, respectively.

At pH 5.0–7.4, intestine environment and blood circulation, the carboxylic group in **ProD 1** and **ProD 2** will equilibrate with the related carboxylate form. Consequently, the free acid form will undergo proton transfer reaction after being transferred by the membrane to release gabapentin. The synthesized gabapentin **ProD 1-2** will be designed for oral use in the form of enteric coated tablets. Enteric coated tablets are completely stable at high acidic pH found in the stomach, but dissolve quickly at less acidic pH. For instance, enteric coated tablets will not dissolve in the acidic juices of the stomach (pH ~3), but they will at higher pH (above pH 5.5) in the small intestine. In the intestine, prodrugs **ProD 1-2** will present in the ionic and acidic forms where the equilibrium constant for the exchange between both forms is dependent on the pKa of the given prodrug.

The pKa's of gabapentin **ProD 1-2** are in the range of 5-6 because experimentally determined pKa's for **ProD 1-2** linkers are in the range of 5.0-6.0. Therefore, it is predicted that the pKa's of the related prodrugs will be in the same range.

Thus, we predict that at pH 6.8 and pH 7.4 the ratio of the free acid form that undergoes acid-catalyzed hydrolysis will be comparatively low and the anionic form of the prodrugs will be dominant. At 0.1N HCl and pH 3, most of the prodrug will present as the free acid form. This interpreted the differences in rates at the different pH buffers.

Thus, both gabapentin **ProD 1-2** will release active drug in a sustained release manner as indicated by their  $t_{1/2}$ , but immediate release of drug from prodrug will be achieved by using carboxylic linkers having pKa close to that of the blood circulation (pH 7.4).

On the other hand, **ProD 1** was found to have a higher hydrolysis rate than **ProD 2**, this is due to a structural feature of 4-methylcyclohexane moiety of the **ProD 1** linker, which contains a methyl group on the cyclohexane (strained system) which results in a decrease of the distance between the two reactive centers (hydroxyl oxygen of the carboxylic group and the amide carbonyl carbon). Hence, the hydrolysis of gabapentin **ProD 1** is faster than that of gabapentin **ProD 2**.

However, the linker of gabapentin **ProD 3** has the lowest pKa, which is about 4. Thus, it is predictable that the pKa of the **ProD 3** will be about 4. Therefore, most of **ProD 3** will exist as the anionic form at pH 6.8 and pH 7.4. This explains why **ProD 3** was completely stable and no liberation of gabapentin was observed in both buffers. In addition, **ProD 3** was extremely insoluble in the acidic buffers of 0.1N HCl and pH 3. Thus, no reaction happened in the acidic environment for this prodrug

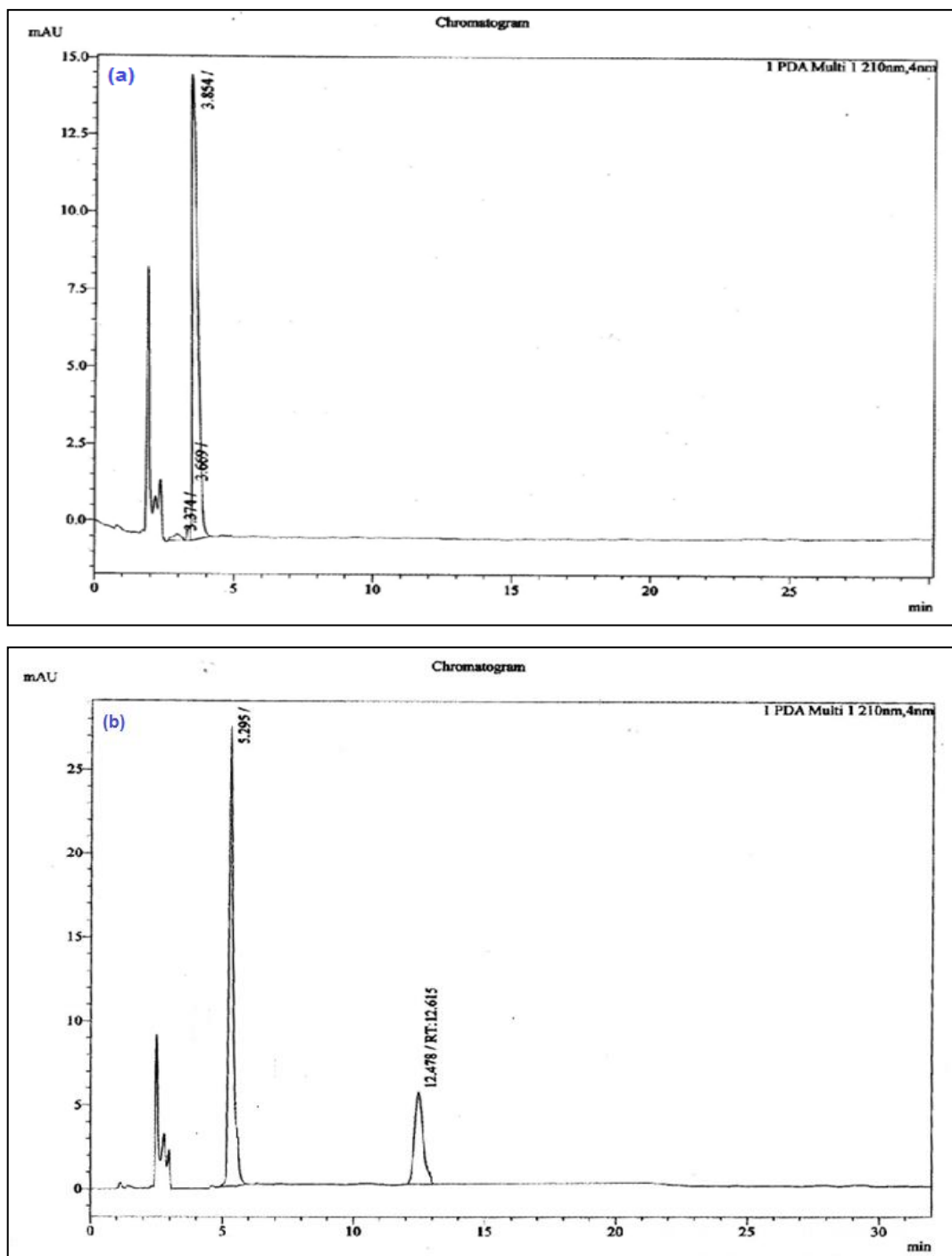


**Figure 4-15:** Chromatograms showing gabapentin standard (a) and both linker 1 diastereomers (b) at gabapentin **ProD 1** HPLC conditions.

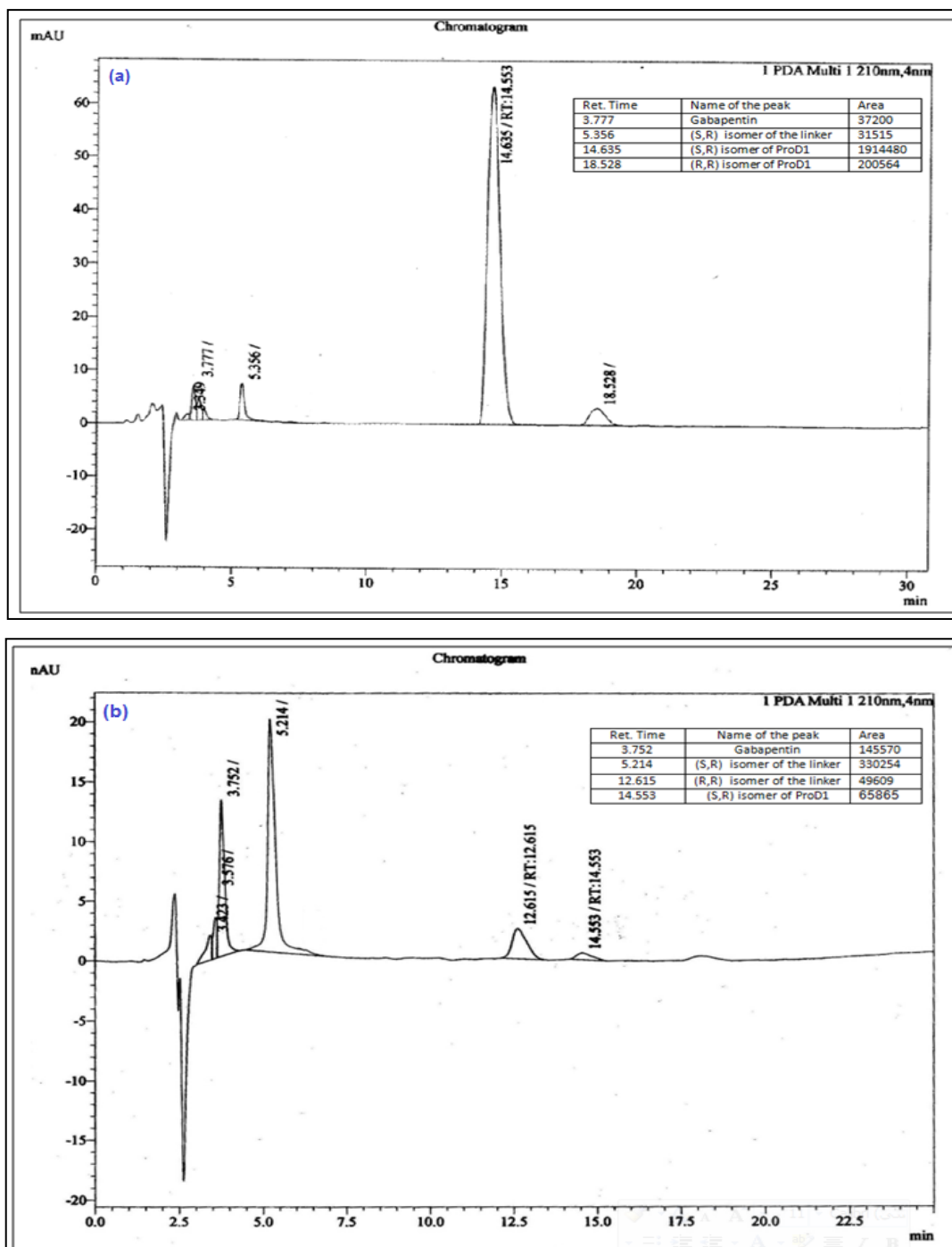


**Figure 4-16:** Chromatograms showing the intraconversion of **ProD 1** at 0.1 N HCl after 15 min (a) and after 72 hrs (b).

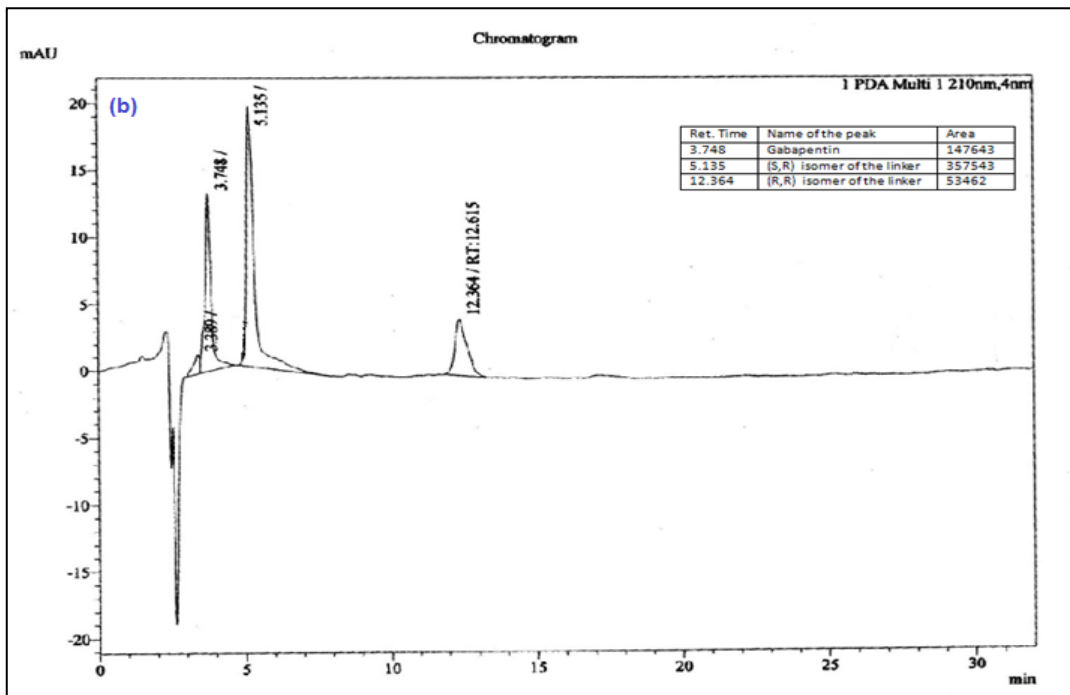
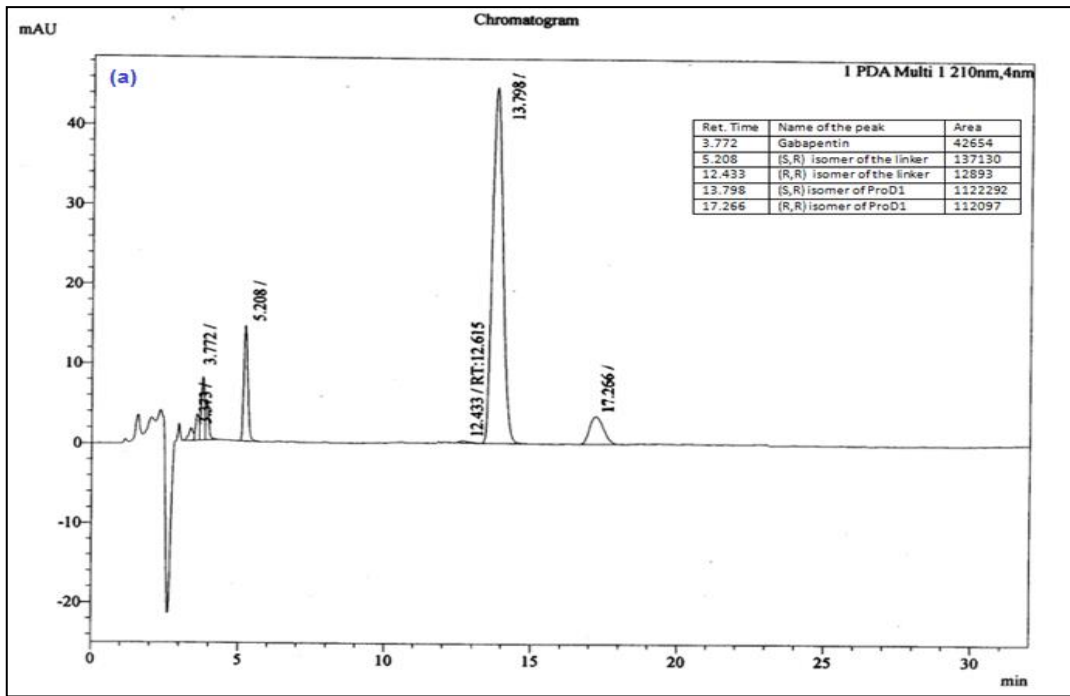


**Figure 4-17:** Chromatograms showing the intraconversion of **ProD 1** at pH 3 after 9 hrs (a) and at end of the reaction (b).

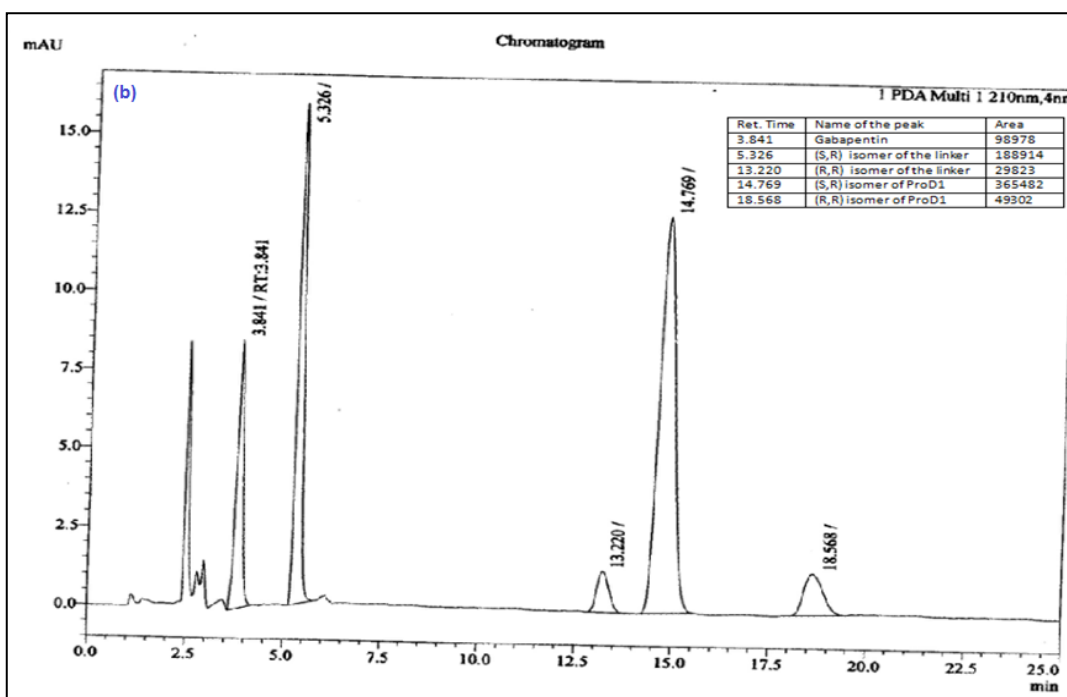
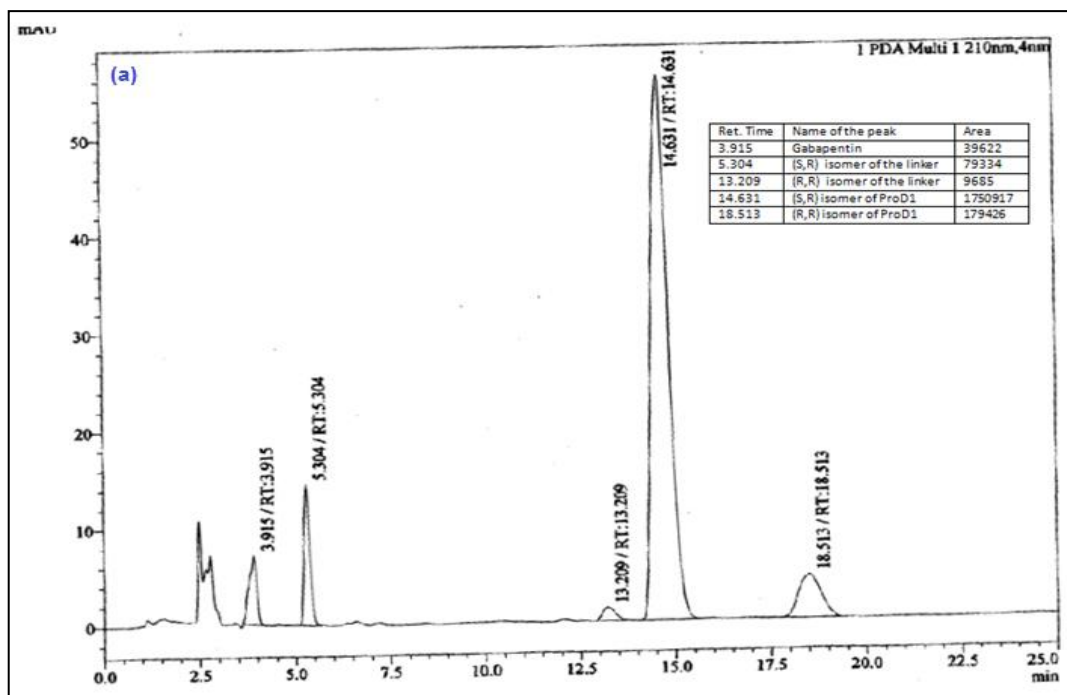


**Figure 4-18:** Chromatograms showing the intraconversion of **ProD 1** at pH 6.8 after 24 hrs (a) and after 240 hrs (b).

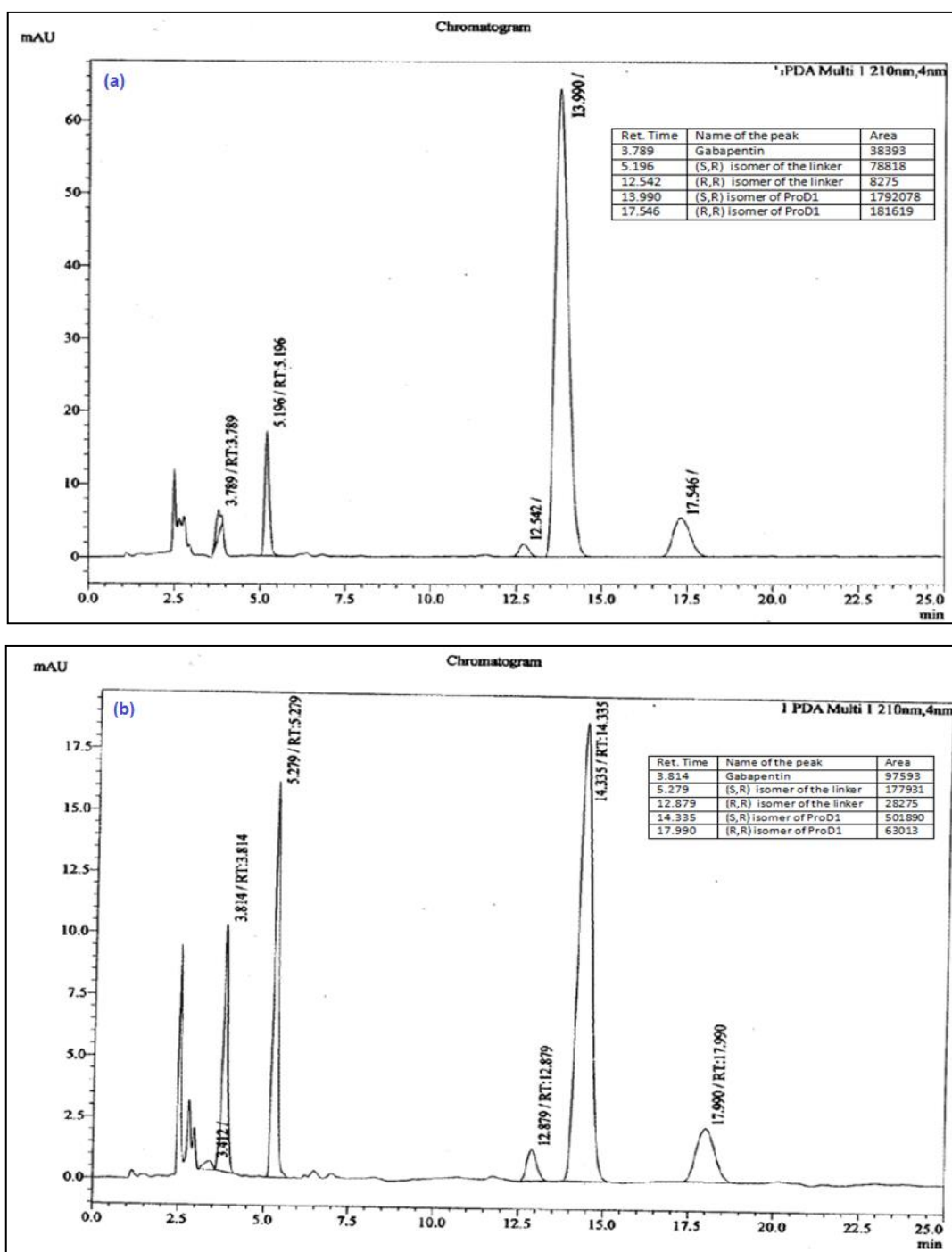


**Figure 4-19:** Chromatograms showing the intraconversion of **ProD 1** at pH 7.4 after 30 hrs (a) and after 240 hrs (b).

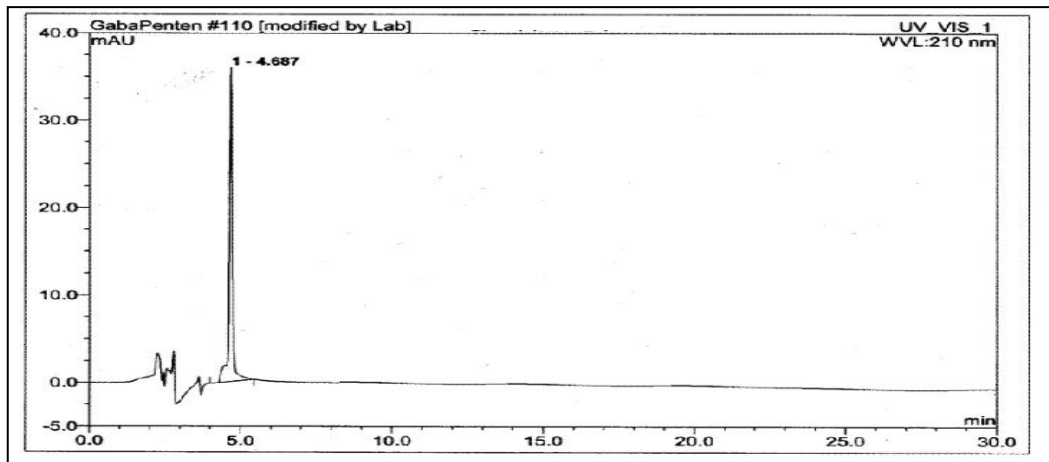


**Figure 4-20:** Chromatograms showing gabapentin standard at gabapentin **ProD 2** HPLC conditions.

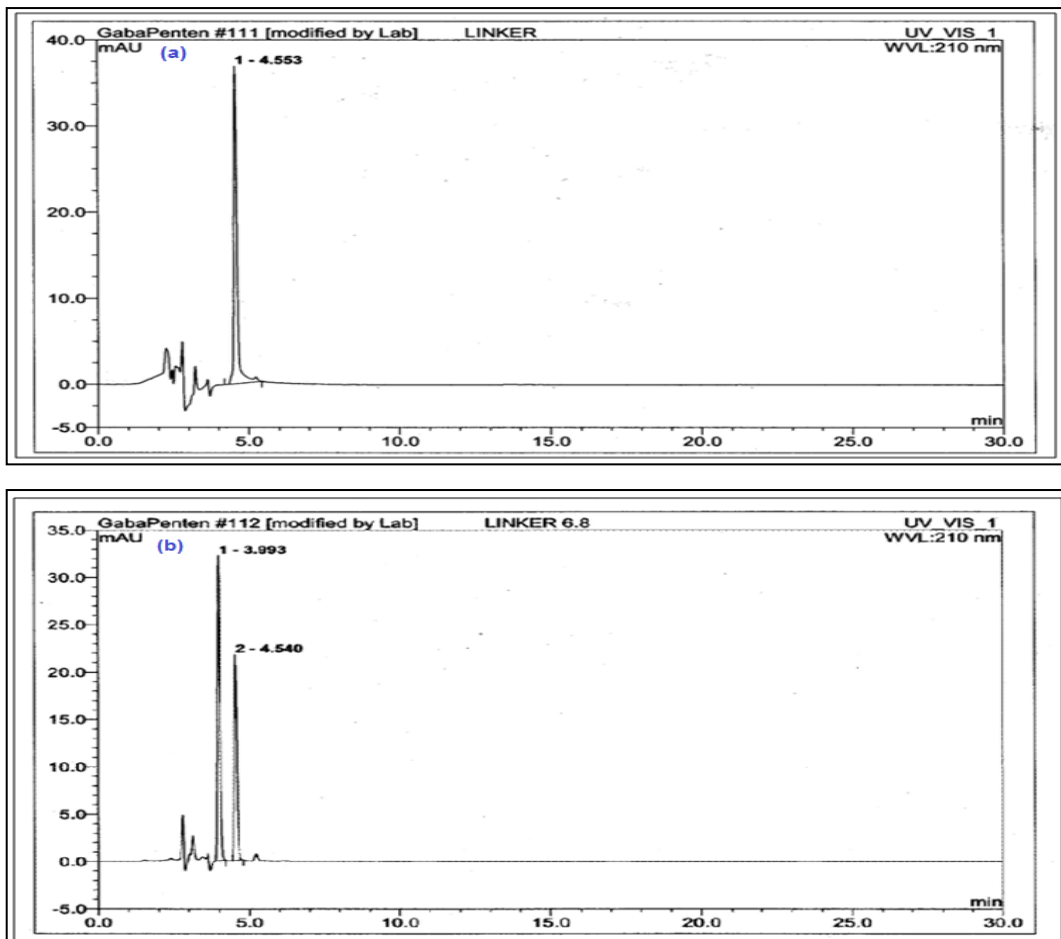


**Figure 4-21:** Chromatograms showing linker 2 standard at pH 0.1N HCl and pH 3 (a) and pH 6.8 and 7.4 (b) at gabapentin **ProD 2** HPLC conditions.

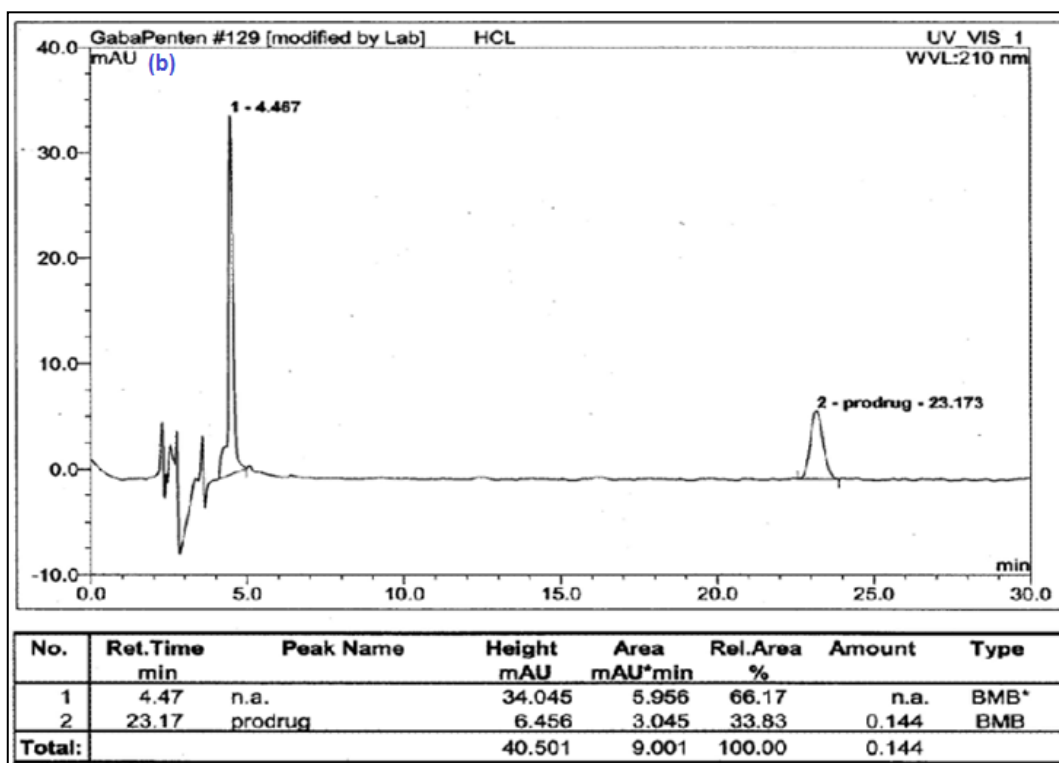
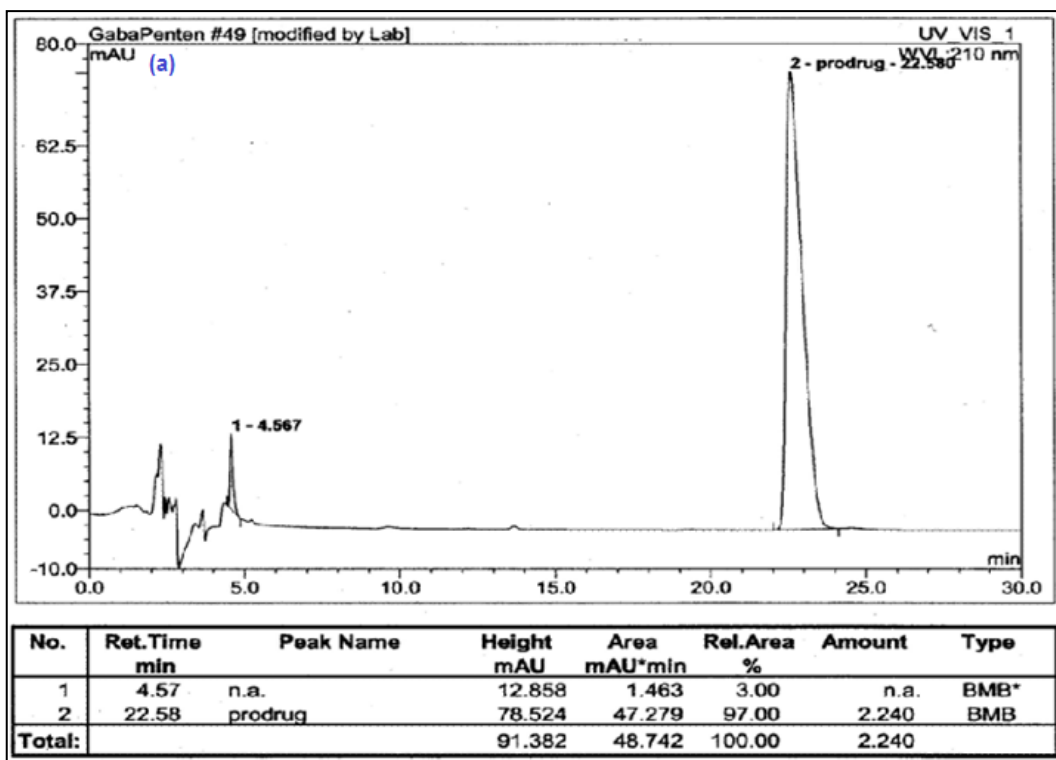


**Figure 4-22:** Chromatograms showing the intraconversion of **ProD 2** at pH 0.1 N HCl after 1 hr (a), and after 73 hrs (b).

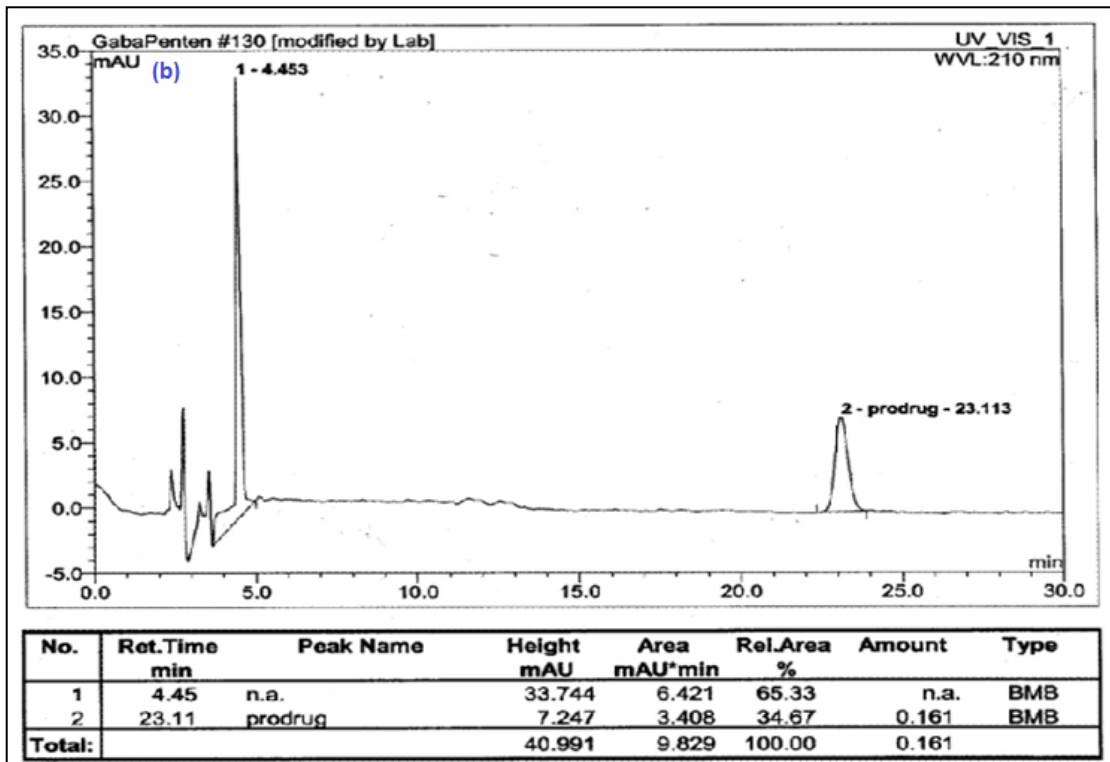
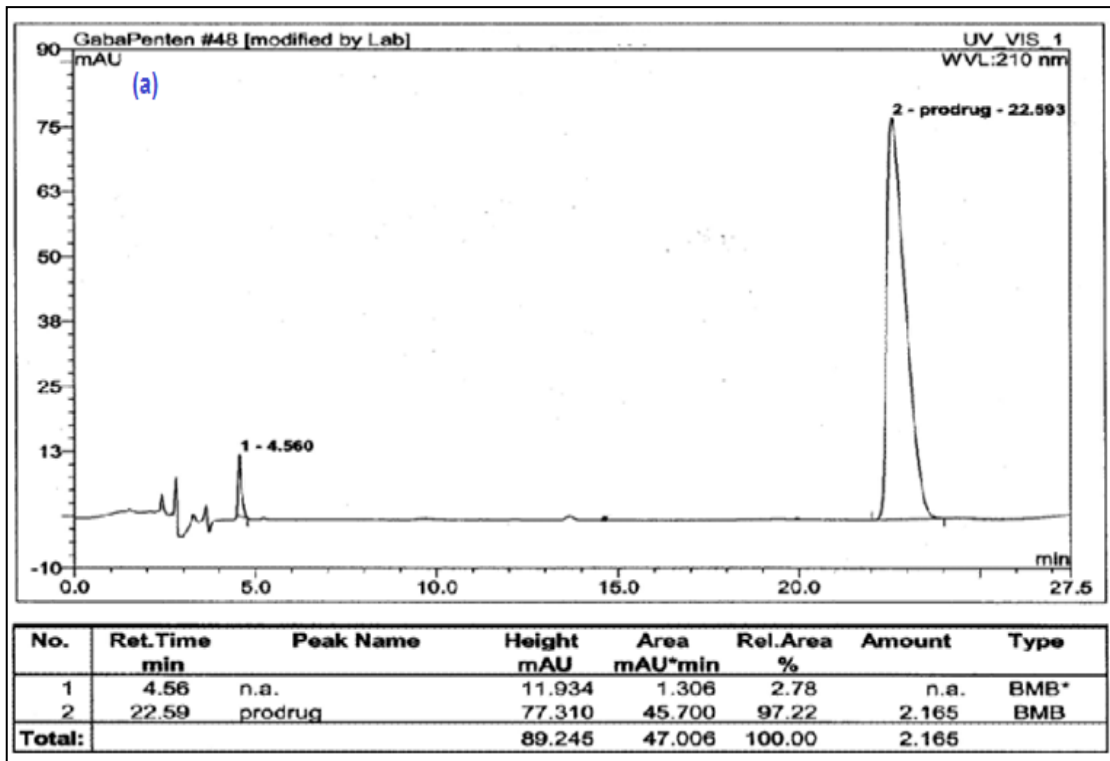
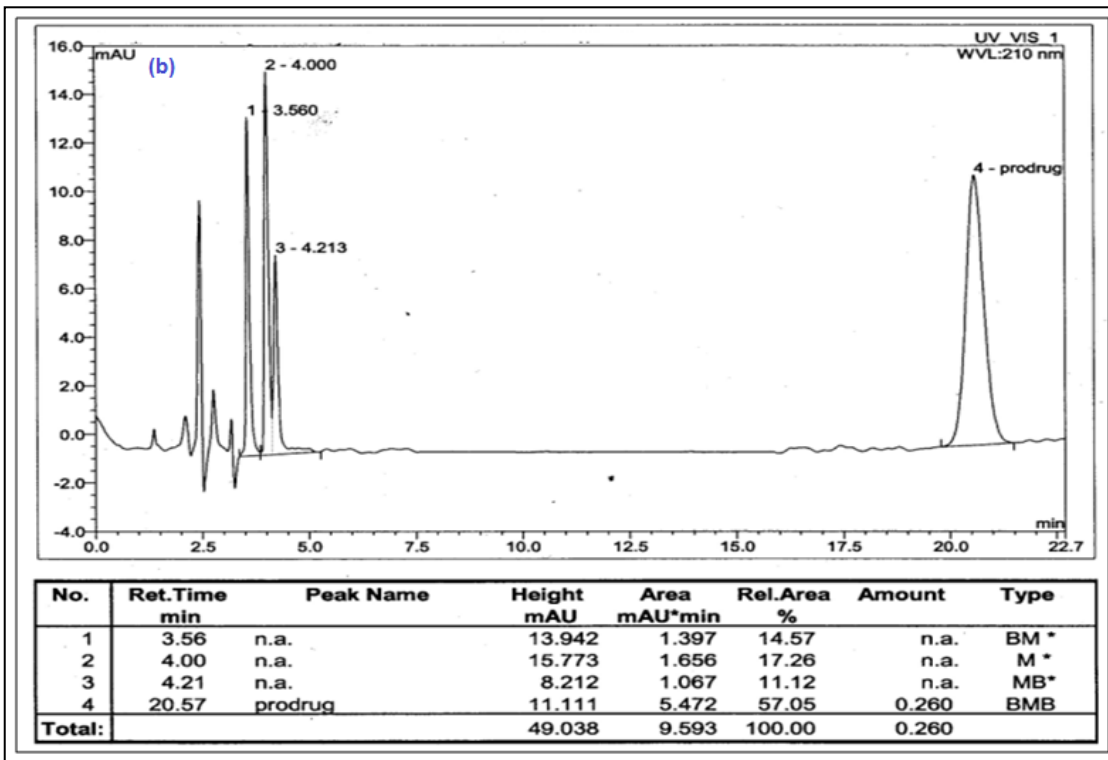
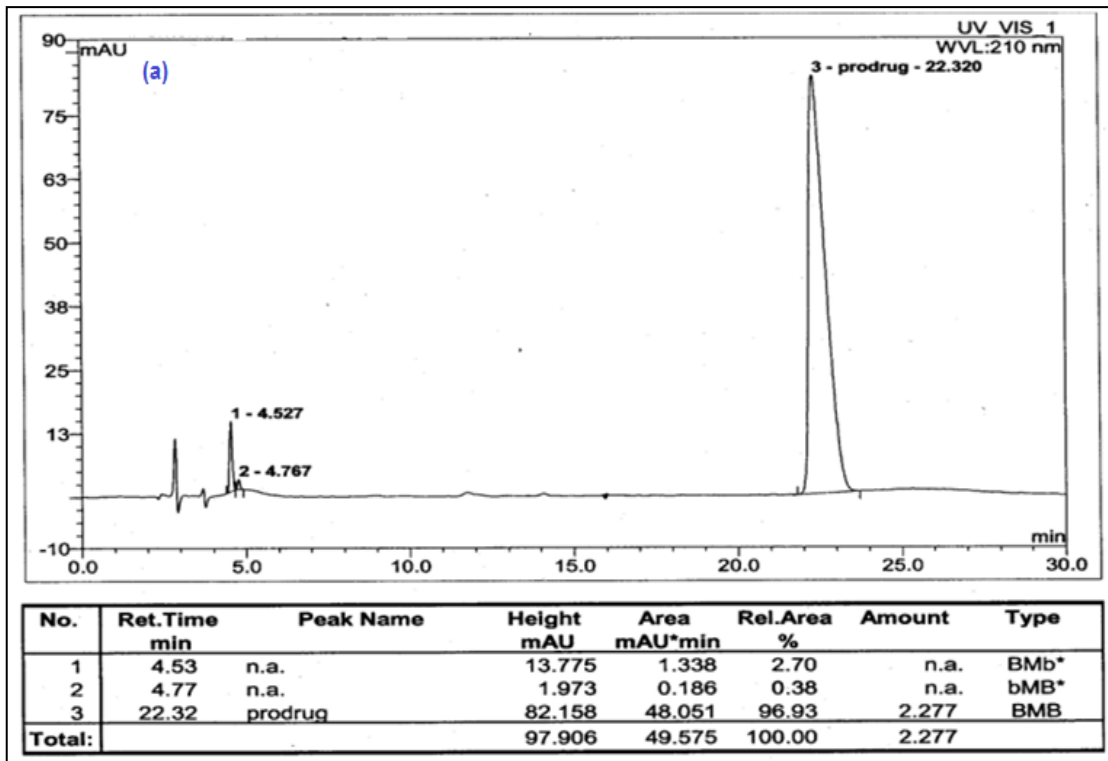


Figure 4-23: Chromatograms showing the intraconversion of ProD 2 at pH 3 after 2 hrs (a) and after 79 hrs (b).



**Figure 4-24:** Chromatograms showing the intraconversion of **ProD 2** at pH 6.8 after 1 hr (a) and after 380 hrs (b).

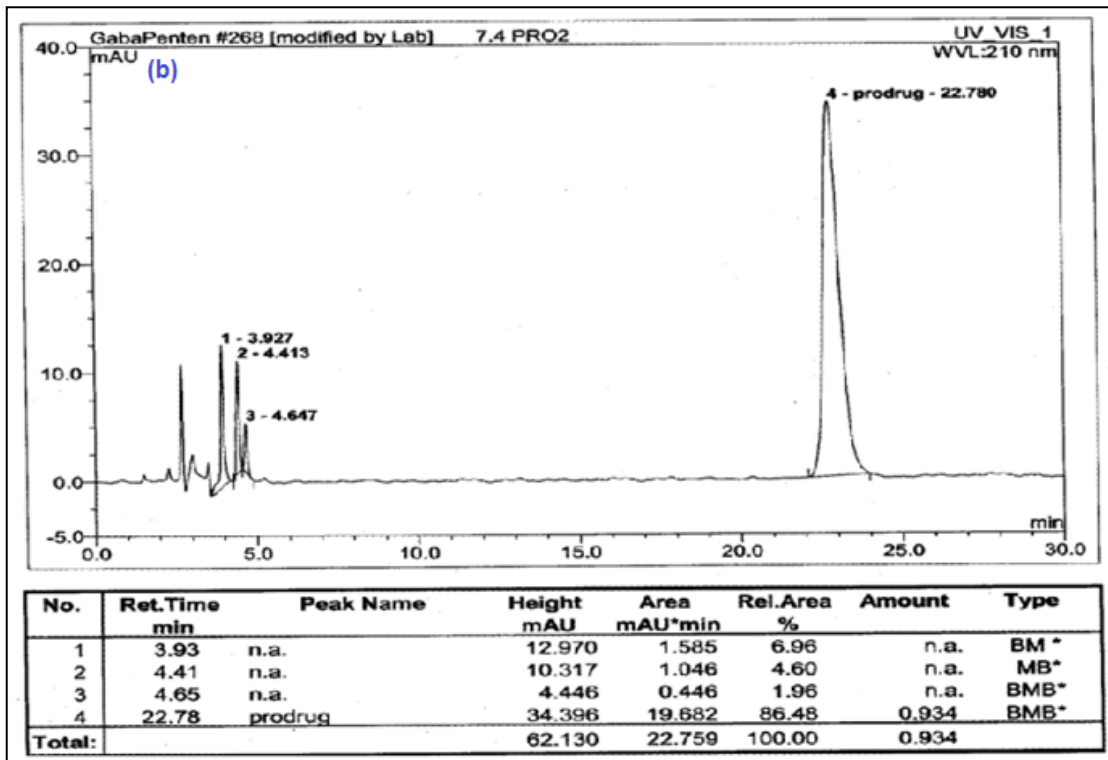
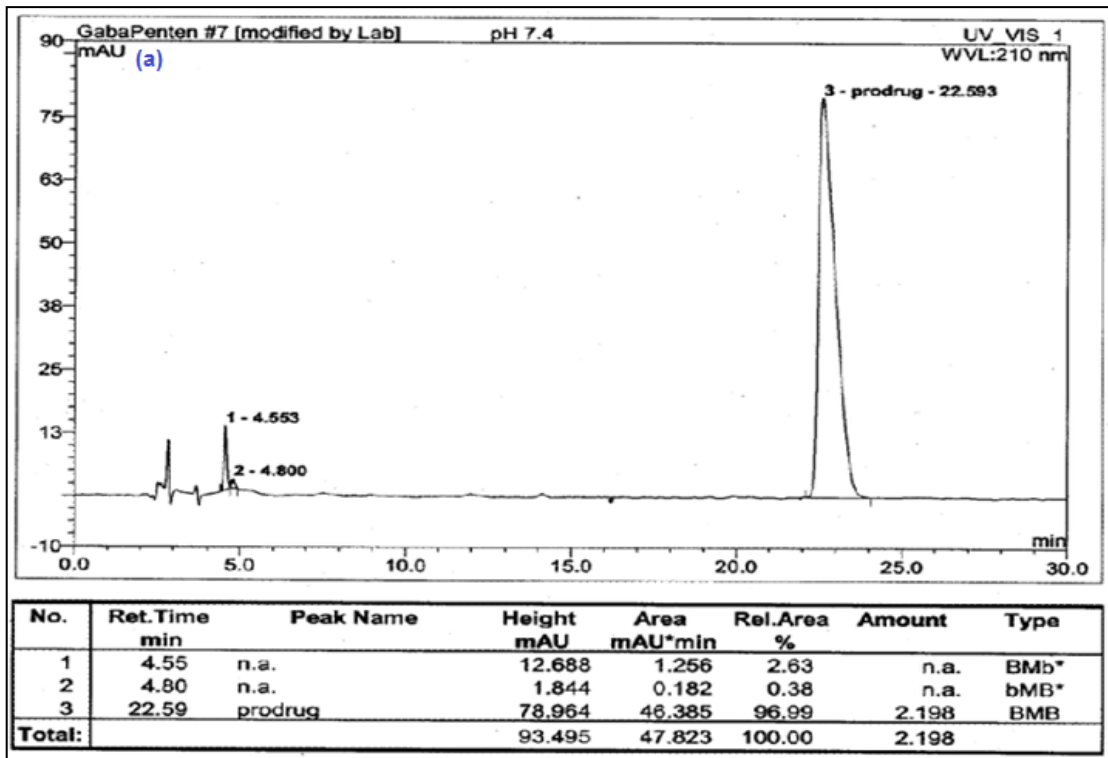
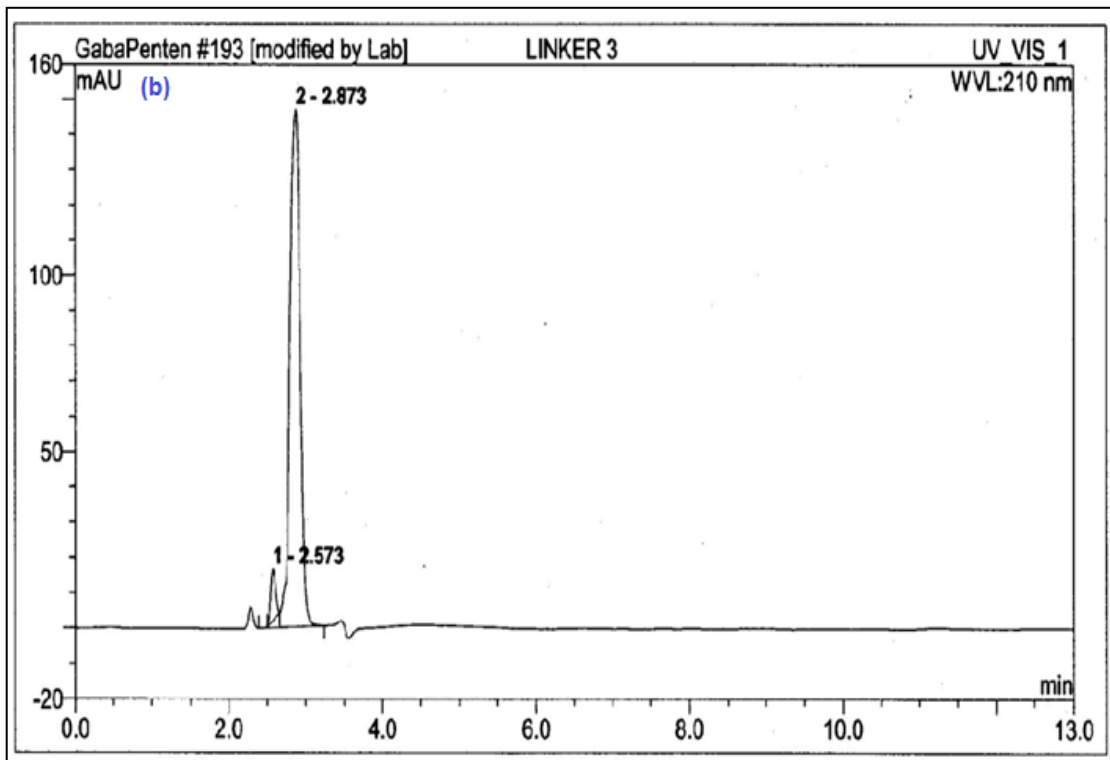
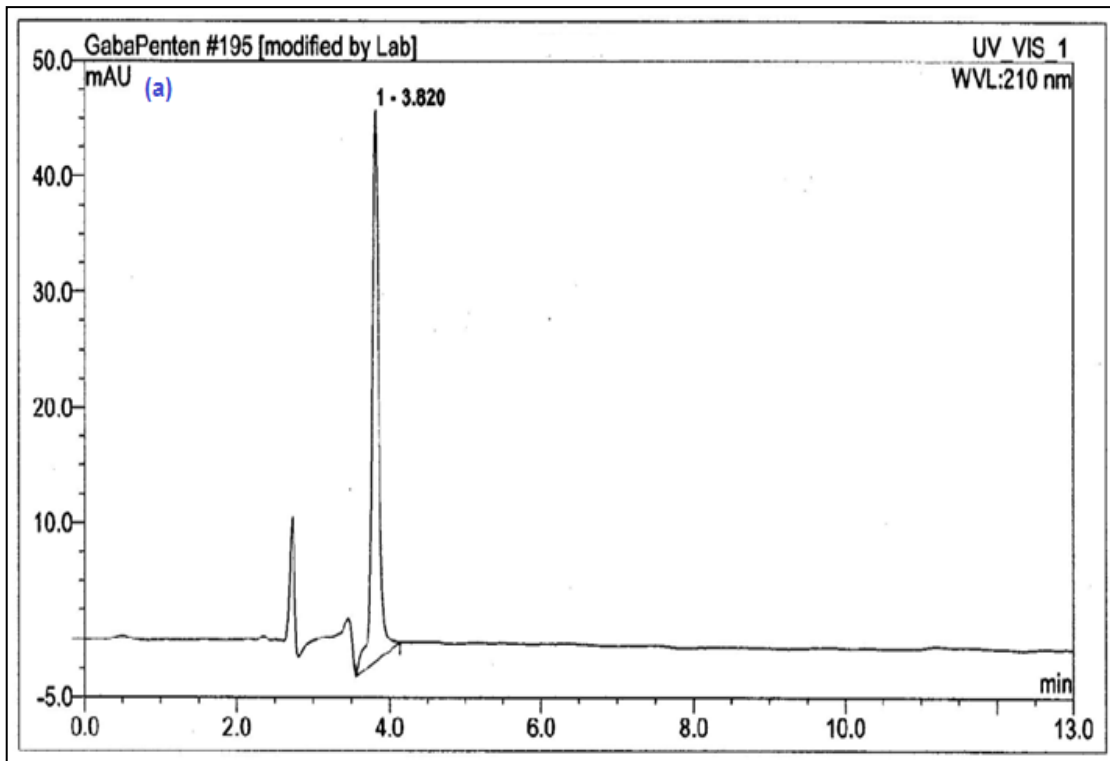
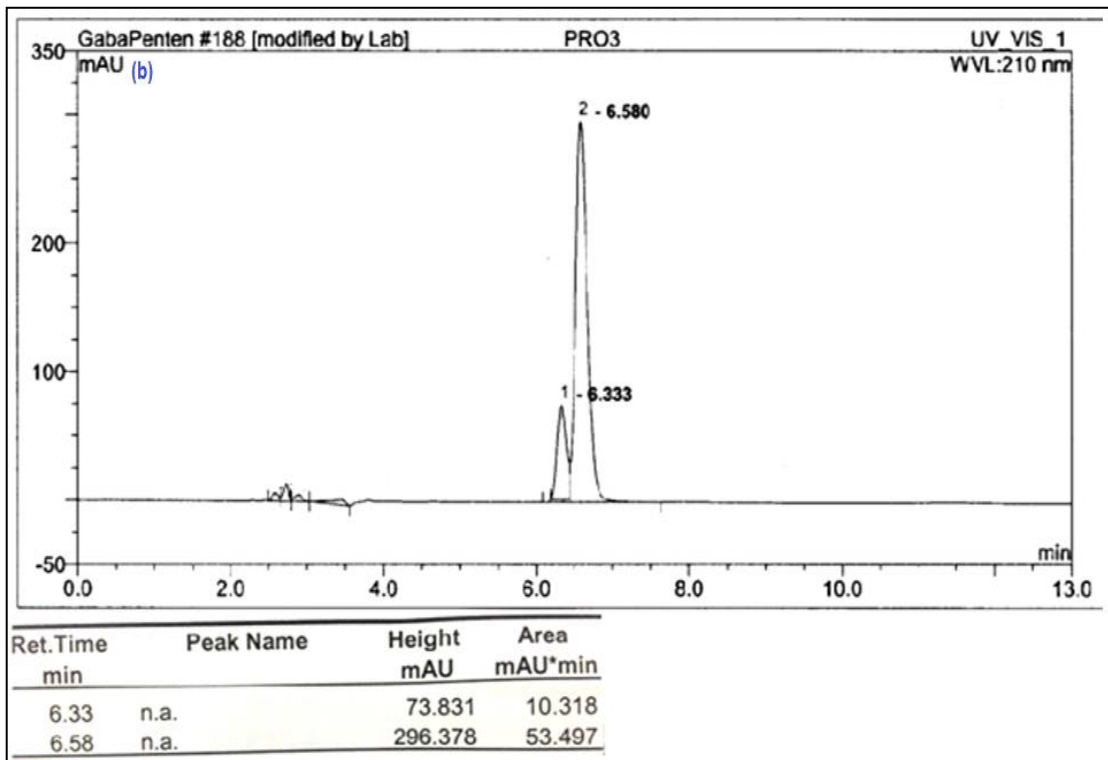
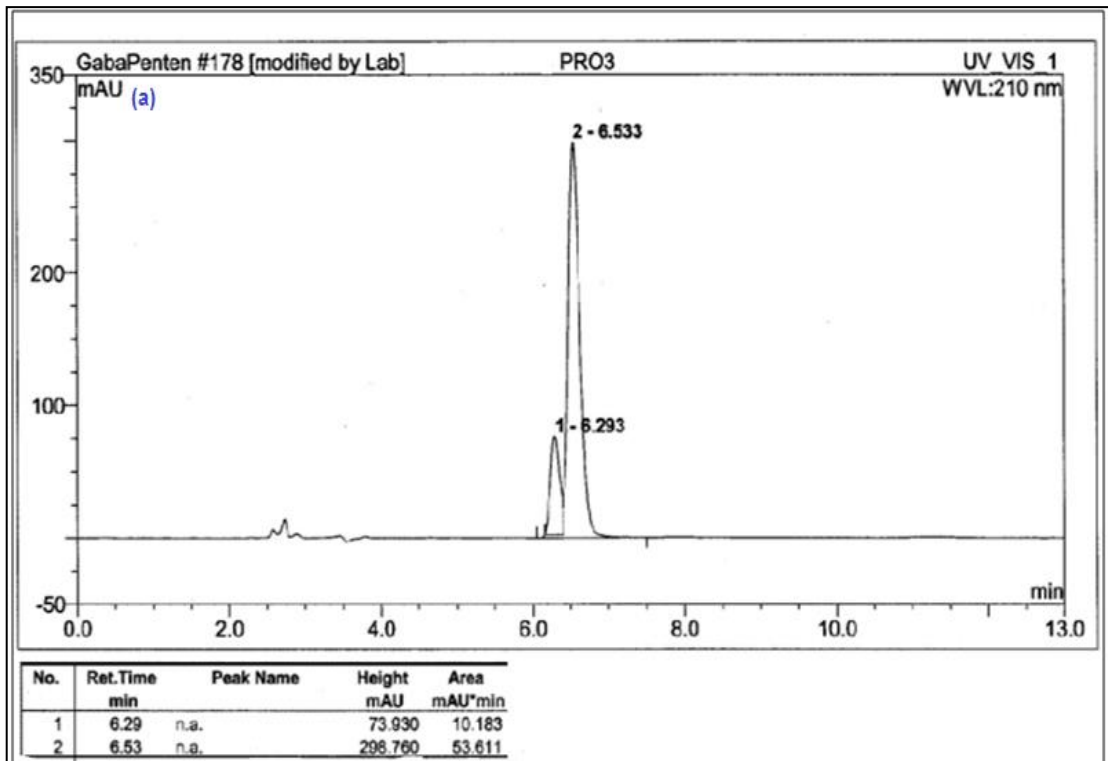


Figure 4-25: Chromatograms showing the intraconversion of ProD 2 at pH 7.4 after 5 hrs (a) and after 355 hrs (b).



**Figure 4-26:** Chromatograms showing gabapentin standard (a) and both linker 3 diastereomers (b) at gabapentin **ProD 3** HPLC conditions.



**Figure 4-27:** Chromatograms showing the stability of **ProD 3** at pH 7.4 after 1 hr (a) and after 168 hrs (b).

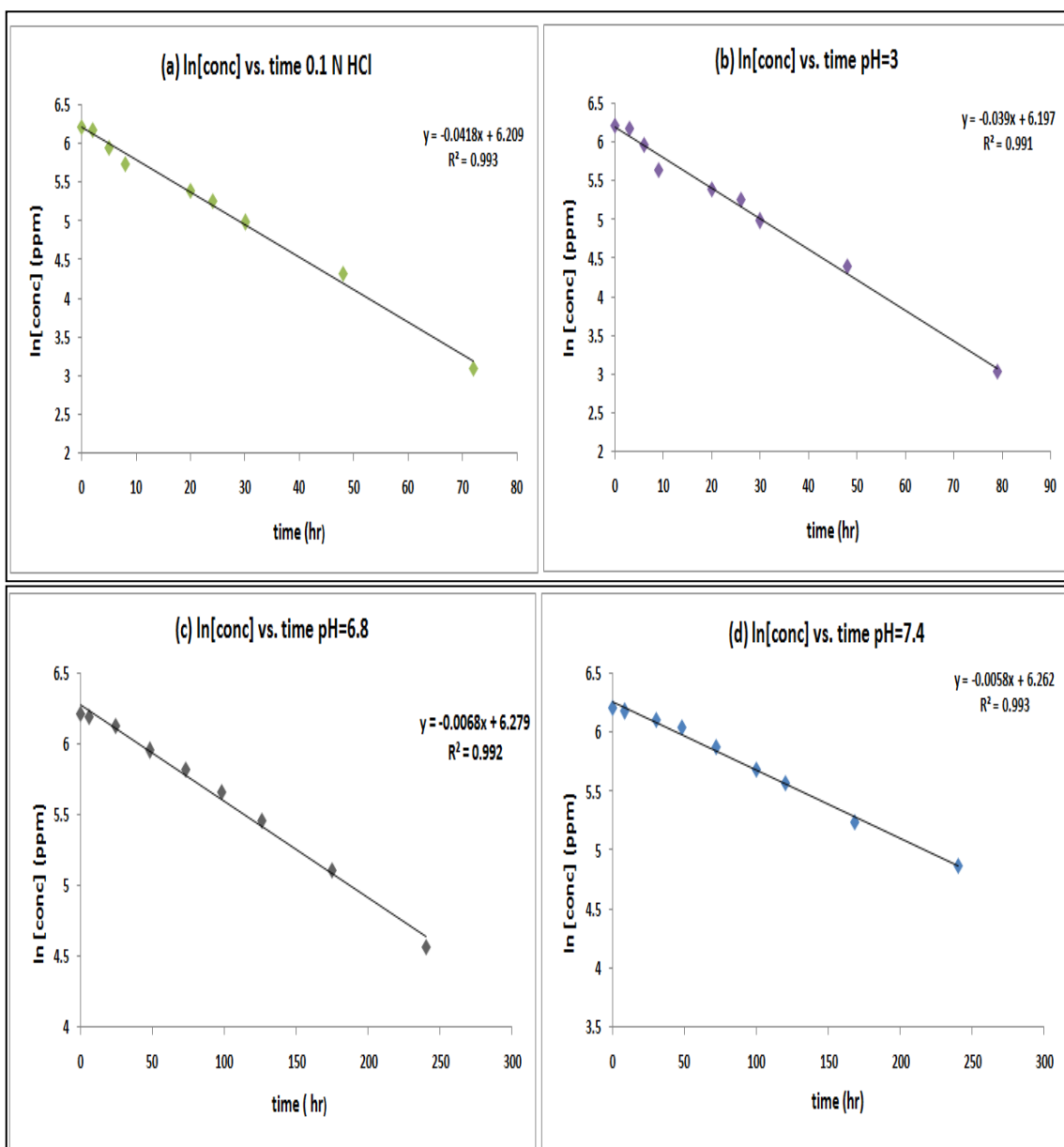


**Figure 4-28:** First order hydrolysis plot for both diastereomers of **ProD 1** in 0.1N HCL (a), buffer pH 3 (b), buffer pH 6.8 (c), and buffer pH 7.4 (d).

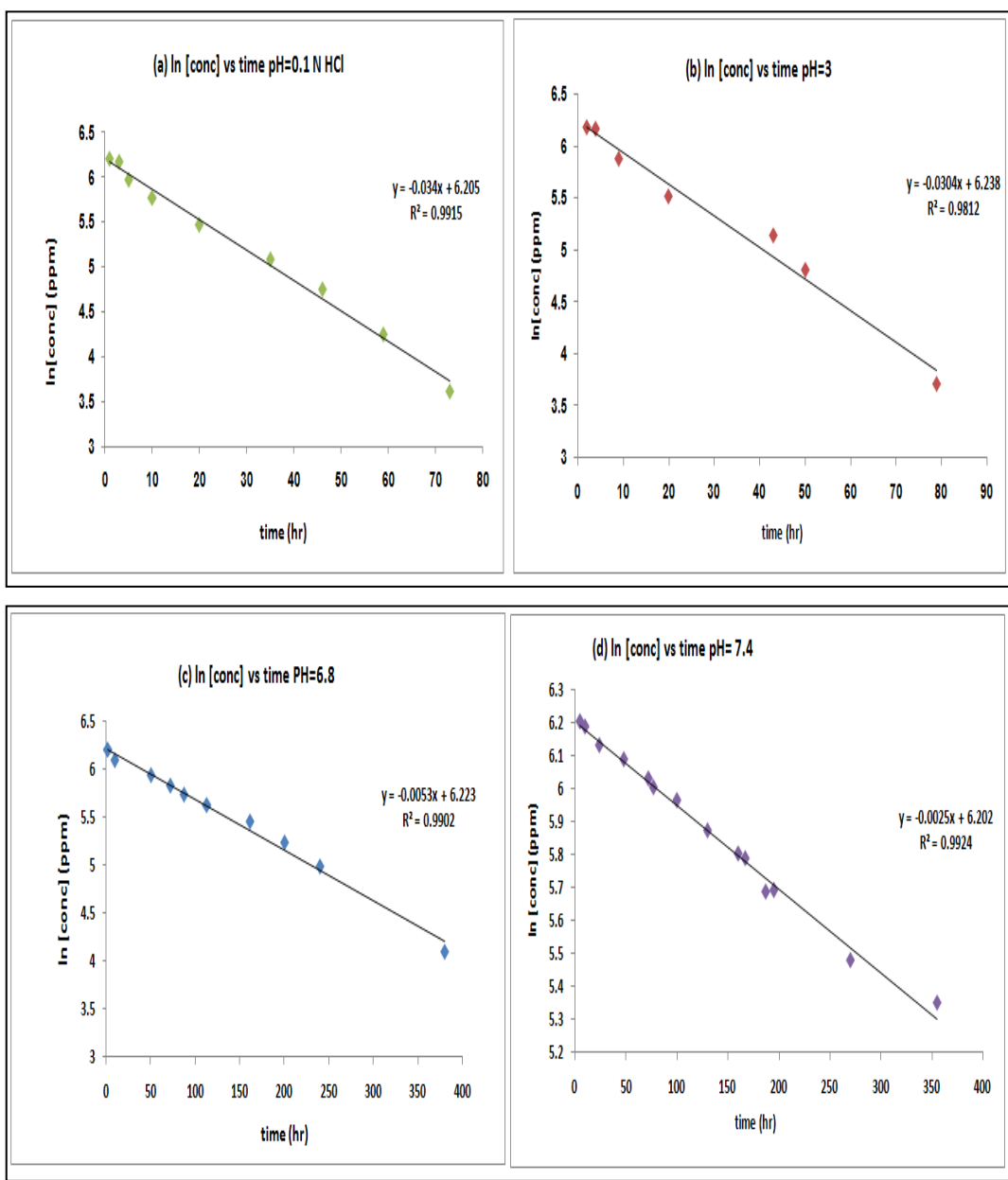


**Figure 4-29:** First order hydrolysis plot for **ProD 2** in 0.1N HCl (a), buffer pH 3 (b), buffer pH 6.8 (c), and buffer pH 7.4 (d).

**Table 4-1:** The  $k_{\text{obs}}$  value and  $t_{1/2}$  for the intraconversion of **ProD 1** in 0.1N HCl, pH 3, pH 6.8, and pH 7.4.

Medium	$k_{\text{obs}}(\text{hr}^{-1})$	$t_{1/2}$ (hr)
0.1N HCl	0.0418	16.57
Buffer pH 3	0.039	17.76
Buffer pH 6.8	0.0068	101.91
Buffer pH 7.4	0.0058	119.48

**Table 4-2:** The  $k_{\text{obs}}$  value and  $t_{1/2}$  for the intraconversion of **ProD 2** in 0.1N HCl, pH 3, pH 6.8, and pH 7.4.

Medium	$k_{\text{obs}}(\text{hr}^{-1})$	$t_{1/2}$ (hr)
0.1N HCl	0.0340	20.3
Buffer pH 3	0.0304	22.79
Buffer pH 6.8	0.0053	130.75
Buffer pH 7.4	0.0025	277.2

**Table 4-3:** The  $k_{\text{obs}}$  value and  $t_{1/2}$  for the intraconversion of **ProD 3** in 0.1N HCl, pH 3, pH 6.8, and pH 7.4.

Medium	$k_{\text{obs}}(\text{hr}^{-1})$	$t_{1/2}$ (hr)
0.1N HCl	No reaction	-----
Buffer pH 3	No reaction	-----
Buffer pH 6.8	No reaction	-----
Buffer pH 7.4	No reaction	-----

### **4.3 *In silico* prediction of physicochemical parameters, drug-likeness and CNS like properties for gabapentin ProD 1-3**

#### **4.3.1. Drug-likeness:**

The physicochemical properties of more than 2,000 biologically active compounds were evaluated by Lipinski *et al.* and subsequently what is known as “Lipinski’s rule of five” was conceived [168]. They concluded that ninety percent of orally active drugs that have successfully reached phase II clinical studies were associated with four physicochemical parameter ranges: (molecular weight < 500, partition coefficient ( $\log P$ ) < 5, H-bond donors < 5 and H-bond acceptors < 10), but it applies only to passive absorption. Thus, compounds that comply with these physicochemical properties, are predicted to be more membrane permeable and have drug-like properties [168,169].

Later, the ranges of some parameters were specified and other criteria added to the rule in order to enhance the prediction of drug-likeness. Such ranges include  $\log P$  -0.4 to +5.6, molecular weight 180 to 500 Da, molar refractivity 40 to 130, and a total number of atoms ranging 20 to 70 [170]. According to the values of physicochemical properties of the synthesized gabapentin prodrugs, all the synthesized prodrugs obey Lipinski’s rule of five and have drug-like properties (Table 4-4).

Moreover, Veber *et al.* suggested that compounds which meet only the two criteria of polar surface area equal to or less than  $140 \text{ \AA}^2$  and has 10 or fewer rotatable bonds are predicted to have high oral bioavailability [171]. All synthesized gabapentin prodrugs in this study meet these criteria (Table 4-4).

### 4.3.2. Molecular lipophilicity:

Lipophilicity is a significant molecular feature in medicinal chemistry and also in rationalized drug development and design. It affects the physiochemical properties of compounds such as permeability, toxicity, and bioavailability [172].

The n-octanol/water partition coefficient has been used to quantify lipophilicity of compounds for many years [173]. This coefficient is frequently defined as  $\log P$ , which is the ratio of the unionized compound concentration in 1-octanol to its concentration in water. Thus this coefficient is a measure of differential solubility of the compound between these two solvents [173]. Hansch and Fujita developed the first method for  $\log P$  calculation [174] and now several computational methods, including *in silico* tools, have been designed in order to predict  $\log P$  value. Lipinski states that a compound is more likely to have good absorption or permeability when the calculated  $\log P$  is  $< 5$  [164]. In addition, Hitchcock *et al.* Suggested a range of 2-5 for calculated  $\log P$  in order to increase the potential for BBB penetration [175]. Results of calculated  $\log P$  values using Chemicalize software showed that all values of the  $\log P$  for the synthesized gabapentin prodrugs were within these limits (Table 4-4).

### 4.3.3. Distribution coefficient ( $\log D$ ):

Log  $D$  is a pH-dependent version of  $\log P$  that takes into account the difference in lipophilicity of a drug in regard to the ionic states present at key biological pH values [176,177].

Since about 95% of all drugs are ionizable, it was suggested that  $\log D$  is a better descriptor for the lipophilicity of chemical compounds in physiological systems. Thus, Bhal *et al.* proposed that  $\log P$  should be replaced with  $\log D$  in ‘drug-likeness filters’ such as the rule of five [177]. Moreover, Van de Waterbeemd *et al.* demonstrated that, of a total of 125 compounds, all those acting in the CNS are within the ranges of  $1 \leq \log D$  (pH 7.5)  $\leq 4$  [178]. Chemicalize software was used for the calculation of  $\log D$  values of the synthesized gabapentin prodrugs. Results showed that all synthesized gabapentin prodrugs were within this range (Table 4-1).

#### 4.3.4. Aqueous solubility ( $\log S$ ):

Solubility is a common and challenging physicochemical parameter for drug discovery. The aqueous solubility of a drug is essential as it considerably affects its absorption and distribution characteristics. Generally, a low soluble drug is avoidable because it frequently has poor absorption. In 2010, Alelyunas *et al.* showed that the aqueous solubility at pH 7.4 is a significant prerequisite for a CNS targeted drug [179]. All the synthesized gabapentin prodrugs were predicted by Chemicalize program to be highly soluble at pH 6.8 and 7.4. However, **ProD 3** has poor solubility at pH 3 and 0.1 N HCl (Table 4-2).

#### 4.3.5. *In silico* prediction of BBB permeability and $\log BB$ :

Designing drugs that can penetrate the BBB and have an adequate concentration at the desired therapeutic target in the CNS is a significant challenge for medicinal chemists working in CNS drug development [180].

BBB permeability software predicted that gabapentin **ProD 1-3** have the capability to pass the BBB. Abraham *et al.* suggested that compounds with log BB less than -1.0 will not cross through the BBB, while compounds with log BB equal to or more than -1.0 are predicted to enter to CNS [180]. All the synthesized gabapentin prodrugs were predicted to have  $\log BB \geq -1$ .

**Table 4-4:** Physiochemical properties and drug-likeness of the gabapentin and its synthesized prodrugs.

Physiochemical properties	Drug-like criteria	Gabapentin	ProD 1	ProD 2	ProD 3	
<b>Molecular weight</b>	< 500	171.23	339.43	325.4	353.45	
<b>No. of Hydrogen Bond Donors</b>	< 5	2	3	3	3	
<b>No. of Hydrogen Bond Acceptors</b>	< 10	3	6	6	6	
<b>log P</b>	< 5	-1.9	2.527	2.326	2.983	
<b>log D at pH 7.4</b>	$-1 \leq \log D (\text{pH } 7.4) \leq 3$	-1.25	1.279	1.078	1.734	
<b>TPSA</b>	<140 Angstrom ( $\text{\AA}^2$ )	63.32 $\text{\AA}^2$	103.7 $\text{\AA}^2$	103.7 $\text{\AA}^2$	103.7 $\text{\AA}^2$	
<b>Molar Refractivity</b>	40 to 130 $\text{cm}^3$	46.33 $\text{cm}^3$	87.76 $\text{cm}^3$	83.05 $\text{cm}^3$	92.37 $\text{cm}^3$	
<b>No. of Rotatable Bonds</b>	$\leq 10$	3	6	6	6	
<b>Total number of atoms</b>	20 to 70	29	53	50	56	

**Table 4-5:** CNS like properties for gabapentin and its synthesized prodrugs.

Physiochemical properties.	CNS-like criteria	Gabapentin	ProD1	ProD2	ProD3	✓ ✗
<b>log BB</b>	Log BB $\geq$ -1 [180].	-0.19	-0.704	-0.89	-1	✓
<b>Molecular weight</b>	MW < 450 [181,182].	171.25	339.43	325.4	353.45	✓
<b>log P</b>	2-5 [175].	-1.9	2.527	2.326	2.983	✓
<b>log D at pH 7.4</b>	$1 \leq \log D$ (pH 7.4) $\leq$ 4 [181].	-1.25	1.279	1.078	1.734	✓
<b>Log S</b>	$-4 < \log S < 0$ [182].	-1.6	-3.499	-3.125	-3.769	✓

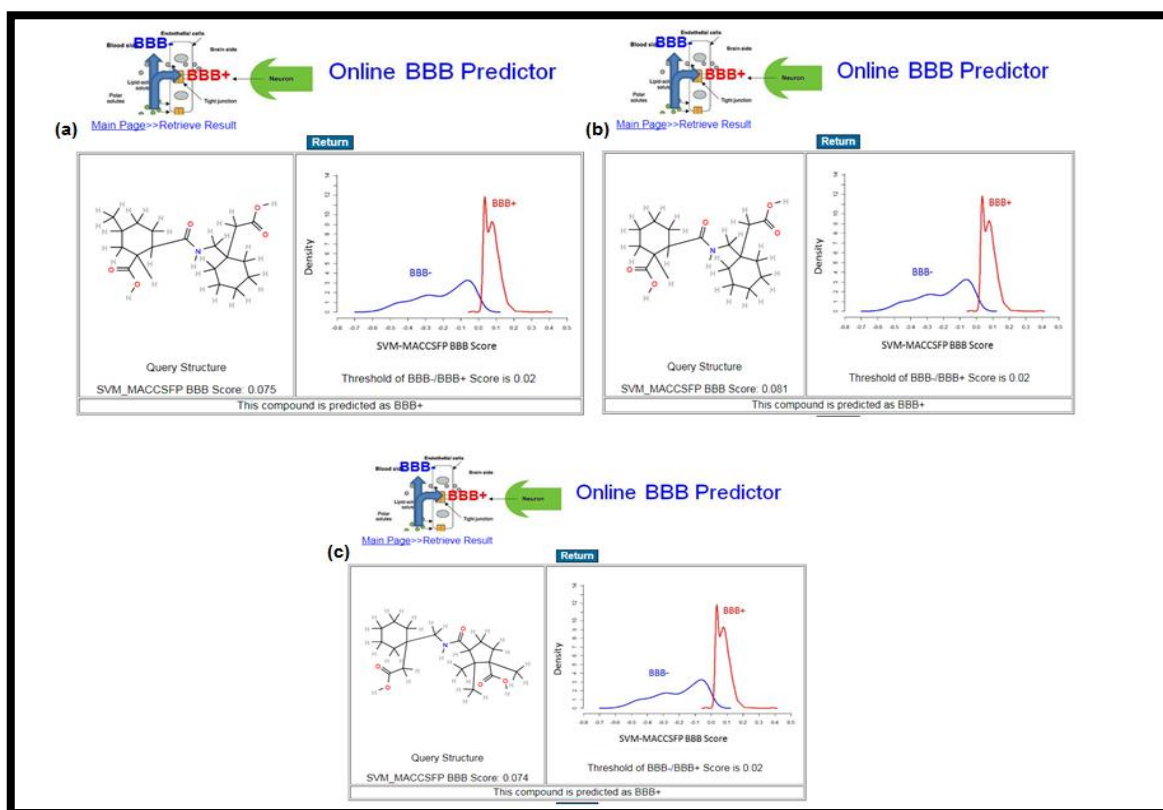


**Figure 4-30:** BBB permeability prediction for **ProD 1** (a), **ProD 2** (b), and **ProD 3** (c).

#### 4.4 *In silico* ADMET prediction

*In silico* pharmacokinetic properties and toxicity were studied using PreADME software for all three gabapentin prodrugs. The results of the pharmacokinetic and toxicity predictions (Table 4-6) showed that all the prodrugs showed good pharmacokinetic properties. For example, Yee *et al.* suggested that compound with human intestinal absorption (HIA) more than 70 will be classified as a well-absorbed compound and compound with colorectal adenocarcinoma cell lines (caco2) value more than 4 will be absorbed by the intestine [183]. All synthesized gabapentin prodrugs predicted to have HIA values more than 70 and caco2 values more than 4 (Table 4-6). Furthermore, the synthesized gabapentin prodrugs are predicted to be non-inhibitors for the CYP enzymes or P-glycoprotein (Pgp), which means to have less drug-drug interactions [101,184] (Table 4-6). In addition, none of the prodrugs had a high risk of toxicity or mutagenicity.

**Table 4-6:** ADMET prediction for **ProD 1** (a), **ProD 2** (b), and **ProD 3** (c).

(a). ADME – PreADMET		(b).ADME – PreADMET		(c).ADME – PreADMET	
ID	Value	ID	Value	ID	Value
BBB	0.197529	BBB	0.126739	BBB	0.0885924
Buffer_solubility_mg_L	351877	Buffer_solubility_mg_L	370206	Buffer_solubility_mg_L	622239
Caco2	20.6114	Caco2	20.4834	Caco2	20.9996
CYP_2C19_inhibition	Non	CYP_2C19_inhibition	Non	CYP_2C19_inhibition	Non
CYP_2C9_inhibition	Non	CYP_2C9_inhibition	Non	CYP_2C9_inhibition	Non
CYP_2D6_inhibition	Non	CYP_2D6_inhibition	Non	CYP_2D6_inhibition	Non
CYP_2D6_substrate	Non	CYP_2D6_substrate	Non	CYP_2D6_substrate	Non
CYP_3A4_inhibition	Non	CYP_3A4_inhibition	Non	CYP_3A4_inhibition	Non
CYP_3A4_substrate	Weakly	CYP_3A4_substrate	Non	CYP_3A4_substrate	Substrate
HIA	77.109811	HIA	74.179022	HIA	79.651273
Plasma_Protein_Binding	84.195908	Plasma_Protein_Binding	85.685802	Plasma_Protein_Binding	75.739832
Pgp_inhibition	Non	Pgp_inhibition	Non	Pgp_inhibition	Non
Plasma_Protein_Binding	84.195908	Plasma_Protein_Binding	85.685802	Plasma_Protein_Binding	75.739832
Pure_water_solubility_mg_L	107.575	Pure_water_solubility_mg_L	243.71	Pure_water_solubility_mg_L	60.1225

## **Chapter Five**

### **Conclusion and Future direction**

## Chapter Five

### 5. Conclusion and Future direction

#### 5.1 Conclusion

Gabapentin has pharmacokinetic limitations which limit its clinical effectiveness. For example, it has dose-dependent bioavailability. Consequently, there is need to synthesize prodrugs of gabapentin that have the potential for higher and more predictable bioavailability than the current medications when given in different dosage forms. Moreover, they should have the ability to hydrolyze to gabapentin *via* intramolecular reaction and without any need for enzyme catalysis.

Based on Kirby's enzyme model (Proton transfer in N-alkylmaleamic acids), three different gabapentin prodrugs were synthesized and characterized. These prodrugs have a carboxylic group as a hydrophilic moiety and the rest of the prodrug as a lipophilic moiety, where the combination of both moieties secures a modified HLB. Thus, the synthesized gabapentin prodrugs were expected to have predictable and enhanced bioavailability in comparison to gabapentin as a result of improving its passive transport. Moreover, the synthesized prodrugs can be used in many dosage forms such as enteric coated tablets. In *vitro* intraconversion of these prodrugs to their parent drug, gabapentin, showed that  $t_{1/2}$  was highly affected by the pH of the medium, the pKa of the linker, and the distance between the two reactive centers. Gabapentin **ProD 1** was readily hydrolyzed in 0.1N HCl, buffer pH 3, buffer pH 6.8, and buffer pH 7.4 with experimental  $t_{1/2}$  values of 16.57 hrs, 17.76 hrs, 101.91 hrs and 191.48 hrs, respectively. The experimental  $t_{1/2}$  values for gabapentin **ProD 2** in 0.1N HCl and pH 3, pH 6.8 and pH 7.4 were 20.3 hrs, 22.79 hrs, 130.75 hrs and 277.2 hrs, respectively.

However, **ProD 3** was extremely insoluble in 0.1 N HCl and pH 3. Moreover, it was found to be completely stable at pH 6.8 and pH 7.4 and no reaction was observed. This is due to the comparatively low pKa of its linker.

*In silico* prediction of the pharmacokinetic and toxicity parameters of the synthesized gabapentin prodrugs found that all have favorable pharmacokinetic features, drug-like, and have a low risk of toxicity.

## 5.2 Future directions

Synthesis of additional gabapentin prodrugs that may be immediately intraconverted to their parent drug, gabapentin, at pH 7.4 (blood circulation system) by using linkers having pKa close to that of the blood circulation (pH 7.4).

Moreover, *In vivo* pharmacokinetic studies will be done for both **ProD 1** and **ProD 2** in order to determine the bioavailability and the duration of action of the tested prodrugs.

Finally, we will evaluate if our newly synthesized prodrugs have pharmacological activity before they undergo hydrolysis because they have a programmable release manner.

## References

1. Costigan, M., Scholz, J., & Woolf, C. J. (2009). Neuropathic pain: a maladaptive response of the nervous system to damage. *Annual review of neuroscience*, 32, 1-32.
2. Fields, H. L., Rowbotham, M., & Baron, R. (1998). Postherpetic neuralgia: irritable nociceptors and deafferentation. *Neurobiology of disease*, 5(4), 209-227.
3. Bennett, M. I., Attal, N., Backonja, M. M., Baron, R., Bouhassira, D., Freynhagen, R., ... & Jensen, T. S. (2007). Using screening tools to identify neuropathic pain. *Pain*, 127(3), 199-203.
4. Finnerup, N. B., Haroutounian, S., Kamerman, P., Baron, R., Bennett, D. L., Bouhassira, D., ... & Raja, S. N. (2016). Neuropathic pain: an updated grading system for research and clinical practice. *Pain*, 157(8), 1599.
5. Garry, E. M., Delaney, A., Anderson, H. A., Sirinathsinghji, E. C., Clapp, R. H., Martin, W. J., ... & Fleetwood-Walker, S. M. (2005). Varicella zoster virus induces neuropathic changes in rat dorsal root ganglia and behavioral reflex sensitisation that is attenuated by gabapentin or sodium channel blocking drugs. *Pain*, 118(1-2), 97-111.
6. Baron, R., Binder, A., & Wasner, G. (2010). Neuropathic pain: diagnosis, pathophysiological mechanisms, and treatment. *The Lancet Neurology*, 9(8), 807-819.
7. Premkumar, L. S. (2010). Targeting TRPV1 as an alternative approach to narcotic analgesics to treat chronic pain conditions. *The AAPS journal*, 12(3), 361-370.
8. VanDenKerkhof, E. G., Mann, E. G., Torrance, N., Smith, B. H., Johnson, A., & Gilron, I. (2016). An epidemiological study of neuropathic pain symptoms in Canadian adults. *Pain Research and Management*, 2016.
9. Bowsher, D. (1999). The lifetime occurrence of herpes zoster and prevalence of post-herpetic neuralgia: a retrospective survey in an elderly population. *European journal of pain*, 3(4), 335-342.
10. Hall, G. C., Carroll, D., Parry, D., & McQuay, H. J. (2006). Epidemiology and treatment of neuropathic pain: the UK primary care perspective. *Pain*, 122(1-2), 156-162.
11. Doth, A. H., Hansson, P. T., Jensen, M. P., & Taylor, R. S. (2010). The burden of neuropathic pain: a systematic review and meta-analysis of health utilities. *Pain®*, 149(2), 338-344.
12. Langley, P. C., Van Litsenburg, C., Cappelleri, J. C., & Carroll, D. (2013). The burden associated with neuropathic pain in Western Europe. *Journal of medical economics*, 16(1), 85-95.
13. Dworkin, R. H., Backonja, M., Rowbotham, M. C., Allen, R. R., Argoff, C. R., Bennett, G. J., ... & Hewitt, D. J. (2003). Advances in neuropathic pain: diagnosis, mechanisms, and treatment recommendations. *Archives of neurology*, 60(11), 1524-1534.
14. Foley, P. L., Vesterinen, H. M., Laird, B. J., Sena, E. S., Colvin, L. A., Chandran, S., ... & Fallon, M. T. (2013). Prevalence and natural history of pain in adults with multiple sclerosis: systematic review and meta-analysis. *PAIN®*, 154(5), 632-642.

15. Woolf, C. J., & Mannion, R. J. (1999). Neuropathic pain: aetiology, symptoms, mechanisms, and management. *The lancet*, 353(9168), 1959-1964.
16. Marchettini, P., Lacerenza, M., Mauri, E., & Marangoni, C. (2006). Painful peripheral neuropathies. *Current neuropharmacology*, 4(3), 175-181.
17. Singh, R., Kishore, L., & Kaur, N. (2014). Diabetic peripheral neuropathy: current perspective and future directions. *Pharmacological research*, 80, 21-35.
18. Oates, P. J. (2002). Polyol pathway and diabetic peripheral neuropathy. *International review of neurobiology*, 50, 325-392.
19. Ishii, H., Koya, D., & King, G. L. (1998). Protein kinase C activation and its role in the development of vascular complications in diabetes mellitus. *Journal of Molecular Medicine*, 76(1), 21-31.
20. Kemp, J. A. (2001). The South African Dental Association and dentists in the field. *SADJ: journal of the South African Dental Association= tydskrif van die Suid-Afrikaanse Tandheelkundige Vereniging*, 56(1), 10-1.
21. Brisson, M., Edmunds, W. J., Law, B., Gay, N. J., Walld, R., Brownell, M., ... & De Serres, G. (2001). Epidemiology of varicella zoster virus infection in Canada and the United Kingdom. *Epidemiology & Infection*, 127(2), 305-314.
22. Insinga, R. P., Itzler, R. F., Pellissier, J. M., Saddier, P., & Nikas, A. A. (2005). The incidence of herpes zoster in a United States administrative database. *Journal of general internal medicine*, 20(8), 748-753.
23. Dworkin, R. H., & Schmader, K. E. (2001). The epidemiology and natural history of herpes zoster and postherpetic neuralgia. *Pain Research and Clinical Management*, 11, 39-64.
24. Drolet, M., Brisson, M., Schmader, K., Levin, M., Johnson, R., Oxman, M., ... & Mansi, J. A. (2010). Predictors of postherpetic neuralgia among patients with herpes zoster: a prospective study. *The Journal of Pain*, 11(11), 1211-1221.
25. Baron, R. (2008). Mechanisms of postherpetic neuralgia—we are hot on the scent.
26. Burchiel, K. J. (2003). A new classification for facial pain. *Neurosurgery*, 53(5), 1164-1167.
27. Eller, J. L., Raslan, A. M., & Burchiel, K. J. (2005). Trigeminal neuralgia: definition and classification. *Neurosurgical focus*, 18(5), 1-3.
28. Love, S., & Coakham, H. B. (2001). Trigeminal neuralgia: pathology and pathogenesis. *Brain*, 124(12), 2347-2360.
29. Max, M. B., Schafer, S. C., Culnane, M., Smoller, B., Dubner, R., & Gracely, R. H. (1988). Amitriptyline, but not lorazepam, relieves postherpetic neuralgia. *Neurology*, 38(9), 1427-1427.
30. Moore, R. A., Chi, C. C., Wiffen, P. J., Derry, S., & Rice, A. S. C. (2013). Oral nonsteroidal anti-inflammatory drugs for neuropathic pain. *Cochrane Database Syst Rev*, 12.
31. Derry, S., Rice, A. S., Cole, P., Tan, T., & Moore, R. A. (2017). Topical capsaicin (high concentration) for chronic neuropathic pain in adults. *The Cochrane Library*.
32. Seidel, S., Aigner, M., Wildner, B., Sycha, T., & Pablik, E. (2018). Antipsychotics for the treatment of neuropathic pain in adults. *The Cochrane Library*.
33. Stannard, C., Gaskell, H., Derry, S., Aldington, D., Cole, P., Cooper, T. E., ... & Moore, R. A. (2016). Hydromorphone for neuropathic pain in adults. *The Cochrane Library*.
34. Gaskell, H., Derry, S., Stannard, C., & Moore, R. A. (2016). Oxycodone for neuropathic pain in adults. *The Cochrane Library*.

35. Derry, S., & Moore, R. A. (2012). Topical capsaicin (low concentration) for chronic neuropathic pain in adults. *The Cochrane Library*.
36. Derry, S., Wiffen, P. J., Moore, R. A., & Quinlan, J. (2014). Topical lidocaine for neuropathic pain in adults. *Cochrane Database Syst Rev*, 7.
37. Cruccu, G., & Truini, A. (2017). A review of Neuropathic Pain: From Guidelines to Clinical Practice. *Pain and therapy*, 6(1), 35-42.
38. Sultan, A., Gaskell, H., Derry, S., & Moore, R. A. (2008). Duloxetine for painful diabetic neuropathy and fibromyalgia pain: systematic review of randomised trials. *BMC neurology*, 8(1), 29.
39. Sumpton, J. E., & Moulin, D. E. (2001). Treatment of neuropathic pain with venlafaxine. *Annals of Pharmacotherapy*, 35(5), 557-559.
40. Moore, R. A., Cai, N., Skljarevski, V., & Tölle, T. R. (2014). Duloxetine use in chronic painful conditions—individual patient data responder analysis. *European Journal of Pain*, 18(1), 67-75.
41. Moore, R. A., Derry, S., Aldington, D., Cole, P., & Wiffen, P. J. (2015). Amitriptyline for neuropathic pain in adults. *The Cochrane Library*.
42. Moore, R. A., Straube, S., Wiffen, P. J., Derry, S., & McQuay, H. J. (2009). Pregabalin for acute and chronic pain in adults. *The Cochrane Library*.
43. Moore, R. A., Wiffen, P. J., Derry, S., & McQuay, H. J. (2011). Gabapentin for chronic neuropathic pain and fibromyalgia in adults. *Cochrane Database Syst Rev*, 3.
44. Wiffen, P. J., Derry, S., Moore, R. A., Aldington, D., Cole, P., Rice, A. S., ... & Kalso, E. A. (2013). Antiepileptic drugs for neuropathic pain and fibromyalgia. *status and date: New, published in*, (6).
45. O'Connor, A. B., & Dworkin, R. H. (2009). Treatment of neuropathic pain: an overview of recent guidelines. *The American journal of medicine*, 122(10), S22-S32.
46. Gore, M., Brandenburg, N. A., Dukes, E., Hoffman, D. L., Tai, K. S., & Stacey, B. (2005). Pain severity in diabetic peripheral neuropathy is associated with patient functioning, symptom levels of anxiety and depression, and sleep. *Journal of pain and symptom management*, 30(4), 374-385.
47. Remick, R. A. (1988). Anticholinergic side effects of tricyclic antidepressants and their management. *Progress in neuro-psychopharmacology & biological psychiatry*.
48. Jefferson, J. W. (1975). A review of the cardiovascular effects and toxicity of tricyclic antidepressants. *Psychosomatic Medicine*.
49. Roose, S. P., Laghrissi-Thode, F., Kennedy, J. S., Nelson, J. C., Bigger Jr, J. T., Pollock, B. G., ... & Gergel, I. (1998). Comparison of paroxetine and nortriptyline in depressed patients with ischemic heart disease. *Jama*, 279(4), 287-291.
50. Dworkin, R. H., O'connor, A. B., Backonja, M., Farrar, J. T., Finnerup, N. B., Jensen, T. S., ... & Portenoy, R. K. (2007). Pharmacologic management of neuropathic pain: evidence-based recommendations. *Pain*, 132(3), 237-251.
51. Raskin, J., Smith, T. R., Wong, K., Pritchett, Y. L., D'souza, D. N., Iyengar, S., & Wernicke, J. F. (2006). Duloxetine versus routine care in the long-term management of diabetic peripheral neuropathic pain. *Journal of palliative medicine*, 9(1), 29-40.

52. Mowla, A., Dastgheib, S. A., & Jahromi, L. R. (2016). Comparing the Effects of Sertraline with Duloxetine for Depression Severity and Symptoms: A Double-Blind, Randomized Controlled Trial. *Clinical drug investigation*, 36(7), 539-543.
53. Schukro, R. P., Oehmke, M. J., Geroldinger, A., Heinze, G., Kress, H. G., & Pramhas, S. (2016). Efficacy of Duloxetine in Chronic Low Back Pain with a Neuropathic Component A Randomized, Double-blind, Placebo-controlled Crossover Trial. *Anesthesiology: The Journal of the American Society of Anesthesiologists*, 124(1), 150-158.
54. Rowbotham, M. C., Goli, V., Kunz, N. R., & Lei, D. (2004). Venlafaxine extended release in the treatment of painful diabetic neuropathy: a double-blind, placebo-controlled study. *Pain*, 110(3), 697-706.
55. Whyte, I. M., Dawson, A. H., & Buckley, N. A. (2003). Relative toxicity of venlafaxine and selective serotonin reuptake inhibitors in overdose compared to tricyclic antidepressants. *Qjm*, 96(5), 369-374.
56. Möller, H. J., Baldwin, D. S., Goodwin, G., Kasper, S., Okasha, A., Stein, D. J., ... & Versiani, M. (2008). Do SSRIs or antidepressants in general increase suicidality?. *European Archives of Psychiatry and Clinical Neuroscience*, 258(3), 3-23.
57. Simon, G. E., Savarino, J., Operskalski, B., & Wang, P. S. (2006). Suicide risk during antidepressant treatment. *American Journal of Psychiatry*, 163(1), 41-47.
58. Taylor, C. P. (2009). Mechanisms of analgesia by gabapentin and pregabalin—Calcium channel  $\alpha 2\text{-}\delta$  [Cava $2\text{-}\delta$ ] ligands. *Pain*, 142(1-2), 13-16.
59. Gilron, I. (2007). Gabapentin and pregabalin for chronic neuropathic and early postsurgical pain: current evidence and future directions. *Current Opinion in Anesthesiology*, 20(5), 456-472.
60. Ho, J. M., Tricco, A. C., Perrier, L., Chen, M., Juurlink, D. N., & Straus, S. E. (2013). Risk of heart failure and edema associated with the use of pregabalin: a systematic review. *Systematic reviews*, 2(1), 25.
61. Murphy, N., Mockler, M., Ryder, M., Ledwidge, M., & McDonald, K. (2007). Decompensation of chronic heart failure associated with pregabalin in patients with neuropathic pain. *Journal of cardiac failure*, 13(3), 227-229.
62. Robert Lee Page, I. I., Cantu, M., Lindenfeld, J., Hergott, L. J., & Lowes, B. D. (2008). Possible heart failure exacerbation associated with pregabalin: case discussion and literature review. *Journal of Cardiovascular Medicine*, 9(9), 922-925.
63. Thurman, D. J., Beghi, E., Begley, C. E., Berg, A. T., Buchhalter, J. R., Ding, D., ... & Kroner, B. (2011). Standards for epidemiologic studies and surveillance of epilepsy. *Epilepsia*, 52(s7), 2-26.
64. Moshé, S. L., Perucca, E., Ryvlin, P., & Tomson, T. (2015). Epilepsy: new advances. *The Lancet*, 385(9971), 884-898.
65. French, J. A., Kanner, A. M., Bautista, J., Abou-Khalil, B., Browne, T., Harden, C. L., ... & Bergen, D. (2004). Efficacy and tolerability of the new antiepileptic drugs I: Treatment of new onset epilepsy Report of the Therapeutics and Technology Assessment Subcommittee and Quality Standards Subcommittee of the American Academy of Neurology and the American Epilepsy Society. *Neurology*, 62(8), 1252-1260.

66. Chadwick, D. W., Anhut, H., Greiner, M. J., Alexander, J., Murray, G. H., Garofalo, E. A., & Pierce, M. W. (1998). A double-blind trial of gabapentin monotherapy for newly diagnosed partial seizures. *Neurology*, *51*(5), 1282-1288.
67. O'keeffe, S. T. (1996). Restless legs syndrome. *Archives of Internal Medicine*, *156*, 243-248.
68. Trenkwalder, C., Wetter, T. C., Stiasny, K., & Clarenbach, P. (2001). Restless-legs-Syndrom und "periodic limb movements in sleep". *Der Nervenarzt*, *72*(6), 425-436.
69. Allen, R. P., Picchietti, D. L., Garcia-Borreguero, D., Ondo, W. G., Walters, A. S., Winkelman, J. W., ... & Lee, H. B. (2014). Restless legs syndrome/Willis–Ekbom disease diagnostic criteria: updated International Restless Legs Syndrome Study Group (IRLSSG) consensus criteria–history, rationale, description, and significance. *Sleep medicine*, *15*(8), 860-873.
70. Karlsson, A., Fonnum, F., Malthe-Sørensen, D., & Storm-Mathisen, J. (1974). Effect of the convulsive agent 3-mercaptopropionic acid on the levels of GABA, other amino acids and glutamate decarboxylase in different regions of the rat brain. *Biochemical pharmacology*, *23*(21), 3053-3061.
71. Rose, M. A., & Kam, P. C. A. (2002). Gabapentin: pharmacology and its use in pain management. *Anaesthesia*, *57*(5), 451-462.
72. O'Neil, M. J. (Ed.). (2013). *The Merck index: an encyclopedia of chemicals, drugs, and biologicals*. RSC Publishing.
73. Stewart, B. H., Kugler, A. R., Thompson, P. R., & Bockbrader, H. N. (1993). A saturable transport mechanism in the intestinal absorption of gabapentin is the underlying cause of the lack of proportionality between increasing dose and drug levels in plasma. *Pharmaceutical research*, *10*(2), 276-281.
74. Yuen, P. W. (2006).  $\alpha 2\delta$  Ligands: Neurontin®(Gabapentin) and Lyrica®(Pregabalin). *The Art of Drug Synthesis*, 225-240.
75. Backonja, M., Beydoun, A., Edwards, K. R., Schwartz, S. L., Fonseca, V., Hes, M., ... & Gabapentin Diabetic Neuropathy Study Group. (1998). Gabapentin for the symptomatic treatment of painful neuropathy in patients with diabetes mellitus: a randomized controlled trial. *Jama*, *280*(21), 1831-1836.
76. Albert, A. (1958). Chemical aspects of selective toxicity. *Nature*, *182*(4633), 421.
77. Higuchi, T., & Stella, V. (Eds.). (1975). *Pro-drugs as novel drug delivery systems*. American Chemical Society.
78. Rautio, J., Kumpulainen, H., Heimbach, T., Oliyai, R., Oh, D., Järvinen, T., & Savolainen, J. (2008). Prodrugs: design and clinical applications. *Nature Reviews Drug Discovery*, *7*(3), 255.
79. Gupta, S. K. (2004). *Drug screening methods*. Jaypee Brothers.
80. Jana, S., Mandlekar, S., & Marathe, P. (2010). Prodrug design to improve pharmacokinetic and drug delivery properties: challenges to the discovery scientists. *Current medicinal chemistry*, *17*(32), 3874-3908.
81. Stella, V. J. (2010). Prodrugs: Some thoughts and current issues. *Journal of pharmaceutical sciences*, *99*(12), 4755-4765.
82. Rautio, J. (2010). Prodrug strategies in drug design. *Prodrugs and targeted delivery: towards better ADME properties*, 1-30.
83. Zawilska, J. B., Wojcieszak, J., & Olejniczak, A. B. (2013). Prodrugs: a challenge for the drug development. *Pharmacological reports*, *65*(1), 1-14.

84. Liederer, B. M., & Borchardt, R. T. (2006). Enzymes involved in the bioconversion of ester-based prodrugs. *Journal of pharmaceutical sciences*, 95(6), 1177-1195.
85. Taylor, M. D. (1996). Improved passive oral drug delivery via prodrugs. *Advanced drug delivery reviews*, 19(2), 131-148.
86. Huttunen, K. M., Raunio, H., & Rautio, J. (2011). Prodrugs—from serendipity to rational design. *Pharmacological reviews*, 63(3), 750-771.
87. Hörter, D., & Dressman, J. B. (2001). Influence of physicochemical properties on dissolution of drugs in the gastrointestinal tract1. *Advanced drug delivery reviews*, 46(1-3), 75-87.
88. Stegemann, S., Leveiller, F., Franchi, D., De Jong, H., & Lindén, H. (2007). When poor solubility becomes an issue: from early stage to proof of concept. *European journal of pharmaceutical sciences*, 31(5), 249-261.
89. Choudhary, S., Gupta, L., Rani, S., Dave, K., & Gupta, U. (2017). Impact of dendrimers on solubility of hydrophobic drug molecules. *Frontiers in pharmacology*, 8, 261.
90. Stella, V. J., & Nti-Addae, K. W. (2007). Prodrug strategies to overcome poor water solubility. *Advanced drug delivery reviews*, 59(7), 677-694.
91. Müller, C. E. (2009). Prodrug approaches for enhancing the bioavailability of drugs with low solubility. *Chemistry & Biodiversity*, 6(11), 2071-2083.
92. Karaman, R. (2014). Prodrugs for Masking the Bitter Taste of Drugs. In *Application of Nanotechnology in Drug Delivery*. InTech.
93. Kwan, K. C. (1997). Oral bioavailability and first-pass effects. *Drug metabolism and disposition*, 25(12), 1329-1336.
94. Singh, B., & Ahuja, N. (2002). Development of controlled-release buccoadhesive hydrophilic matrices of diltiazem hydrochloride: optimization of bioadhesion, dissolution, and diffusion parameters. *Drug development and industrial pharmacy*, 28(4), 431-442.
95. Chu, W. W. (1987). *Prodrug strategies for bypassing the first-pass metabolism of propranolol* (Master's thesis, Dept. of Pharmaceutics, University of Utah).
96. Merali, Z., Ross, S., & Paré, G. (2014). The pharmacogenetics of carboxylesterases: CES1 and CES2 genetic variants and their clinical effect. *Drug metabolism and drug interactions*, 29(3), 143-151.
97. Lewis, J. P., Horenstein, R. B., Ryan, K., O'Connell, J. R., Gibson, Q., Mitchell, B. D., ... & Peer, C. J. (2013). The functional G143E variant of carboxylesterase 1 is associated with increased clopidogrel active metabolite levels and greater clopidogrel response. *Pharmacogenetics and genomics*, 23(1), 1.
98. Tarkiainen, E. K., Backman, J. T., Neuvonen, M., Neuvonen, P. J., Schwab, M., & Niemi, M. (2012). Carboxylesterase 1 polymorphism impairs oseltamivir bioactivation in humans. *Clinical Pharmacology & Therapeutics*, 92(1), 68-71.
99. Marsh, S., & Hoskins, J. M. (2010). Irinotecan pharmacogenomics. *Pharmacogenomics*, 11(7), 1003-1010.
100. Kubo, T., Kim, S. R., Sai, K., Saito, Y., Nakajima, T., Matsumoto, K., ... & Ohtsu, A. (2005). Functional characterization of three naturally occurring single nucleotide polymorphisms in the CES2 gene encoding carboxylesterase 2 (HCE-2). *Drug metabolism and disposition*, 33(10), 1482-1487.
101. CYP2C9, C., & CYP2D6, C. (2007). The effect of cytochrome P450 metabolism on drug response, interactions, and adverse effects. *Am Fam Physician*, 76, 391-6.

102. Belpaire, F. M., & Bogaert, M. G. (1996). Cytochrome P450: genetic polymorphism and drug interactions. *Acta Clinica Belgica*, 51(4), 254-260.
103. Karaman, R. (2012). Computationally designed enzyme models to replace natural enzymes in prodrug approaches. *J Drug Design*, 1, e111.
104. Moser, V. C., Chanda, S. M., Mortensen, S. R., & Padilla, S. (1998). Age- and gender-related differences in sensitivity to chlorpyrifos in the rat reflect developmental profiles of esterase activities. *Toxicological sciences*, 46(2), 211-222.
105. Draganov, D. I., & La Du, B. N. (2004). Pharmacogenetics of paraoxonases: a brief review. *Naunyn-Schmiedeberg's archives of pharmacology*, 369(1), 78-88.
106. Ngawhirunpat, T., Kawakami, N., Hatanaka, T., Kawakami, J., & Adachi, I. (2003). Age dependency of esterase activity in rat and human keratinocytes. *Biological and Pharmaceutical Bulletin*, 26(9), 1311-1314.
107. Karaman, R., & Pascal, R. (2010). A computational analysis of intramolecularity in proton transfer reactions. *Organic & biomolecular chemistry*, 8(22), 5174-5178.
108. Karaman, R. (2010). The efficiency of proton transfer in Kirby's enzyme model, a computational approach. *Tetrahedron Letters*, 51(16), 2130-2135.
109. Karaman, R. (2011). Analyzing the efficiency of proton transfer to carbon in Kirby's enzyme model—a computational approach. *Tetrahedron Letters*, 52(6), 699-704.
110. Karaman, R. (2011). Analyzing the efficiency in intramolecular amide hydrolysis of Kirby's N-alkylmaleamic acids—A computational approach. *Computational and Theoretical Chemistry*, 974(1-3), 133-142.
111. Karaman, R. (2014). Prodrugs-Current and Future Drug Development Strategy. *Drug discovery*, 1, 11.
112. Madan, J., Chawla, G., Arora, V., Malik, R., & Bansal, A. K. (2005). Unbiased membrane permeability parameters for gabapentin using boundary layer approach. *The AAPS journal*, 7(1), E224-E230.
113. Gidal, B. E., Radulovic, L. L., Kruger, S., Rutecki, P., Pitterle, M., & Bockbrader, H. N. (2000). Inter- and intra-subject variability in gabapentin absorption and absolute bioavailability. *Epilepsy research*, 40(2-3), 123-127.
114. Gidal, B. E., DeCerce, J., Bockbrader, H. N., Gonzalez, J., Kruger, S., Pitterle, M. E., ... & Ramsay, R. E. (1998). Gabapentin bioavailability: effect of dose and frequency of administration in adult patients with epilepsy. *Epilepsy research*, 31(2), 91-99.
115. Beydoun, A., Fakhoury, T., Nasreddine, W., & Abou-Khalil, B. (1998). Conversion to high dose gabapentin monotherapy in patients with medically refractory partial epilepsy. *Epilepsia*, 39(2), 188-193.
116. Karaman, R. (2013). Prodrugs Design Based on Inter- and Intramolecular Chemical Processes. *Chemical biology & drug design*, 82(6), 643-668.
117. Satzinger, G., Hartenstein, J., Herrmann, M., & Heldt, W. (1977). *U.S. Patent No. 4,024,175*. Washington, DC: U.S. Patent and Trademark Office.
118. Su, T. Z., Lunney, E., Campbell, G., & Oxender, D. L. (1995). Transport of Gabapentin, a  $\gamma$ -Amino Acid Drug, by System L  $\alpha$ -Amino Acid Transporters: A Comparative Study in Astrocytes, Synaptosomes, and CHO Cells. *Journal of neurochemistry*, 64(5), 2125-2131.
119. Kukkar, A., Bali, A., Singh, N., & Jaggi, A. S. (2013). Implications and mechanism of action of gabapentin in neuropathic pain. *Archives of pharmacal research*, 36(3), 237-251.

120. Offord, J., & Isom, L. L. (2016). Drugging the undruggable: gabapentin, pregabalin and the calcium channel  $\alpha 2\delta$  subunit. *Critical reviews in biochemistry and molecular biology*, 51(4), 246-256.
121. Rogawski, M. A., Tofighy, A., White, H. S., Matagne, A., & Wolff, C. (2015). Current understanding of the mechanism of action of the antiepileptic drug lacosamide. *Epilepsy research*, 110, 189-205.
122. Toth, C. (2010). Substitution of gabapentin therapy with pregabalin therapy in neuropathic pain due to peripheral neuropathy. *Pain Medicine*, 11(3), 456-465.
123. Bockbrader, H. N., Wesche, D., Miller, R., Chapel, S., Janiczek, N., & Burger, P. (2010). A comparison of the pharmacokinetics and pharmacodynamics of pregabalin and gabapentin. *Clinical pharmacokinetics*, 49(10), 661-669.
124. Bonnet, U., & Scherbaum, N. (2017). How addictive are gabapentin and pregabalin? A systematic review. *European Neuropsychopharmacology*, 27(12), 1185-1215.
125. Agarwal, M. M., & Elsi Sy, M. (2017). Gabapentinoids in pain management in urological chronic pelvic pain syndrome: Gabapentin or pregabalin?. *Neurourology and urodynamics*, 36(8), 2028-2033.
126. Beydoun, A., Uthman, B. M., Kugler, A. R., Greiner, M. J., Knapp, L. E., Garofalo, E. A., & Pregabalin 1008–009 Study Group. (2005). Safety and efficacy of two pregabalin regimens for add-on treatment of partial epilepsy. *Neurology*, 64(3), 475-480.
127. McLean, M. J. (1994). Clinical pharmacokinetics of gabapentin. *Neurology*, 44(6 Suppl 5), S17-22.
128. Cundy, K. C., Sastry, S., Luo, W., Zou, J., Moors, T. L., & Canafax, D. M. (2008). Clinical pharmacokinetics of XP13512, a novel transported prodrug of gabapentin. *The Journal of Clinical Pharmacology*, 48(12), 1378-1388.
129. Rais, R., Fletcher, S., & Polli, J. E. (2011). Synthesis and *in vitro* evaluation of gabapentin prodrugs that target the human apical sodium-dependent bile acid transporter (hASBT). *Journal of pharmaceutical sciences*, 100(3), 1184-1195.
130. Cundy, K. C., Annamalai, T., Bu, L., De Vera, J., Estrela, J., Luo, W., ... & Barrett, R. W. (2004). XP13512, a novel gabapentin prodrug: II. Improved oral bioavailability, dose proportionality, and colonic absorption compared with gabapentin in rats and monkeys. *J Pharmacol Exp Ther*, 311, 324-333.
131. Kume, A. (2014). Gabapentin enacarbil for the treatment of moderate to severe primary restless legs syndrome (Willis-Ekbom disease): 600 or 1,200 mg dose?. *Neuropsychiatric disease and treatment*, 10, 249.
132. Thomas, B. M., & Farquhar-Smith, P. (2013). Gabapentin enacarbil extended release for the treatment of postherpetic neuralgia in adults. *Therapeutics and clinical risk management*, 9, 469.
133. Cundy, K. C., Branch, R., Chernov-Rogan, T., Dias, T., Estrada, T., Hold, K., ... & Raillard, S. P. (2004). XP13512, a novel gabapentin prodrug: I. design, synthesis, enzymatic conversion to gabapentin, and transport by intestinal solute transporters. *J Pharmacol Exp Ther*, 311, 315-323.
134. Jung, D., Fried, M., & Kullak-Ublick, G. A. (2002). Human apical sodium-dependent bile salt transporter gene (SLC10A2) is regulated by the peroxisome proliferator-activated receptor  $\alpha$ . *Journal of Biological Chemistry*, 277(34), 30559-30566.
135. Balakrishnan, A., & Polli, J. E. (2006). Apical sodium dependent bile acid transporter (ASBT, SLC10A2): a potential prodrug target. *Molecular pharmaceuticals*, 3(3), 223-230.

136. Karaman, R. (2016). From Conventional Prodrugs to Prodrugs Designed By Molecular Orbital Methods. In *Frontiers in Computational Chemistry* (pp. 187-249).
137. Ala'Abu-Jaish, S. J., & Karaman, R. Prodrug Overview. *PRODRUGS DESIGN*, 1, 77.
138. Fattash, B., & Karaman, R. (2014). Chemical approaches used in prodrugs design. *Nova Science Publishers, Inc. NY, USA*, 103-138.
139. Salameh, F., Karaman, D., Mecca, G., Scrano, L., Bufo, S. A., & Karaman, R. (2015). Prodrugs targeting the central nervous system (CNS). *World J Pharm Pharm Sci*, 4(8), 208-37.
140. Karaman, R. (2008). Analysis of Menger's 'spatiotemporal hypothesis'. *Tetrahedron Letters*, 49(41), 5998-6002.
141. Karaman, R. (2009). Cleavage of Menger's aliphatic amide: a model for peptidase enzyme solely explained by proximity orientation in intramolecular proton transfer. *Journal of Molecular Structure: THEOCHEM*, 910(1-3), 27-33.
142. Karaman, R. (2010). A general equation correlating intramolecular rates with 'attack' parameters: distance and angle. *Tetrahedron Letters*, 51(39), 5185-5190.
143. Karaman, R. (2009). A new mathematical equation relating activation energy to bond angle and distance: a key for understanding the role of acceleration in lactonization of the trimethyl lock system. *Bioorganic chemistry*, 37(1), 11-25.
144. Karaman, R. (2010). Proximity vs. strain in intramolecular ring-closing reactions. *Molecular Physics*, 108(13), 1723-1730.
145. Karaman, R. (2011). The role of proximity orientation in intramolecular proton transfer reactions. *Computational and Theoretical Chemistry*, 966(1-3), 311-321.
146. Karaman, R. (2013). Prodrug design vs. drug design. *J Drug Design*, 2, e114.
147. Karaman, R. (2012). The future of prodrugs designed by computational chemistry. *Drug Des*, 1, e103.
148. Karaman, R. (2013). Prodrugs design by computation methods-a new era. *Journal of Drug Designing*, 1, e113.
149. Karaman, R. (2011). Analyzing Kemp's amide cleavage: A model for amidase enzymes. *Computational and Theoretical Chemistry*, 963(2-3), 427-434.
150. Karaman, R., Ghareeb, H., Dajani, K. K., Scrano, L., Hallak, H., Abu-Lafi, S., ... & Bufo, S. A. (2013). Design, synthesis and *in vitro* kinetic study of tranexamic acid prodrugs for the treatment of bleeding conditions. *Journal of computer-aided molecular design*, 27(7), 615-635.
151. Karaman, R., Dajani, K. K., Qtait, A., & Khamis, M. (2012). Prodrugs of Acyclovir—A Computational Approach. *Chemical biology & drug design*, 79(5), 819-834.
152. Karaman, R., Dajani, K., & Hallak, H. (2012). Computer-assisted design for atenolol prodrugs for the use in aqueous formulations. *Journal of molecular modeling*, 18(4), 1523-1540.
153. Karaman, R., Amly, W., Scrano, L., Mecca, G., & Bufo, S. A. (2013). Computationally designed prodrugs of statins based on Kirby's enzyme model. *Journal of molecular modeling*, 19(9), 3969-3982.
154. Karaman, R., Karaman, D., & Zeiadeh, I. (2013). Computationally-designed phenylephrine prodrugs—a model for enhancing bioavailability. *Molecular Physics*, 111(21), 3249-3264.
155. Karaman, R. (2015). Computationally Designed Prodrugs Based on Enzyme Models| *Aperito Journal of Drug Designing and Pharmacol* 2015, 2: 111.

156. Karaman, R., Jumaa, S., Awwadallah, H., Salah, S., Khawaja, Y., & Karaman, D. (2016). Intramolecular Processes and Their Applications in Prodrugs Approaches-Experimental and Computational Studies. *Current Organic Chemistry*, 20(3), 289-315.
157. Karaman, R. (2011). Computational-Aided Design for Dopamine Prodrugs Based on Novel Chemical Approach. *Chemical biology & drug design*, 78(5), 853-863.
158. Kirby, A. J., & Williams, N. H. (1994). Efficient intramolecular general acid catalysis of enol ether hydrolysis. Hydrogen-bonding stabilisation of the transition state for proton transfer to carbon. *Journal of the Chemical Society, Perkin Transactions 2*, (4), 643-648.
159. Johnson, D. E., & Wolfgang, G. H. (2000). Predicting human safety: screening and computational approaches. *Drug discovery today*, 5(10), 445-454.
160. Sketch, C. ACD-LAB Software for calculating the refferd physiochemical parameters. *Chem Sketch*.
161. Swain, M. (2012). Chemicalize. org.
162. Lee, S. K., Lee, I. H., Kim, H. J., Chang, G. S., Chung, J. E., & No, K. T. (2003). The PreADME Approach: Web-based program for rapid prediction of physico-chemical, drug absorption and drug-like properties. *EuroQSAR 2002 Designing Drugs and Crop Protectants: processes, problems and solutions*, 2003, 418-420.
163. Lee, S. K., Chang, G. S., Lee, I. H., Chung, J. E., Sung, K. Y., & No, K. T. (2004). The PreADME: pc-based program for batch prediction of adme properties. *EuroQSAR*, 9, 5-10.
164. Lipinski, C. A. (2004). Lead-and drug-like compounds: the rule-of-five revolution. *Drug Discovery Today: Technologies*, 1(4), 337-341.
165. Misra, A., Ganesh, S., Shahiwala, A., & Shah, S. P. (2003). Drug delivery to the central nervous system: a review. *J Pharm Pharm Sci*, 6(2), 252-273.
166. Predictor, B. B. B. (2017). [cbligand.org/BBB/predictor.php](http://cbligand.org/BBB/predictor.php).
167. Kirby, A. J., & Lancaster, P. W. (1972). Structure and efficiency in intramolecular and enzymic catalysis. Catalysis of amide hydrolysis by the carboxy-group of substituted maleamic acids. *Journal of the Chemical Society, Perkin Transactions 2*, (9), 1206-1214.
168. Lipinski, C. A. (2000). Drug-like properties and the causes of poor solubility and poor permeability. *Journal of pharmacological and toxicological methods*, 44(1), 235-249.
169. Lipinski, C. A., Lombardo, F., Dominy, B. W., & Feeney, P. J. (2001). Experimental and computational approaches to estimate solubility and permeability in drug discovery and development settings1. *Advanced drug delivery reviews*, 46(1-3), 3-26.
170. Ghose, A. K., Viswanadhan, V. N., & Wendoloski, J. J. (1999). A knowledge-based approach in designing combinatorial or medicinal chemistry libraries for drug discovery. 1. A qualitative and quantitative characterization of known drug databases. *Journal of combinatorial chemistry*, 1(1), 55-68.
171. Veber, D. F., Johnson, S. R., Cheng, H. Y., Smith, B. R., Ward, K. W., & Kopple, K. D. (2002). Molecular properties that influence the oral bioavailability of drug candidates. *Journal of medicinal chemistry*, 45(12), 2615-2623.

172. Waring, M. J. (2010). Lipophilicity in drug discovery. *Expert Opinion on Drug Discovery*, 5(3), 235-248.
173. Kwon, Y. (2001). *Handbook of essential pharmacokinetics, pharmacodynamics and drug metabolism for industrial scientists*. Springer Science & Business Media.
174. Hansch, C., & Fujita, T. (1964).  $\rho$ - $\sigma$ - $\pi$  Analysis. A method for the correlation of biological activity and chemical structure. *Journal of the American Chemical Society*, 86(8), 1616-1626.
175. Hitchcock, S. A., & Pennington, L. D. (2006). Structure– brain exposure relationships. *Journal of medicinal chemistry*, 49(26), 7559-7583.
176. Comer, J. E. (2003). High-Throughput Measurement of log *D* and pKa. *Drug bioavailability: Estimation of solubility, permeability, absorption and bioavailability*, 21-45.
177. Bhal, S. K., Kassam, K., Peirson, I. G., & Pearl, G. M. (2007). The Rule of Five revisited: applying log *D* in place of log *P* in drug-likeness filters. *Molecular pharmaceutics*, 4(4), 556-560.
178. van de Waterbeemd, H., & Kansy, M. (1992). Hydrogen-bonding capacity and brain penetration. *CHIMIA International Journal for Chemistry*, 46(7-8), 299-303.
179. Alelyunas, Y. W., Empfield, J. R., McCarthy, D., Spreen, R. C., Bui, K., Pelosi-Kilby, L., & Shen, C. (2010). Experimental solubility profiling of marketed CNS drugs, exploring solubility limit of CNS discovery candidate. *Bioorganic & medicinal chemistry letters*, 20(24), 7312-7316.
180. Abraham, M. H., Takács-Novák, K., & Mitchell, R. C. (1997). On the partition of ampholytes: application to blood–brain distribution. *Journal of pharmaceutical sciences*, 86(3), 310-315.
181. van de Waterbeemd, H., Camenisch, G., Folkers, G., Chretien, J. R., & Raevsky, O. A. (1998). Estimation of blood-brain barrier crossing of drugs using molecular size and shape, and H-bonding descriptors. *Journal of drug targeting*, 6(2), 151-165.
182. Pajouhesh, H., & Lenz, G. R. (2005). Medicinal chemical properties of successful central nervous system drugs. *NeuroRx*, 2(4), 541-553.
183. Yee, S. (1997). *In vitro* permeability across Caco-2 cells (colonic) can predict *in vivo* (small intestinal) absorption in man—fact or myth. *Pharmaceutical research*, 14(6), 763-766.
184. Rautio, J., Humphreys, J. E., Webster, L. O., Balakrishnam, A., Keogh, J. P., Kunta, J. R., ... & Polli, J. W. (2006). *In vitro* p-glycoprotein inhibition assays for assessment of clinical drug interaction potential of new drug candidates: a recommendation for probe substrates. *Drug metabolism and disposition*.

تصنيع ودراسة مواصفات وحركية الدواء المخبرية لطلائع الغابابنتين.

إعداد: فاطمة عصام عبد القادر حداد

إشراف: البروفيسور الدكتور رفيع قرمان

الملخص

يمتلك الغابابنتين حركية دوائية منتظمة تحد من فعاليته السريرية؛ وذلك لأن إمتصاصه يتم من خلال نظام نقل الأحماض الأمينية نوع L- بواسطة ناقل المغذيات منخفض السعة والذي يتواجد في مكان محدود من الجزء العلوي للأمعاء الدقيقة. نظام النقل هذا هو نظام نقل يحتاج إلى ناقل ويحدث له إشباع؛ وهذا أدى إلى اعتماد حركية الدواء للغابابنتين على الجرعة؛ أي أنه كلما زادت الجرعة ينخفض التوافر الحيوي (الامتصاص) للغابابنتين.

استناداً إلى نموذج إنزيم كيربي، تم اقتراح ثلاثة طلائع للغابابنتين يتوقع أن تكون ذات توافر حيوي عالي وتمتلك حركية دوائية خطية، على النقيض من الغابابنتين، نتيجة لتحسين امتصاصه عبر الانتشار البسيط. علاوة على ذلك، يمكن استخدام الطلائع المقترحة في أشكال صيدلانية مختلفة بسبب احتمالية قابليتها للذوبان في الوسطين العضوي والمائي.

تم تحضير وتشخيص هذه الطلائع المقترحة عن طريق قياس درجة الإنصهار، أطياف الأشعة تحت الحمراء، والرنين النووي المغناطيسي للبروتون، و كروماتوغرافيا المقترن بالمطياف الكتلي للتأكد من أن المركبات المصنعة نقية. و تم دراسة تحلل هذه الطلائع داخل المختبر إلى دواءه الأصلي -دون أي تدخل من الإنزيمات- باستخدام كروماتوغرافيا السائل ذات الكفاءة العالية على درجة حرارة ثابتة (37°C) و درجات حموضة مختلفة مثل 0.1N HCl و 3 و 6.8 و 7.4 ، التي تشبه درجات الحموضة في جسم الإنسان. و قد تم التنبؤ بخصائص هذه الطلائع الفيزيوكيميائية،

والامتصاص، والتوزيع، والأيض، والإخراج، والسمية، و قابليتها للنفاذ من خلال الحاجز الدموي للدماغ من خلال برامج معلوماتية متعددة.

وقد تبين أن قيم العمر النصفى التجريبي لطلية الغابانتين الأول في حمض الهيدروكلوريد 0.1 N HCl، ودرجة الحموضة 3، ودرجة الحموضة 6.8، ودرجة الحموضة 7.4 كانت 16.57، و17.76، و101.91، و 119.48 ساعة، على التوالي. وأيضاً تم تحليل طليعة الغابانتين الثاني إلى دوائه الأساسي في حمض الهيدروكلوريد 0.1 N HCl، ودرجات حموضة 3، و6.8، و7.4 وكانت قيم العمر النصفى التجريبي 20.3، و22.70، و130.75، و277.2 ساعة، على التوالي. بالمقابل، كان طليعة الغابانتين الثالث غير قابل للذوبان إطلاقاً في البيئة الحمضية ومستقر تماماً في درجة الحموضة 6.8 ودرجة الحموضة 7.4.

وقد أظهرت نتائج تنبؤ خصائص هذه الطلائع من خلال البرامج المعلوماتية أن جميع هذه الطلائع تتوافق مع قاعدة لبنسكي ولديها خصائص حركية دوائية جيدة وليس لديها مخاطر عالية من السمية و لديها قابليته للنفاذ إلى الجهاز العصبي المركزي.

لقد تم تصنيع و دراسة مواصفات ثلاثة طلائع للغابانتين و قد بينت نتائج تحليلها الي أن العمر النصفى يتأثر بشكل أساسي بالرقم الهيدروجيني للوسط والمسافة بين المركزين المتفاعلين (ذرة الأكسجين بالهيدروكسيل التابعة لمجموعة الكربوكسيل وذرة الكربون بمجموعة الكربونيل بالربطة الأميدية) وال pka للرابط. سوف يتم دراسة حركية طليعة الغابانتين الأول و الثاني في جسم الانسان لحساب التوفر الحيوي و مدة عملها.